

UNIVERSITY OF CALGARY

Adaptive Controller for SVC

by

Abdullatif M. E. Barnawi

A THESIS

**SUBMITTED TO THE FACULTY OF GRADUATE STUDIES
IN PARTIAL FULFILMENT OF THE REQUIREMENTS FOR THE
DEGREE OF MASTER OF SCIENCE**

DEPARTMENT OF ELECTRICAL AND COMPUTER ENGINEERING

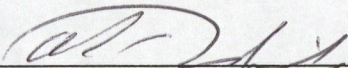
CALGARY, ALBERTA

JULY, 2007

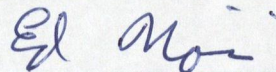
© Abdullatif M. E. Barnawi 2007

UNIVERSITY OF CALGARY
FACULTY OF GRADUATE STUDIES

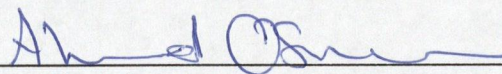
The undersigned certify that they have read, and recommend to the Faculty of Graduate Studies for acceptance, a thesis entitled, "Adaptive Controller for SVC", submitted by Abdullatif M. E. Barnawi in partial fulfilment of the requirements of the degree of Master of Science.



Supervisor, Dr. O. P. Malik
Department of Electrical and Computer Engineering



Dr. Ed Nowicki
Department of Electrical and Computer Engineering



Dr. Ahmed Osman
Department of Electrical and Computer Engineering



Dr. Alejandro Ramirez-Serrano
Department of Mechanical & Manufacturing Engineering

2027.07.06
Date

Abstract

Flexible AC Transmission Systems (FACTS) devices are playing an increasingly important role in electrical power systems. They have been used to enhance the power system stability and performance. A Static VAR Compensator (SVC), one of the first breed of FACTS devices, is a fast controllable generator and/or absorber of reactive power and can contribute to improve system performance in a number of areas.

This dissertation gives a survey of the prospective applications of SVC in power systems with particular emphasis on the use of SVC with supplementary adaptive controller to enhance system damping. The application areas are briefly outlined and the SVC is compared with other possible techniques. A relatively detailed description of the SVC, Recursive Least Squares (RLS) identification algorithm, Kalman Filter (KF) operating as parameters estimator algorithm and variable Pole-Shifting (PS) linear feedback control theory are given, supported by simulation studies to evaluate the SVC adaptive control performance.

Acknowledgements

First of all, I want to thank God almighty for giving me the strength and motivation to pursue this degree.

Then, I wish to express my sincere gratitude and deep feeling of indebtedness to my supervisor, Dr. O. P. Malik for his constant guidance, encouragement and support throughout the whole program. He rebuilt my knowledge in Electrical Engineering area and I have learned so much from him not only in the area of my study but also in teaching, research, and life style. My foremost thanks go to him and all professors and support staff in the Department of Electrical and Computer Engineering and The University of Calgary, for their help during my study here.

I also wish to acknowledge the financial support provided by the Government of the Kingdom of Saudi Arabia through The General Organization of Technical Education and Vocational Training. I also wish to acknowledge the great support supplied from Ministry of Higher Education through the Saudi Arabian Cultural Bureau in Canada and my hearty thanks goes to Cultural Attache and the Staff for their help and encouragement.

Special appreciation goes to all the friends I met and work together during my study period for their companionship and assistance especially my colleague Mr. A. Albakkar and Dr. W. Hussain.

Finally, these acknowledgments can not be complete without my expressing my great indebtedness to my Mother and my Wife for their patience, understanding and constant spiritual support especially during times of difficulty.

Dedication

*To
My Parents
My Brothers, My Sisters
My Wife, My Children*

Table of Contents

Approval Page.....	ii
Abstract.....	iii
Acknowledgements.....	iv
Dedication.....	v
Table of Contents.....	vi
List of Tables.....	ix
List of figures and Illustrations.....	x
List of Abbreviations and Symbols.....	xv
Epigraph.....	xxi
 CHAPTER 1	 1
INTRODUCTION	1
1.1 Power System Interconnection and Control Systems	1
1.2 Power System Damping Controller	2
1.2.1 Damping Control at Generation Locations	3
1.2.2 Damping Control in the Transmission Path.....	4
1.3 Types of Power System Stabilizers	5
1.3.1 Conventional Power System Stabilizers	6
1.3.2 Adaptive Power System Stabilizers	7
1.4 Applications of the Static VAR Compensator	12
1.5 Dissertation Objective.....	17
1.6 Dissertation Contributions	18
1.7 Dissertation Organizations.....	19
 CHAPTER 2	 20
SYSTEM IDENTIFICATION AND MODEL	20
2.1 Introduction.....	20
2.2 System and Model	21
2.2.1 ARMA Model	22
2.2.2 ARMAX Model	24
2.2.3 Test Signal	25
2.3 Identification Scheme	26
2.3.1 Recursive Least Squares Identifier	27
2.3.2 Kalman Filter as Parameter Estimator	34
 CHAPTER 3	 38
VARIABLE POLE-SHIFT LINEAR FEEDBACK CONTROL	38
3.1 Introduction.....	38
3.2 Pole-Shifting Control.....	38
3.2.1 Background	38
3.2.2 Concepts.....	39
3.2.3 Taylor Series Expansion of Control Signal $u(t)$ in Terms of α	42
3.2.4 System Output Prediction, $\hat{y}(t+1)$	43

3.2.5 Performance Index and Constraints	44
3.2.6 Properties of the PS Algorithm	46
CHAPTER 4	51
APPLICATION OF SAPSS IN A SINGLE-MACHINE INFINITE-BUS SYSTEM ..	51
4.1 Introduction.....	51
4.2 Self-Tuning Control	52
4.3 System Configuration and Model	55
4.4 System Identification	57
4.4.1 On-line Identification Using RLS Algorithm	58
4.4.2 On-line Identification Using KF Algorithm.....	61
4.4.3 Discussion	64
4.5 Control Strategy	66
4.5.1 Controller Start-Up:	68
4.6 Simulation Studies	68
4.6.1 Normal Load Conditions.....	69
4.6.2 Light Load Conditions	73
4.6.3 Leading Power Factor Load Conditions	75
4.6.4 Change in Voltage Reference of the Generator Bus	77
4.6.5 Voltage Reference Change of the Middle Bus	79
4.6.6 The Effectiveness of Changing the Sampling Rate and Test of the Coordination with the Generator PSS	81
4.6.7 Three-Phase to Ground Short Circuit.....	86
4.6.8 Comparison between Using the Output of SVC (Bsvc) and the Generator Speed Deviation as Supplementary Stabilizing Signal to the Identifier and the Controller	88
4.6.9 Dynamic Stability	88
4.7 Summary	90
CHAPTER 5	91
APPLICATION OF SAPSS IN A MULTI-MACHINE SYSTEM.....	91
5.1 Introduction.....	91
5.2 System Configuration and Model	92
5.2.1 Placement of SVC.....	93
5.3 System Identification	94
5.4 Control Strategy	99
5.5 Simulation Studies	100
5.5.1 Change of the Input Reference Torque	102
5.5.2 Three-Phase to Ground Short Circuit.....	106
5.6 Summary	108
CHAPTER 6	109
CONCLUSIONS	109
6.1 Conclusions.....	109
6.2 Future Work	111
REFERENCES	113

APPENDIX A	123
SINGLE MACHINE POWER SYSTEM.....	123
A.1. Generator Model	123
A.2. Governor Model.....	124
A.3. AVR and Exciter Models.....	125
A.4. SVC.....	126
A.5. CPSS for Generator AND SVC	127
A.6. Transmission System	127
APPENDIX B	128
MULTI-MACHINE POWER SYSTEM.....	128
B.1. Generator Model	128
B.2. Parameters of the Power System.....	128
B.3. Loads and Operating Condition	130

List of Tables

Table 4.1 Maximum values of the torque applied to the system in the stability margin test	90
Table A.1. Generator parameters used in simulation studies.....	124
Table A.2. Governor parameters used in simulation studies	125
Table A.3. AVR and exciter parameters used in simulation studies	125
Table A.4. SVC parameters used in simulation studies.....	127
Table A.5. CPSS parameter used in simulation studies.....	127
Table A.6. Transmission line parameters used in simulation studies	127
Table B.1. Generators parameters used in simulation studies	129
Table B.2. AVR and ST1A exciter parameters used in simulation studies	129
Table B.3. Governor parameters used in simulation studies	130
Table B.4. Transmission line parameters used in simulation studies	130
Table B.5. Load parameters used in simulation studies.....	130
Table B.6. Power flow parameters used in simulation studies	131

List of figures and Illustrations

Fig. 1.1 Model reference adaptive control	8
Fig. 1.2 Self-tuning adaptive control	9
Fig. 1.3 A typical SVC structure.....	12
Fig. 1.4 (a) Two machine power system, (b) corresponding phasor diagram and (c) power transmission vs. angle characteristic.....	14
Fig. 1.5 Supplementary damping scheme for SVC.....	16
Fig. 2.1 Block diagram of a stochastic system.....	22
Fig. 2.2 Block diagram of an ARMA model	23
Fig. 2.3 A general scheme for RLS.....	28
Fig. 2.4 A general scheme for kalman filter	34
Fig. 3.1 A general system model with a feed-back control	40
Fig. 3.2 Schematic diagram of optimization.....	46
Fig. 3.3 Pole-shifting process.....	47
Fig. 3.4 Illustration of performance index	48
Fig. 3.5 Illustration of control signal	49
Fig. 4.1 Block diagram of a self-tuning adaptive controller	53
Fig. 4.2. System model	55
Fig. 4.3 Block diagram of SVC with adaptive control	57
Fig. 4.4 Generator angular speed deviation and RLS output.....	59
Fig. 4.5 Variation of A parameters on-line	60
Fig. 4.6 Variation of B parameters on-line	60
Fig. 4.7 Forgetting factor variation	61
Fig. 4.8 Generator angular speed deviation and KF output	62

Fig. 4.9 Variation of A parameters on-line	63
Fig. 4.10 Variation B parameters on-line.....	63
Fig. 4.11 Mean square error for the RLS-identifier	65
Fig. 4.12 Mean square error for the KF-identifier	65
Fig. 4.8 Generator angular speed deviation in response to a 0.15 p.u. step increase in mechanical torque at 0.5 s. initial condition, $P = 0.7$ p.u., p.f.= 0.9 lag.	70
Fig. 4.9 SVC controller output in response to a 0.15 step increase in mechanical torque.	70
Fig. 4.10 Middle bus voltage in response to a 0.15 p.u. step increase in mechanical torque.	71
Fig. 4.11 Generator terminal voltage in response to a 0.15 p.u step increase in mechanical torque.	71
Fig. 4.12 Controls output of SAPSS & SCPSS in response to a 0.15 p.u. step increase in mechanical torque.	72
Fig. 4.13 Generator angular speed deviation in response to a 0.15 p.u. step increase in mechanical torque at 0.5 s., initial condition $P = 0.2$ p.u., p.f.= 0.8 lag	73
Fig. 4.14 SVC controller output in response to a 0.15 p.u. step increase in mechanical torque.	74
Fig. 4.15 Middle bus voltage in response to a 0.15 p.u. step increase in mechanical torque.	74
Fig. 4.16 Angular speed deviation in response to a 0.15 p.u. step increase in mechanical torque at time 0.5 s., initial condition $P = 0.7$ p.u., p.f.= 0.9 lead.....	75
Fig. 4.17 SVC controller output in response to a 0.15 p.u. step increase in mechanical torque	76

Fig. 4.18 Middle bus voltage in response to a 0.15 p.u. step increase in mechanical torque	76
Fig. 4.19 Angular speed deviation in response to a 5% step increase in the generator terminal voltage reference and back to the initial condition.....	78
Fig. 4.20 SVC controller output in response to a 5% step increase in the terminal voltage reference and back to the initial condition.....	78
Fig. 4.21 Middle bus voltage in response to a 5% step increase in the terminal voltage reference and back to the initial condition.....	79
Fig. 4.22 Angular speed deviation in response to a 5% step increase in the middle bus voltage reference and back to the initial condition	80
Fig. 4.23 SVC controller output in response to a 5% step increase in the terminal voltage reference and back to the initial condition.....	80
Fig. 4.24 Middle bus voltage in response to a 5% step increase in the terminal voltage reference and back to the initial condition.....	81
Fig. 4.25 Angular speed deviation in response to a 0.15 p.u. step increase in mechanical torque at 0.5 s. and back to initial condition, $P = 0.7$ p.u., $p.f. = 0.9$ lag, for different sampling periods and the APSS on the generator only.....	83
Fig. 4.26 Angular speed deviation in response to a 0.15 p.u. step increase in mechanical torque at 0.5 s, initial condition, $P = 0.7$ p.u., $p.f. = 0.9$ lag, for different sampling periodss and the APSS on the SVC only	84
Fig. 4.27 Angular speed deviation in response to a 0.15 p.u. step increase in mechanical torque at 0.5 s, initial condition, $P = 0.7$ p.u., $p.f. = 0.9$ lag, for different sampling periods and the APSS on the generator and SVC	85

Fig. 4.28 Angular speed deviation in response to a three phase to ground fault at the middle of one transmission line and successful reclosure	86
Fig. 4.29 SVC controller output in response to a three phase to ground fault at the middle of one transmission line and successful reclosure	87
Fig. 4.30 Middle bus voltage in response to a three phase to ground fault at the middle of one transmission line and successful reclosure.....	87
Fig. 4.31 Response of the angular speed deviation to different input signals	89
Fig. 4.32 Loss of synchronism in the stability margin test.....	89
Fig. 5.1 A five machine power system model including the SVC.....	92
Fig. 5.2 Response of speed deviation of G1-G2	94
Fig. 5.3 Response of the angular speed deviation of G3 and RLS output	95
Fig. 5.4 Forgetting factor variation.....	96
Fig. 5.5 Response of A parameters on-line variation.....	96
Fig. 5.6 Response of B parameters on-line variation.....	97
Fig. 5.7 Response of power deviation of tie-line 6-7 and RLS output	97
Fig. 5.8 Forgetting factor variation.....	98
Fig. 5.9 Response of A parameters on-line variation.....	98
Fig. 5.10 Response of B parameters on-line variation.....	99
Fig. 5.11 Response of speed deviation of G1-G2	101
Fig. 5.12 Response of speed deviation of G2-G3	101
Fig. 5.13 Response of speed deviation of G3-G1	102
Fig. 5.14 Response of speed deviation of G1-G2	103
Fig. 5.15 Response of speed deviation of G2-G3	103

Fig. 5.16 Response of speed deviation of G3-G1	104
Fig. 5.17 Response of speed deviation of G1-G2	105
Fig. 5.18 Response of speed deviation of G2-G3	105
Fig. 5.19 Response of speed deviation of G3-G1	106
Fig. 5.20 Response of speed deviation of G1-G2	107
Fig. 5.21 Response of speed deviation of G2-G3	107
Fig. 5.22 Response of speed deviation of G3-G1	108
Fig. A.1. AVR and excitation model type ST1A, IEEE standard P421.5-1992	126

List of Abbreviations and Symbols

Abbreviation or symbol	Definition
$A(z^{-1})$	System polynomial in the backward shift operator z^{-1} corresponding to system output
a, b	Governor gain constants
AC	Alternating Current
a_i	Elements of the system polynomial $A(z^{-1})$
APSS	Adaptive Power System Stabilizer
ARMA	Auto Regressive Moving Average
ARMAX	Auto-Regressive Moving-Average Exogenous
AVR	Automatic Voltage Regulator
$B(z^{-1})$	System polynomial in the backward shift operator z^{-1} corresponding to system input
b_i	Elements of the system polynomial $B(z^{-1})$
B_{svc}	The SVC variable susceptance
$B_{svc_{ini}}$	The initial value of the SVC susceptance
$B_{svc_{max}}$	The SVC variable susceptance upper limit
$B_{svc_{min}}$	The SVC variable susceptance lower limit
$C(z^{-1})$	System noise polynomial
c_i	Elements of the system polynomial $C(z^{-1})$
CPSS	Conventional Power System Stabilizer
DAPSS	Duplicate Adaptive Power System Stabilizer
DC	Direct Current
E	Expectation function
$e(t)$	Identification error
e_d	Generator d-axis voltage
e_f	Generator field voltage

e_q	Generator q-axis voltage
ERLS	Extended Recursive Least Squares
$F(z^{-l})$	Denominator polynomial in the backward shift operator z^{-l} corresponding to the feed-back loop
FACTS	Flexible AC Transmission Systems
f_i	Elements of the system polynomial $F(z^{-l})$
G	Generator
g	Governor output
$G(z^{-l})$	Numerator polynomial in the backward shift operator z^{-l} corresponding to the feed-back loop
GAVR	Generator Automatic Voltage Regulator
g_i	Elements of the system polynomial $G(z^{-l})$
GMV	Generalized Minimum Variance
H	Generator inertia
HV	High-Voltage
HVDC	High Voltage Direct Current
Hz	Hertz
i_d	Generator d-axis current
i_f	Generator field current
i_q	Generator q-axis current
I_s	SVC current
I_T	Generator terminal current
J	Performance index
$K(l)$	Modifying gain vector for parameter identification
K_A, K_C, K_F	AVR gains
K_d	Generator damping ratio coefficient
KF	Kalman Filter
K_{LF}, I_{LF}	AVR gains
K_{svc}	SVC gain constant

l	System delay
L_o	Load
LR	Linear Regression
MV	Minimum Variance
N	Notation for total iteration number
n_a, n_b	Orders of the system polynomials $A(z^{-1}), B(z^{-1})$
n_a, n_b, n_c	Orders of the system polynomials $A(z^{-1}), B(z^{-1}), C(z^{-1})$
n_f, n_g	Orders of the system control polynomials $F(z^{-1}), G(z^{-1})$
NMP	Non-Minimum-Phase
NO SPSS	The system without any supplementary control on the
P	Active power
$P(l)$	Covariance matrix for parameter identification
p.f.	Power Factor
p.u.	Per-Unit representation of electrical variables
PA	Pole Assignment
p_i	i th term of the row vector $X_c^T(t)M^I$
PRBS	Pseudo-Random Binary Signal
PS	Pole Shifting
PSS	Power System Stabilizers
PT	Potential Transformer
Q	Reactive power
R	Error Covariance matrix
r_a	Generator armature resistance
R_C, X_C	Voltage transducer compensation constants
r_c	Transmission line resistance
RELS	Recursive Extended Least Squares
r_f	Generator field winding resistance
r_{kd}	Generator d-axis damper winding resistance
r_{kq}	Generator q-axis damper winding resistance

RLS	Recursive Least Squares
RML	Recursive Maximum Likelihood
SAPSS	SVC Adaptive Power System Stabilizer
SCPSS	SVC Conventional Power System Stabilizer
SDC	Supplementary Damping Controller
s_i	ith order sensitivity constant
STATCOM	Static synchronous compensator
SVC	Static VAr Compensators
$T(z^{-1})$	Closed-loop characteristic polynomial
T_1, T_2, T_3, T_4	AVR time constants
TCR	Thyristor-Controlled Reactor
TCSC	Thyristor Controlled Series Capacitor
T_{do}'	Transient d-axis time constant
T_{do}''	Sub transient d-axis time constant
T_e	Generator electric torque output
T_g	Governor time constant
T_m	Generator mechanical torque input
T_{qo}''	Sub transient q-axis time constant
TSC	Thyristor-Switched Capacitor
T_{svc}	SVC time constant
T_w	AVR time constants
$U(t)$	Controller output
$u_c(l)$	steady-state control signal
u_{max}	Absolute physical value of the upper control limit
u_{min}	Absolute physical value of the lower control limit
UPFC	Unified power flow controller
U_{ref}	the steady state system input reference
V	Voltage
V_{AMAX}	AVR command signal upper limit

V_{AMIN}	AVR command signal lower limit
V_{aux}	SVC auxiliary signal
V_{IMAX}	AVR input signal upper limit
V_{IMIN}	AVR input signal lower limit
V_m	Middle bus voltage
V_{OEL}	AVR over-excitation limit
V_{PSS}	PSS output
V_{Ref}	AVR voltage reference setting
V_{RMAX}	AVR regulator upper limit
V_{RMIN}	AVR regulator lower limit
V_{STMAX}	PSS output upper limit
V_{STMIN}	PSS output lower limit
V_{svc}	Voltage of the SVC
$V_{svc(ref)}$	SVC voltage reference
V_t	Generator terminal voltage
V_{UEL}	AVR under-excitation limit
X_c	Measurement variable vector (system output, controller
X_d	Generator d-axis reactance
X_d'	Transient d-axis reactance
X_d''	Sub transient d-axis reactance
X_e	Transmission line reactance
X_f	Generator field reactance
X_i	Measurement variable vector (System output, system
X_{kd}	Generator d-axis damper winding reactance
X_{kq}	Generator q-axis damper winding reactance
X_q	Generator q-axis reactance
y_p	Controlled coordinates of the system
$\hat{y}(t)$	Predicted system output
ε	Mismatch error

X_q''	Sub transient q-axis reactance
$y(t)$	System output signal
λ_d	Generator d-axis flux linkage
λ_f	Generator field flux linkage
λ_{kd}	Generator d-axis damper winding flux linkage
λ_c	Absolute value of the largest characteristic root of $A(z-1)$
λ_{kq}	Generator q-axis damper winding flux linkage
α_{limit}	The initial value of pole-shifting factor
β_m	Identified system parameter vector
α_{opt}	Optimal value of the pole-shifting factor α
λ_q	Generator q-axis flux linkage
λ	Forgetting factor
Σ	Constant for forgetting factor calculation
α	Pole-shift factor
σ	Security coefficient
β	Identified System Parameter vector
δ	Generator power angle
ω	Generator speed
ΔP	The deviation of the active power
$\Delta \omega$	The deviation of angular speed
$\theta(t)$	Identified system parameter vector
$\xi(t)$	White noise signal
$\varphi(t)$	Measurement vector
ω_0	Rated value of generator speed

Epigraph

Allah will exalt in degree those of you who believe, and those who have been granted knowledge. And Allah is Well-Acquainted with what you do.

[Surat Al-Mujadilah, 11], The Holy Qur'an.

For him who adopts a path of seeking knowledge, Allah eases the way in Paradise, and Angels spread their wings for the seekers of knowledge, being pleased with his occupation, and all that is in the heavens and the Earth including the fish in the water, ask for his forgiveness. The learned are the heirs of the Prophets and the Prophets do not leave an inheritance of Dirhams and Dinars (gold, silver and money), but only of knowledge. He who acquires knowledge acquires a vast portion.

The prophet Muhammad peace be upon him

Chapter 1

INTRODUCTION

1.1 Power System Interconnection and Control Systems

Electric power interconnections and their control systems play a prominent role in reliable and stable operation of power systems. Growth in the interconnections such as the interconnections between the operating plants and distribution stations or substations, and the use of new technologies has increased the complexity of power systems. At the same time, financial and regulatory constraints have forced utility companies to operate the system closer than ever to its stability limits. As a result, proper analysis and design of controls in power systems has become very important. Adequate overall system performance will depend largely on the proper operation and performance of critical controls such as excitation systems, power system stabilizers (PSSs), static VAR compensators (SVCs), and the latest breed of control devices often referred to as flexible AC transmission systems (FACTS). The heavy reliance on controls requires a systematic procedure to analyze and design controls that demonstrate good performance for a wide range of operating conditions.

Accompanying the above-mentioned trends has been an increasing tendency of power systems to exhibit oscillatory instability. For example, several instances of low frequency oscillations, associated with some machines in one part of the system swinging against machines in another part of the system, have been observed in the North American interconnected power systems in the past decade [1]. These phenomena are referred to as inter-area oscillations and have frequencies typically in the range of 0.1Hz

to 0.7Hz in multi machine interconnections. Those oscillations are due to the dynamics of inter-area power transfer and often exhibit poor damping where the aggregate power transfer over a corridor is high relative to the transmission strength [2]. With the growth of interconnections and the advent of open access and competition in the industry, inter-area oscillations are more likely to happen, even under normal operating conditions.

Controls once again have been the main tools used for the mitigation of inter-area oscillations. While power system stabilizers (PSSs) remain the main damping method, there is an increasing interest in using FACTS devices to aid the damping of these oscillations [3], especially when the damping effect from the PSSs alone is not enough. SVC is one of these FACTS devices where potential for damping inter-area oscillations is studied in this dissertation.

1.2 Power System Damping Controller

The primary function of introducing artificial damping is to make net damping positive. Even if the natural damping is already positive, there is a considerable benefit in increasing it to achieve stronger damping. However, if for example the natural damping of a power system is negative, one of the cures is to introduce artificial positive damping. Powerful damping decreases both the ratio of each successive swing to the preceding one and the amplitude of the first swing, thus enhancing the stability margin of the system.

During the past few decades many methods have been investigated to improve the stability of the power systems. Generally, the damping control strategies can be divided into two major groups:

- Damping control at generation locations.
- Damping control in the transmission path.

1.2.1 Damping Control at Generation Locations

Considerable effort has been devoted over many years to enhance power system stability in various ways such as system operating condition, configuration control [4, 5, 6], generator input power control [7], and excitation control [8, 9]. Among the artificial damping methods discussed in the literature, it is found that the most economical one is the generator excitation control (with a supplementary signal in addition to the usual terminal-voltage signal), because the additional equipment required operates at a low power level (mW to Watts), whereas other methods (such as resistor braking and capacitor switching) need a much higher power level (MW or MVar, respectively). Other advantages of the generator excitation control are:

- It has much smaller time constant than the mechanical system.
- An electrical control system is effectively a continuous acting system because of its small loop time constant and small sampling period. Therefore, it can give a smooth system response [10].

Effectiveness of damping produced by excitation control has been demonstrated both by simulation studies and by field tests.

Several kinds of supplementary signals such as speed or frequency deviation, and accelerating power have been used with this type of control.

Generator supplementary excitation controller commonly referred to as power system stabilizer (PSS) has been studied since the 1950s.

1.2.2 Damping Control in the Transmission Path

There are two common ways used for damping control in the transmission path:

1. High-Voltage Direct Current (HVDC) Transmission - This plays an important role in improving system stability [11, 12] since there is no requirement to maintain synchronism for HVDC. On the other hand, HVDC provides positive oscillation damping because an HVDC link can change its power flow, in accordance with AC system needs, much faster than any power plant.

The principal disadvantage of HVDC is the cost and complexity of the rectification-inversion equipment. Another disadvantage is that HVDC will generate harmonics in the AC system [10].

2. Flexible AC Transmission System (FACTS) - The FACTS controllers have the ability to manage the interrelated parameters that constrain power system, such as series impedance, shunt impedance, phase angle, etc [5, 6, 13, 14]. Some FACTS controllers are listed below [15]:

Static VAR Compensator (SVC) - uses thyristor valves to rapidly add or remove shunt-connected reactors and/or capacitors.

Thyristor Controlled Series Capacitor (TCSC) - can vary the impedance continuously to levels below and up to the transmission line's natural impedance.

Static synchronous compensator (STATCOM) - generates and/or absorbs reactive power and can be controlled by controlling the voltage.

Unified power flow controller (UPFC) - obtains a net phase and amplitude voltage change that confers control of both active power and reactive power.

Cost is the main drawback of FACTS controllers as well.

1.3 Types of Power System Stabilizers

The basic function of a PSS, supplying supplementary control through generator excitation system, is to extend the stability limits by modulating generator excitation to damp the oscillations of synchronous machine rotors relative to one another. These oscillations of concern typically occur in the frequency range of approximately 0.2Hz to 2.5 Hz, and insufficient damping of these oscillations may limit the ability to transmit power. To provide damping, the stabilizer must produce a component of electrical torque on the rotor that is in phase with speed variations. The implementation details differ, depending upon the stabilizer input signal and control strategy employed. However, for any input signal the transfer function of the stabilizer must compensate for the gain and phase characteristics of the excitation system, the generator, and the power system, which collectively determine the transfer function from the stabilizer output to the component of electrical torque that can be modulated via excitation control. This transfer function is strongly influenced by voltage regulator gain, generator power level, and AC system strength.

1.3.1 Conventional Power System Stabilizers

The first Conventional Power System Stabilizer (CPSS), proposed in the 1950s, was based on the use of a transfer function designed using classical control theory [16, 17, 18]. It is the most commonly used fixed parameter analog-type device. A supplementary stabilizing signal derived from speed deviation, power deviation or accelerating power, and a lead-lag compensating network to compensate for the phase difference from the excitation controller input to the damping torque output, is introduced to the excitation controller. By appropriately tuning the phase and gain characteristics of the compensation network, it is possible to make a system have the desired damping ability [19]. The CPSS is widely used in today's excitation controls and has proved effective in enhancing power system dynamic stability [20, 21].

However, CPSSs are designed for a particular operating condition around which a linearized transfer function model of the system is obtained and it has its inherent drawbacks. Usually the operating condition where control is needed most is chosen [17]. The high non-linearity, very wide operating conditions and stochastic properties of the actual power system present the following problems to the CPSS:

- How to choose a proper transfer function for the CPSS that gives satisfactory supplementary stabilizing signal covering all frequency ranges of interest?
- How to effectively tune the PSS parameters?
- How to automatically track the variation of the system operating conditions?

- How to consider the interaction between the various machines?

Extensive research has been carried out to solve the above problems. Different CPSS transfer functions associated with different systems have been proposed [16, 17]. Various tuning techniques have been introduced to effectively tune PSS parameters [22, 23]. Effective placement and mutual cooperation between the PSSs in multi-machine systems have also been presented [24, 25]. To solve the parameter-tracking problem, variable structure control theory was introduced to design the CPSS [26]. All this research has resulted in great progress in understanding the operation of the PSS and effectively applying PSS in power systems. However, it cannot change the basic fact - the CPSS is a fixed-parameter controller designed for a specific operating point, which generally cannot maintain the same quality of performance at other operating points [27]. For this reason adaptive control, control that adapts its behaviour to changing system characteristics has so much potential to improve power system performance. The idea has led to the research and development of adaptive power system stabilizers (APSSs). This dissertation is an attempt to explore the effectiveness of an APSS, acting through a FACTS device, to improve power system damping.

1.3.2 Adaptive Power System Stabilizers

Most of above-mentioned problems relating to the CPSS can be solved practically by using adaptive control theories [28]. All adaptive control techniques can be classified in two categories [29], Direct Adaptive Control and Indirect Adaptive Control:

- 1. Direct Adaptive Control** – The main objective of this type of control is to

adjust controller parameters, so that the output coordinate of the controlled system can agree with that of a reference model. It is named the model reference adaptive control as shown in Fig. 1.1.

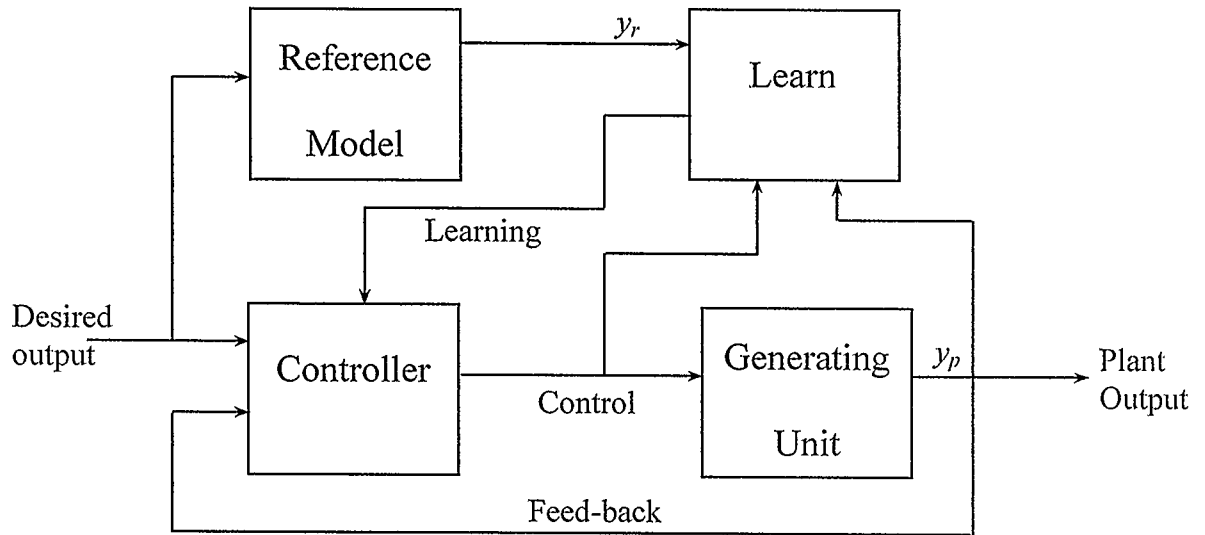


Fig. 1.1 Model reference adaptive control

The value of mismatch, Eqn. 1.1, between the model, y_r , and the controlled coordinate, y_p , of the system usually is used to perform parameter adjustment in the controller.

$$||y_r - y_p|| = \varepsilon \quad (1.1)$$

where ε is the mismatch error.

The derivation of an appropriate learning mechanism and the choice of a suitable reference model will determine the performance of this algorithm.

2. Indirect Adaptive Control - The objective of this type of adaptive control is to control the system so that its behaviour has the given properties. The controller can be

thought in terms of two loops. The first loop, called the outer loop, consists of the controlled process and an ordinary linear feedback controller. The parameters of the controller are adjusted by the second loop, or inner loop, which is composed of an on-line parameter identifier. This kind of adaptive control is often referred as the self-tuning adaptive control shown in Fig. 1.2

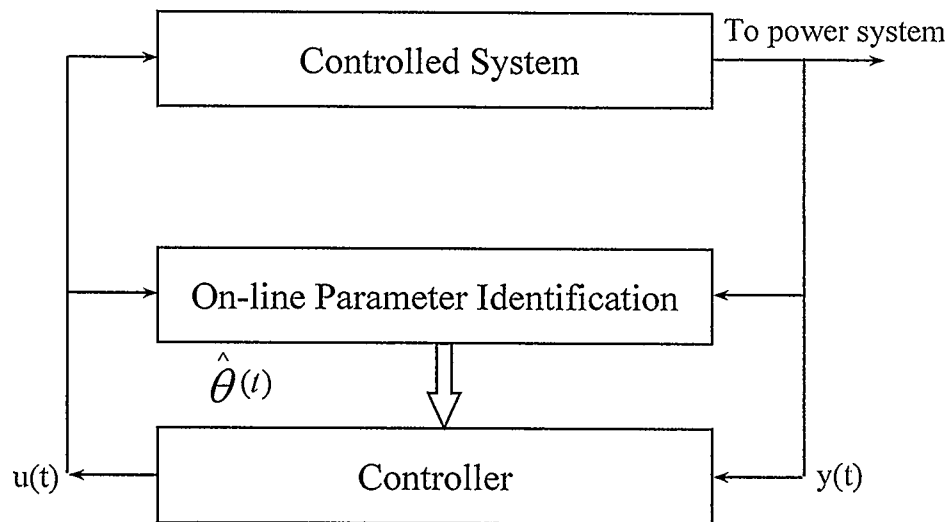


Fig. 1.2 Self-tuning adaptive control

1.3.2.1 On-line Parameter Identifier

On-line parameter identifier is the essence of the APSS that gives the PSS the ability to adapt. At each sampling instant, the input and output of the system are sampled, while a mathematical model is obtained by some on-line identification method to represent the dynamic behaviour of the system at that instant of time. For a time varying stochastic system, such as a power system, its dynamic behaviour varies from time to

time. With this on-line identifier, it is expected that the mathematical model obtained can track changes in the controlled system each sampling period. Obviously, the extent to which the identified model fits the dynamics of the actual system determines the failure or success of the APSS. For the above reason, the on-line identification methods have always been an important subject of research.

1.3.2.2 Control Strategy

Based on the identified model, the controller produces the control signal for the system. The control strategy is generally developed by assuming that the identified model is the true mathematical description of the system. However, since the power system is a high-order nonlinear stochastic continuous complex system, it is hard for the discrete identified model to precisely describe the dynamic behaviour of the power system. Consequently, it is desirable that the control strategy have good tolerance to the errors in the identified model.

The above discussion on identifier and controller highlights two main points:

Firstly, the on-line identifier should be improved to achieve an identified model that represents the controlled system as closely as possible. Secondly, the control strategy should have the ability to tolerate the identification errors. With these two parts working together, successful application of the APSS can be achieved.

In the power system, the identified model of the system can be a Non-Minimum-Phase (NMP) system, which restricts the application of some control strategies. Minimum Variance (MV) control strategy is one example [28, 41]. To overcome the

excessive control signal amplitude problem and the unstable feature of the NMP closed-loop system, a Generalized Minimum Variance (GMV) technique has been proposed and widely used [42, 43, 44]. Though it is simple, its closed-loop performance does not often meet the needs of the controller designer. For example, stability, which is an important issue in control design, is not taken into consideration in the GMV control.

Pole Assignment (PA) control strategy is also well known in adaptive control applications [45, 46]. It puts the emphasis on the closed-loop stability rather than the time domain responses. By choosing the closed-loop poles properly, the closed-loop system can be robust to some extent even if the identified model has some errors. However, selection of the proper closed-loop pole locations to meet the need of both the stability and time domain response requirements offers a hard task to the designer.

Pole Shifting (PS) control strategy is a modified version of the PA control strategy [24, 47, 48]. In this strategy, controller parameters are selected on the basis that the closed-loop poles are shifted from the identified open-loop poles in a stabilizing direction (radially inward away from the unit circle in the z -domain). The amount of shift is determined by one parameter, called the pole-shifting factor, which can be adjusted to achieve desired damping. This control strategy simplifies the PA strategy because only one parameter needs to be selected. Obviously, the way to select the pole-shifting factor determines the behaviour of the controller.

There are many other control strategies though not listed here individually. From past studies and experimental tests a fact that has been made quite clear is that the more

the number of controller parameters that need to be tuned manually, the more difficult it can be to apply in practice. A good controller not only produces satisfactory results, but it is also easy to use. Pole shifting control strategy exhibits such potential and thus is given the main attention in the dissertation.

1.4 Applications of the Static VAR Compensator

Static VAR compensators are shunt-connected VAR generators and/or absorbers whose output is varied so as to control specific parameters of the power system.

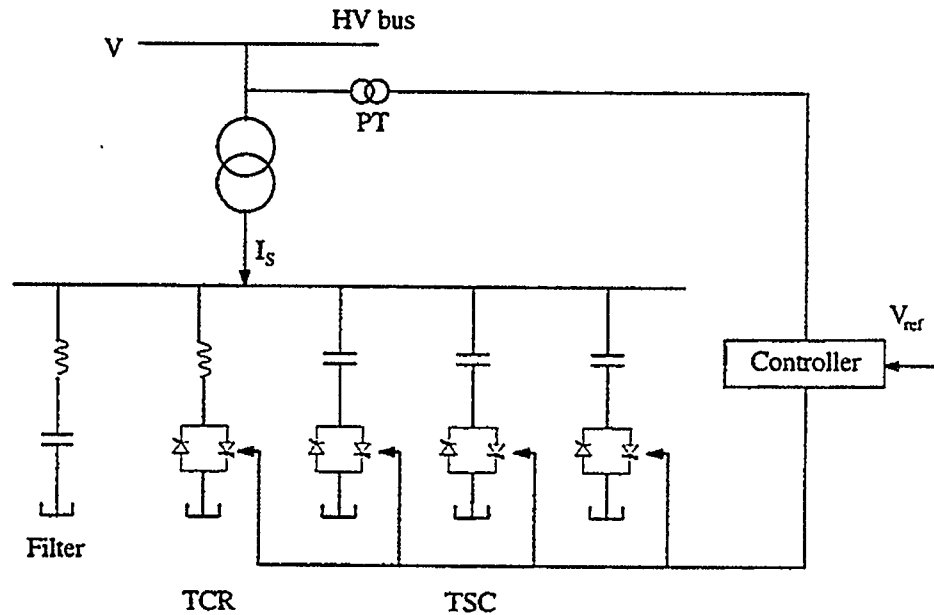


Fig. 1.3 A typical SVC structure

The term "static" is used to indicate that SVCs, unlike synchronous condensers, have no moving or rotating main components [49]. A typical structure of the SVC that consists of a thyristor-controlled reactor (TCR), a three-unit thyristor-switched capacitor (TSC) and a harmonic filter for filtering harmonics generated by TCR is shown in Fig. 1.3. The TCR and TSC are connected in such a manner that the bus voltage stays at or

close to a constant level depending on the control scheme used.

Since its first application in the late 1970s, the use of SVC in transmission system has been increasing steadily. By virtue of the ability to provide continuous and rapid control of reactive power and voltage, the SVC can enhance several aspects of transmission system performance including:

Control of temporary overvoltages.

Prevention of voltage collapse.

Enhancement of transient stability.

Increase in power transmission capability.

The capability of the power transmission is the essential reason to locate the SVC and most of FACTS devices in the middle of the transmission line. The late E. W. Kimbark pointed out that with shunt capacitor voltage support at the mid-point of the transmission line (which he proved to be the optimal location) it is possible to transmit twice the power of the uncompensated line and to extend the steady-state stability limit [94]. This conclusion can be extended to the FACTS devices.

Consider the simple two-machine power system shown in Fig. 1.4(a). in which ideal shunt controller is connected at the mid point of the transmission line and assuming that:

$$|V_s| = |V_r| = |V_m| = |V| \quad (1.2)$$

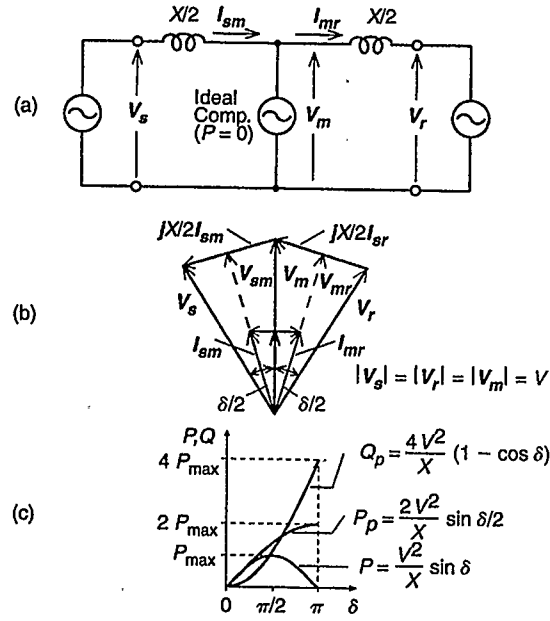


Fig. 1.4 (a) Two machine power system, (b) corresponding phasor diagram and (c) power transmission vs. angle characteristic

The midpoint in effect, segments the transmission line into two parts: the first segment with an impedance of $X/2$, carries power from the sending end to the midpoint and the second segment also with an impedance of $X/2$ carries power from the midpoint to the receiving end. The midpoint compensator exchanges only reactive power with the transmission line in this process. The real power is the same at each part of the line, if lossless system is assumed. The relationship between voltages and currents given is shown in Fig. 1.4(b). such that:

$$V_{sm} = V_{mr} = V \cos(\delta/4) \quad (1.3)$$

$$I_{sm} = I_{mr} = I = \frac{4V}{X} \sin(\delta/4) \quad (1.4)$$

then the transmitted real power is:

$$P = V_{sm} I_{sm} = V_{mr} I_{mr} = V_m I_{sm} \cos(\delta/4) = VI \cos(\delta/4) \quad (1.5)$$

$$P = 2V^2/X(\sin \delta/2) \quad (1.6)$$

$$Q = VI \sin(\delta/4) = 4V^2/X(1 - \cos(\delta/2)) \quad (1.7)$$

The relationship between real power P , reactive power Q and angle δ for the case of ideal shunt compensation is shown in Fig. 1.4(c). It can be observed that the midpoint shunt compensation can significantly increase the transmittable power (doubling its maximum value) at the expense of rapidly increasing reactive power demand on the midpoint and also on the end-generators.

It is also evident that for the single line system, the midpoint of the transmission line is the best location for the compensator and this is because the voltage along the uncompensated transmission line is the largest at the midpoint. Also, the compensation at midpoint breaks the line into two equal segments for each of which the maximum transmittable power is the same. For unequal segments, the transmittable power of the longer segment would clearly determine the overall transmission limit. The concept of transmission line segmentation can be expanded to the use of multiple compensators located at equal segments of the transmission line. The transmittable power would double with each doubling of the segments for the same overall length. Furthermore, with the increase of the number of segments, the voltage variation along the line would rapidly decrease approaching the ideal case of constant voltage profile.

Fast response feature of the SVC also provides other opportunities to improve power system performance. By introducing a supplementary controller superimposed over its voltage control loop, as shown in Fig. 1.5, the SVC can be used to increase the

system damping for undesirable inter-area oscillations. The careful design of the supplementary damping controller (SDC) is again necessary for the SVC to achieve effective damping.

The current industry practice for the design and analysis of controls consists of conventional linear analysis tools coupled with detailed nonlinear simulation of the designed control settings. While this procedure is practical and has served the purpose in the past, it lacks a systematic approach and does not guarantee robustness. Furthermore, it provides little insight and understanding of the parameters that have the most effect on robustness. Consequently, this approach offers little guidance for control design.

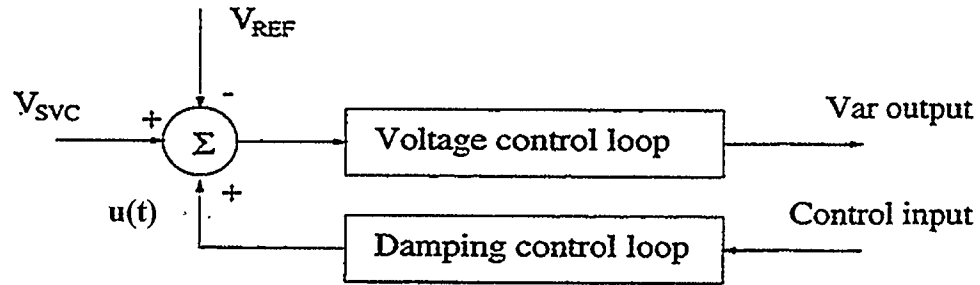


Fig. 1.5 Supplementary damping scheme for SVC

The past few decades have witnessed a significant development in control systems mainly directed at understanding robustness properties of control systems. The purpose of those efforts is to obtain closed-loop systems that are stable and meet performance objectives despite the presence of plant uncertainties and parameter variations, i.e., provide robust stability and performance. The tools that have been developed for robustness analysis and synthesis have the potential to positively impact the way power system controls are analyzed and designed.

1.5 Dissertation Objective

The primary objective of this thesis is to develop and design an Adaptive Power System Stabilizer (APSS) based on the pole-shift linear feedback control algorithm for application on an SVC located at the middle of a transmission line.

In order to achieve this goal, the following topics are studied and discussed in the dissertation. To be more specific, the objective of the dissertation includes the following four aspects:

- 1- A third-order discrete auto-regressive moving average (ARMA) model is used to describe the power system that includes the SVC device installed on the bus in the middle of the system.
- 2- The Recursive Least Square (RLS) and the Kaman Filter (KF) system identification techniques are applied to the system model to track the dynamic behaviour of the power system and update the controller to develop and design an Adaptive Power System Stabilizer (SAPSS).
- 3- Variable Pole-Shifting control uses the on-line, updated regression coefficients to calculate the close-loop poles of the system. The unstable poles are shifted inside the unit circle, in the z -plane, and the control is calculated so as to attain the desired performance.
- 4- Behaviour of the proposed adaptive controller applied to the SVC device under a single machine power system environment and multi-machine power

system environment is studied carefully with different operating conditions in order to investigate and verify the designed controller.

1.6 Dissertation Contributions

The most three important contributions of this dissertation are summarized below:

- 1- Performance of the RLS and the KF identification techniques used to track the behaviour of the system and estimate its parameters in order to update a linear pole shifting feedback controller to perform the proposed adaptive SVC controller, is compared. Although the two identification algorithms are found to have the same accuracy, the RLS-estimator requires less convergence time than the KF-estimator.
- 2- In order to verify the results of the controller and demonstrate that the adaptive SVC controller provides more effective damping than a conventional power system stabilizer, the proposed adaptive SVC controller is simulated on two systems:
 - A single machine connected to an infinite bus system with an SVC at the middle bus.
 - A multi-machine power system with five-machines and an SVC. This system exhibits local and inter-area modes of oscillations.
- 3- The combination of a self-tuning adaptive controller located at the generating unit and an adaptive controller applied to the SVC connected to the middle

bus of a single machine infinite bus system are employed to enhance power system stability.

1.7 Dissertation Organizations

This thesis is composed of 6 Chapters. In addition to the introductory Chapter, the dissertation has five chapters as outlined below:

A third order ARMA-model used to perform the power system simulation model and system identification with the feasibility of RLS and KF identification techniques are discussed in Chapter 2.

In Chapter 3, basic concepts of the pole-shifting control strategy are introduced first. Then, a self-optimizing method to determine the pole-shifting factor for the pole-shifting control strategy is described [50, 51]. Details of the proposed method and its advantages compared with the existing methods are also given.

The simulation results of the proposed SAPSS are carried out on a single-machine power system in Chapter 4. Results are provided for a variety of disturbances and operating conditions.

Chapter 5 presents the simulation studies of the proposed SAPSS on a multi-machine power system environment.

Finally, conclusions and comments on future research are given in Chapter 6.

Chapter 2

SYSTEM IDENTIFICATION AND MODEL

2.1 Introduction

System identification is a very important research area. It is widely used in many disciplines, such as broadcast theory, geology, hydrology, communication, control, etc. The earliest used identification method is the least squares method.

The history of the least squares method began in 1795 when the inventor of this approach, Karl Friedrich Gauss, formulated its concept and used it for astronomic computations [52]. Since that time the method of least squares has been applied to many problems. Its properties have been analyzed and numerical procedures have been proposed in order to obtain better results with a reasonable number of arithmetic operations [53, 54].

The problem of identification can be formulated as the evaluation of a system model representing the essential aspects of an existing dynamic system and representing the knowledge of that system in a useful form [55]. Although system identification includes both the parameters and model identification, only the parameters identification is discussed here for use in self-tuning control.

Identification algorithms may be off-line or on-line. The off-line or non real-time algorithms are generally more accurate than on-line or real-time algorithms since they may reprocess data several times. In self-tuning control applications, on-line algorithms are used since all data must be processed in real time. Another important feature of on-

line identification is that it only stresses the very important features of the system, i.e., the final model should represent only the essential properties of the dynamic system and present these properties in a suitable form. It means that it is not expected to obtain an exact mathematical description of the physical system and that it is preferred to have a model fitted for the specific application. The general requirement for a system identification algorithm can be summarized as follows [56]:

- It should be mathematically tractable.
- It should be easy to implement.
- It should be generally applicable.
- It should yield an optimal identification.
- It should yield an acceptable speed of convergence.

It is generally recognized that an appropriate mathematical model, a proper test input signal and a pre-selected identification scheme are the three main aspects in system identification [40] and all these aspects are closely connected.

2.2 System and Model

The system is a physical object that generates the observed output signal $y(t)$ at time t . Many systems also have a measurable input signal $u_i(t)$. For a stochastic system, any one or both of the system input and system output may be corrupted with noise as shown in Fig. 2.1. In this thesis only the single input and single output system is

discussed.

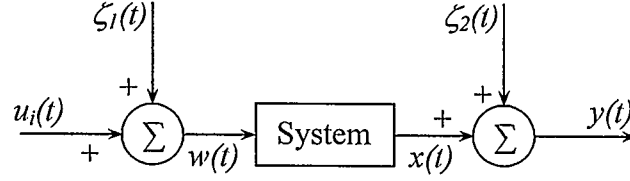


Fig. 2.1 Block diagram of a stochastic system

Knowledge of the system properties is generally called a model. It can be given by any one of several forms, graphical models and/or mathematical models. In order to solve a power system problem, a model of the system is always necessary. For some purposes, the model does not need to be very sophisticated. Mathematical models, however, are necessary when complex design problems are treated. Although all practical problems are non-linear, good regulation can generally be achieved by using a linear model or transfer function given by local linearization around the current operating point. The mathematical models considered in this thesis are of the discrete form (difference equation) due to the digital computer application. There are two main forms of discrete mathematical models frequently used in adaptive control design; Auto-Regressive Moving-Average (ARMA) model and Auto-Regressive Moving-Average Exogenous (ARMAX) model. The following explanation is a brief clarification of these two models.

2.2.1 ARMA Model

The model takes the form:

$$A(z^{-1})y(t) = z^{-l}B(z^{-1})u_i(t) + \zeta(t) \quad (2.1)$$

where

$y(t)$ is the system output signal

$u_i(t)$ is the system input signal

$\zeta(t)$ is a white noise signal

l is the system delay

$A(z^{-l})$ and $B(z^{-l})$, polynomials in the delay operator z^{-l} , are defined as:

$$A(z^{-l}) = 1 + a_1 z^{-l} + a_2 z^{-2l} + \dots + a_{n_a} z^{-n_a l} \quad (2.2)$$

$$B(z^{-l}) = b_1 z^{-l} + b_2 z^{-2l} + \dots + b_{n_b} z^{-n_b l} \quad (2.3)$$

and

$$n_a \geq n_b + 1$$

The graphic representation of this model is shown in Fig. 2.2.

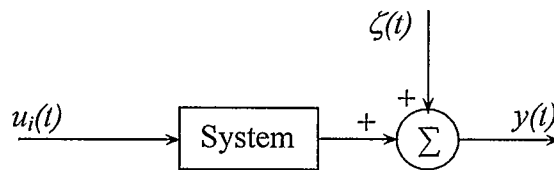


Fig. 2.2 Block diagram of an ARMA model

2.2.2 ARMAX Model

The generalized stochastic system is shown in Fig. 2.1, in which $u_i(t)$ and $y(t)$ are observed as input and output sequences signals, respectively. These signals are corrupted with white noise $\zeta_1(t)$ and $\zeta_2(t)$, respectively. Then the system's input and output can be expressed as:

$$w(t) = u(t) + \zeta_1(t) \quad (2.4)$$

$$x(t) = y(t) - \zeta_2(t) \quad (2.5)$$

Suppose that the system model satisfies the following linear difference equation

$$A(z^{-1})x(t) = z^{-l}B(z^{-1})w(t) \quad (2.6)$$

where $A(z^{-1})$ and $B(z^{-1})$ are defined in Eqns. 2.2 and 2.3, respectively.

Substituting Eqns. 2.4 and 2.5 in Eqn.2.6 and re-arranging gives

$$A(z^{-1})y(t) = z^{-l}B(z^{-1})w(t) + C(z^{-1})\zeta(t) \quad (2.7)$$

where $\zeta(t)$ is a white noise signal and $C(z^{-1})$, a polynomial in z^{-1} , is

$$C(z^{-1}) = 1 + c_1 z^{-1} + c_2 z^{-2} + \dots + c_{n_c} z^{-n_c} \quad (2.8)$$

where

$c_i, (i = 1, \dots, n_c)$ is a function of $a_j, (j = 1, \dots, n_a), b_k, (k = 1, \dots, n_b)$, and $l = 0$.

The model presented by Eqn. 2.7 is called Auto Regressive Moving Average

Exogenous (ARMAX) model.

Other models, such as state space models, are generally used for the multi-input multi-output systems.

The selection of the mathematical model mainly depends on the information known about the system. Mainly, mathematical models decide the identification algorithm that should be used. For this reason, a reasonably simplified mathematical model is sometimes necessary for practical use.

2.2.3 Test Signal

It is commonly recognized that in order to identify a system, the system has to be excited, otherwise no information can be obtained from the system [57]. It is also well known that significant simplification in the computations can be achieved by choosing an input signal of a special type, e.g., impulse function, step function, white noise, sinusoidal signal, pseudo-random binary noise.

From the point of view of the proposed application it seems highly desirable to use techniques that do not need strict limitations on the input. But this is almost impossible in practice. The natural question then becomes; if the input signal can be chosen, how should it be done? It has been proved that the persistent excitation is a sufficient condition to generate consistent estimation for least squares and maximum likelihood identification techniques [58].

Two kinds of input signals, the Pseudo-Random Binary Signal (PRBS) and the

white noise, are commonly used in the self-tuning control. It is verified that these signals can satisfy the persistent excitation conditions as demonstrated in [59].

Many identification procedures require that the input signal be independent of the disturbances acting on the process. If this condition is not fulfilled it might still be possible to identify the parameters, but there is no guarantee that the estimated parameters are the correct parameters. Each specific case must, however, be analyzed in detail.

Apart from persistent excitation condition, many applications require that the output be kept within specified limits during the experiment. In these cases, there is sometimes a constraint on the magnitude of disturbance to the system produced by the input signal. This can usually be satisfied by a constraint on the energy of the input signal. Design of the input signal can significantly influence the accuracy of parameter estimation when the observations are corrupted by noise. There have been many studies concerned with the selection of the best input signal [57].

2.3 Identification Scheme

Different identification quality criteria will result in different identification schemes. As mentioned before, selection of the identification algorithm mainly depends on the mathematical model used, and usually it will affect the next step, i.e. control computation. Generally speaking, more sophisticated identification methods will require more computation time. For this reason, when designing an on-line identifier, a compromise must be made between the quality of identification and a reasonable

computation time among all possible identification methods.

Several methods of recursive identification are used to identify parameters [53, 60, 61, 62, 63], for example:

Recursive Least Squares (RLS) identification

Recursive Extended Least Squares (RELS) identification

Recursive Maximum Likelihood (RML) Method

The Bayesian Estimation

The Square Root Filtering

Kalman Filter as Parameter Estimator

The above list is not exhaustive. In this dissertation, both of the recursive least squares identification technique and the Kalman Filter are used to track the parameters of the system.

2.3.1 Recursive Least Squares Identifier

Among different identification algorithms for on-line identification, Recursive Least Squares (RLS) methods have the advantages of simple calculation and good convergence properties. The Recursive Least Squares identification method has the following general features [64]:

- It is a central part of adaptive systems where the action is based on the most recent model.
- Its requirement on primary memory is relatively modest, since not all data are stored.
- It can be easily incorporated into real-time algorithms that are aimed at tracking time-varying parameters.

The parameter estimates are computed recursively in time. Most adaptive systems are based on recursive identification. As shown in Fig. 2.3, the estimated model of the system is available all the time and is used to determine the parameters of the controller. In this way, the controller will be dependent on the previous behaviour of the system. If an appropriate principle is implemented to design the controller, then the controller should adapt to the changing characteristics of the system.

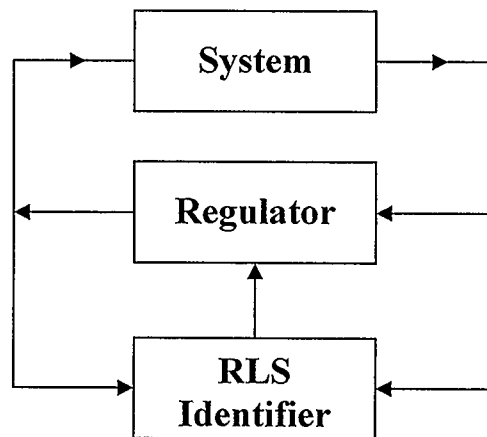


Fig. 2.3 A general scheme for RLS

Theoretically, RLS has been developed for use with time-invariant systems. Mainly, the RLS identification technique is used to treat linear regression models such as

Eqn.2.1.

This algorithm always gives the optimal unbiased parameter estimation for an LR model. For this reason, the model of Eqn. 2.1 is sometimes referred to as the least squares model [60].

Equation 2.1 can be rewritten as:

$$y(t) = \theta^T(t)\varphi(t) + \zeta(t) \quad (2.9)$$

where $\theta(t)$ is the parameter vector

$$\theta(t) = [a_1 \quad a_2 \quad \dots \quad a_{n_a} \quad b_1 \quad b_2 \quad \dots \quad b_{n_b}]^T \quad (2.10)$$

and $\varphi(t)$ is the measurement vector

$$\varphi(t) = [-y(t-1) \quad \dots \quad -y(t-n_a) \quad u_i(t-l-1) \quad \dots \quad u_i(t-l-n_b)]^T \quad (2.11)$$

$\hat{y}(t)$, the predicted value of the system output, $y(t)$, is given by

$$\hat{y}(t) = \hat{\theta}^T(t)\varphi(t) \quad (2.12)$$

and the prediction error is defined as

$$e(t) = y(t) - \hat{y}(t) \quad (2.13)$$

The RLS identification algorithm can be described by the following recursive set of equations [53]:

$$\mathbf{K}(t) = \frac{\mathbf{P}(t-1)\boldsymbol{\varphi}(t)}{\lambda(t) + \boldsymbol{\varphi}^T(t)\mathbf{P}(t-1)\boldsymbol{\varphi}(t)} \quad (2.14)$$

$$\mathbf{P}(t) = \frac{\mathbf{P}(t-1) - \mathbf{K}(t)\boldsymbol{\varphi}^T(t)\mathbf{P}(t-1)}{\lambda(t)} \quad (2.15)$$

$$\hat{\boldsymbol{\theta}}(t) = \hat{\boldsymbol{\theta}}(t-1) + \mathbf{K}(t).e(t) \quad (2.16)$$

where \mathbf{P} is the covariance matrix, \mathbf{K} is the gain vector and λ is the forgetting factor. The criterion of the RLS identification is to determine the most likely value, $\hat{\boldsymbol{\theta}}(t)$, of $\boldsymbol{\theta}(t)$ that will minimize the sum of the squares of the prediction errors:

$$\mathbf{J} = \frac{1}{N} \sum_{i=1}^N \lambda^{N-i} e^2(t) \quad (2.17)$$

where $\lambda < 1$

and N is the simulation sampling rate

The purpose of using the forgetting factor is to overcome problems in the practical use of the RLS. Theoretically, RLS is developed for a time-invariant system. As can be seen from Eqn. 2.16, the estimated parameter set, $\hat{\boldsymbol{\theta}}(t)$, is the weighted sum of the last estimation and the new prediction error, $e(t)$. For a time-invariant system, as time increases, $\hat{\boldsymbol{\theta}}(t)$ tends to converge to the true value. The prediction error, the gain vector, $\mathbf{K}(t)$, and the covariance matrix, $\mathbf{P}(t)$, also tend to be zero. This means the new measurement will not make any contribution to the parameter estimation. This does not cause any serious problems for time-invariant systems because the estimated parameters

have reached the true value. However, the main aim of using the self-tuning control is for time-varying systems. When the RLS is used for this type of system, the following problem will arise [65].

As $K(t)$, used for updating the adaptive parameters, decreases in time, the system model error is less taken into account and that will affect the tracking of the parameters. One way to overcome this problem is to periodically reset the $P(t)$ matrix to either a fixed initial value or a value depending on the latest matrix. However, in this case, all the past information stored in the covariance matrix will be lost [64].

The RLS algorithm with a forgetting factor works best in real time because the gain matrix does not need to be reset. In addition, past errors are gradually forgotten and more attention is paid to recent information [37-65]. The smaller the value of λ , the quicker the information in the previous data will be forgotten [64].

A fixed forgetting factor has been used successfully in practical applications. Many results show that if the system is always properly excited, this algorithm will give good parameter tracking property for the time varying system. However, there exist systems which are not always properly excited. These situations can happen in power systems. In this kind of a system, the injected test signal cannot be too large in order to guarantee normal operation. The random system perturbations then become the main excitation sources. During the normal operating conditions, the system is poorly excited, whereas under the large disturbances, the system is over excited. Use of the fixed forgetting factor RLS identification is likely to face the following problems:

It is difficult to select an appropriate value of λ that always gives the best estimates of the parameters.

A small value of λ gives good parameter tracking for the case of large disturbances but also makes the parameters more sensitive to the system noise.

A large value of λ gives smooth parameter estimation that is useful for the steady state operation but results in a slow parameter tracking speed.

The so called \mathbf{P} matrix ‘blow-up’ some times happens. This problem occurs when the fixed forgetting factor λ is used and the slowly time-varying system operates in steady state for a long time. In this case, as the prediction error tends to zero, Eqn. 2.15 can be approximately represented by [66]

$$\mathbf{P}(t) = \frac{\mathbf{P}(t-1)}{\lambda} \quad (2.18)$$

This can be obtained by putting $\varphi(t) = 0$ in Eqn. 2.15. This means that the $\mathbf{P}(t)$ matrix will exponentially tend to infinity. When $\mathbf{P}(t)$ becomes very large, any disturbance from the system will result in an inappropriate parameter estimation and then a very undesirable control action. This sometimes makes the system unstable.

Many methods have been proposed to solve this problem, such as [57, 67, 68, 69]:

Putting a limit on the $\mathbf{P}(t)$ matrix, keeping the trace of $\mathbf{P}(t)$ matrix constant in each iteration, updating the parameters and the covariance matrix $\mathbf{P}(t)$ when $\mathbf{P}(t)$ or $\varphi(t)$ are sufficiently small, discounting data only when new information is detected, and switching

λ between two values associated with two typical operating conditions (steady state and a certain reasonable disturbance).

For a near deterministic system, the estimation error will tell something about the state of the estimator at each step. If the error is small, a reasonable strategy will be to retain as much old information as possible by choosing a forgetting factor close to unity. If, on the other hand, the error is large, the estimation sensitivity should be increased by choosing a smaller value for the forgetting factor. This will shorten the effective memory length of the estimation until the parameters are readjusted and the error becomes small.

The forgetting factor can be updated on line using the following formula [57]:

$$\lambda(t) = 1 - \frac{[1 + \phi^T(t-1).K(t)]e^2(t)}{\Sigma} \quad (2.19)$$

where Σ a pre-selected constant, can take any value between 0 and 1 ($0 \leq \Sigma \leq 1$).

Equation 2.19 can be explained as follows:

If the system is running at steady state, $e(t)$ will be very small or equal to zero. This forces λ near or equal to one which prevents the $P(t)$ matrix from blowing up. Upon the occurrence of a disturbance, λ decreases as $e(t)$ increases. This improves the parameter tracking property of the identifier.

Combining Eqn. 2.19 with Eqns. 2.14 through 2.16 results in the variable forgetting factor recursive least squares identification. This identification ensures that the estimation is always based on the same amount of information.

2.3.2 Kalman Filter as Parameter Estimator

Within the significant toolbox of mathematical tools that can be used for stochastic estimation from noisy sensor measurements, one of the most well-known and often used tools is what is known as Kalman Filter (KF). The Kalman Filter is named after Rudolph E. Kalman who in 1960 published his famous paper describing a recursive solution to the discrete- data linear filtering problem. Since that time, due in large part to advances in digital computing; the Kalman Filter has been the subject of extensive research and application, particularly in the area of autonomous and assisted navigation.

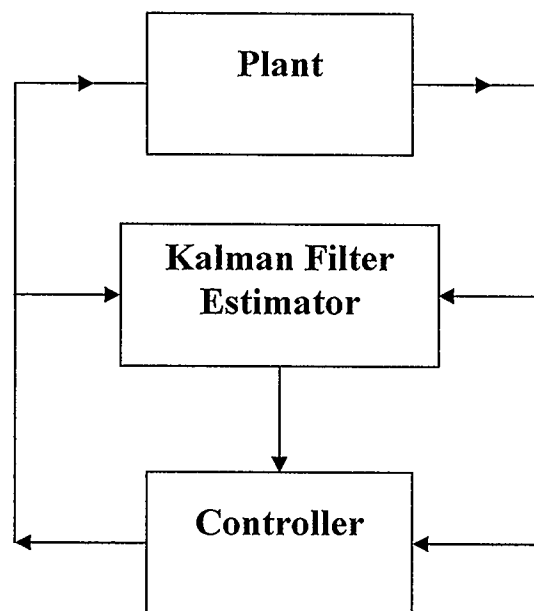


Fig. 2.4 A general scheme for kalman filter

The Kalman Filter is simply a recursive data processing algorithm in the form of a set of mathematical equations that provides an efficient computational means to estimate the behaviour of a process, in a way that minimizes the mean of the squared error between the actual output and the estimated value [90].

Most of the self-tuning systems are based on recursive identification. The parameters, using the Kalman Filter, are also computed recursively in time. As shown in Fig. 2.4, the model of the on-line estimation system should at all time be determining the system parameters and updating the controller, which always depends on the previous values of the estimator.

In addition to good convergence properties and simple calculations, the Kalman filter as parameter estimator has the following important properties [91]:

- The Kalman Filter is a linear, discrete- time finite dimensional system.
- The Kalman Filter gain matrix and the error covariance are independent of the measurement process. Thus they can be pre-computed before the estimator is run. This will substantially reduce the amount of the on-line computation, thereby making it more suitable for real- time work.
- The error covariance matrix is unconditional associated with Kalman Filter.

As it has been mentioned before, the linear regression model of Eqn.2.1 is sometime referred to as the least square model. KF as parameters estimator algorithm is one of the optimal unbiased parameters estimators for the linear regression model [92, 93].

Assuming that the parameters are constant, the linear regression difference equation shown in Eqn. 2.1 can be rewritten simply as:

$$y(t) = \theta^T(t)\phi(t) + \zeta(t) \quad (2.20)$$

where the parameter vector $\theta(t)$ is given by

$$\theta(t) = [a_1 \quad a_2 \quad \dots \quad a_{n_a} \quad b_1 \quad b_2 \quad \dots \quad b_{n_b}]^T \quad (2.21)$$

and the measurement vector $\varphi(t)$ is given by

$$\varphi(t) = [-y(t-1) \quad \dots \quad -y(t-n_a) \quad u_i(t-l-1) \quad \dots \quad u_i(t-l-n_b)]^T \quad (2.22)$$

Then the predicted value $\hat{y}(t)$ for the system output $y(t)$ is given by

$$\hat{y}(t) = \hat{\theta}^T(t) \varphi(t) \quad (2.23)$$

The prediction error is defined as

$$e(t) = y(t) - \hat{y}(t) \quad (2.24)$$

The Recursive Kalman filter identification algorithm can be described by the following recursive set of equations [64]:

$$K(t) = \frac{P(t-1)\varphi(t)}{1 + \varphi^T(t)P(t-1)\varphi(t)} \quad (2.25)$$

$$P(t) = P(t-1) - \frac{P(t-1)\varphi(t)\varphi^T(t)P(t-1)}{[1 + \varphi^T(t)P(t-1)\varphi(t)]} + R \quad (2.26)$$

$$\hat{\theta}(t) = \theta(t-1) + K(t)e(t) \quad (2.27)$$

where K is the gain vector, P is the covariance matrix and R is the error covariance

matrix. The parameter vector $\hat{\theta}(t)$ is based on minimizing the sum of the squares of the prediction errors.

The matrix \mathbf{R} is a constant diagonal matrix with the diagonal elements chosen by a trade-off between alertness and ability to track time variations of the parameters on the one hand and good convergence properties and small variance of the estimates for time –invariant systems on the other.

Chapter 3

VARIABLE POLE-SHIFT LINEAR FEEDBACK CONTROL

3.1 Introduction

A general discussion on the use of the recursive least squares algorithm and kalman filter is given in Chapter 2. RLS and KF algorithmic methods are conceptually understood and have a large body of theoretical results relating to stability and performance.

In this Chapter an adaptive Pole Shifting (PS) control algorithm which combines the advantages of Minimum Variance (MV) and Pole Assignment (PA) control algorithms [70, 71] is described.

3.2 Pole-Shifting Control

3.2.1 Background

The MV control algorithms [30, 41, 42] optimize the system output response directly. They are fast, but are not easily susceptible to stability analysis of the closed-loop system. The PA control algorithm [45] places emphasis on the stability of the closed-loop system rather than the system output response directly. In the PA algorithm, the closed-loop poles are assigned to specific locations within the unit circle in the z -domain corresponding to the desired response and stability margin of the controlled system. With proper choice of the closed-loop poles it can yield satisfactory dynamic response. The algorithm can always assure closed-loop stability as long as the identified

parameters converge to their true values and there are no control limits. However, it is not easy to choose suitable closed-loop pole locations, especially if the system operates over a wide range. Also, there is a conflict between the response speed and the stability of the closed-loop system.

Both MV and PA algorithms have their unique strengths and weaknesses as shown by studies performed on the relationship between these algorithms [72]. Additional control algorithms have been developed in recent years to obtain more effective and flexible adaptive controllers. Among them, the Pole-Shifting control algorithm described in [34, 57, 73] has a special characteristic that makes it suitable for APSS application.

The variable pole-shift control algorithm self-searches the optimal value of the pole shift factor according to the minimization of the performance index. The performance index employs the MV criterion. Also, during optimization, the closed-loop poles are restricted to be within the unit circle in the z -domain for the stability of the closed-loop system. Since no coefficients need to be tuned manually in this control algorithm, manual parameter tuning (which is a drawback of the CPSS) is minimized.

3.2.2 Concepts

Consider the system, shown in Fig. 3.1, is modeled by

$$A(z^{-1})y(t) = B(z^{-1})u_i(t) + \zeta(t) \quad (3.1)$$

where $y(t)$, $u_i(t)$, $\zeta(t)$ are system output, system input and white noise respectively. $A(z^{-1})$,

$B(z^{-1})$ take the form

$$A(z^{-1}) = 1 + a_1 z^{-1} + \dots + a_i z^{-i} + \dots + a_{n_a} z^{-n_a} \quad (3.2)$$

$$B(z^{-1}) = b_1 z^{-1} + \dots + b_i z^{-i} + \dots + b_{n_b} z^{-n_b} \quad (3.3)$$

where $n_a \geq n_b + 1$.

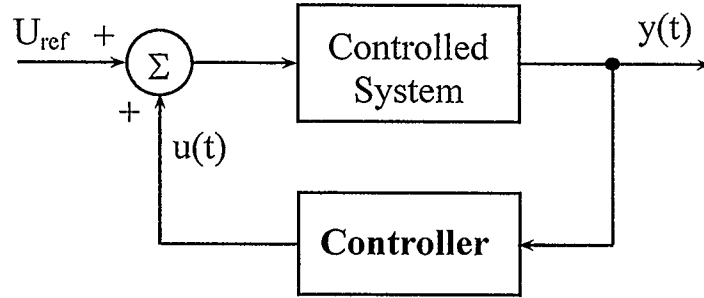


Fig. 3.1 A general system model with a feed-back control

Suppose the system parameters a_i, b_i are fixed or obtained on-line using a system parameter identifier (RLS algorithm). The computation of the control signal $u(t)$ using the PS algorithm [73, 74] is briefly described below.

Assume the feedback loop has the form

$$\frac{u(t)}{y(t)} = -\frac{G(z^{-1})}{F(z^{-1})} \quad (3.4)$$

where

$$F(z^{-1}) = 1 + f_1 z^{-1} + \dots + f_i z^{-i} + \dots + f_{n_f} z^{-n_f} \quad (3.5)$$

$$G(z^{-1}) = g_0 + g_1 z^{-1} + \dots + g_i z^{-i} + \dots + g_{n_g} z^{-n_g} \quad (3.6)$$

and

$$n_f = n_b - 1, \quad n_g = n_a - 1 \quad (3.7)$$

From Eqns. 3.1 and 3.4 the closed-loop characteristics polynomial $T(z^{-1})$ can be derived as

$$T(z^{-1}) = A(z^{-1})F(z^{-1}) + B(z^{-1})G(z^{-1}) \quad (3.8)$$

Unlike the PA control algorithm in which $T(z^{-1})$ is prescribed, the PS control algorithm makes $T(z^{-1})$ take the form of $A(z^{-1})$ but the pole locations are shifted by a factor α , i.e.

$$A(z^{-1})F(z^{-1}) + B(z^{-1})G(z^{-1}) = A(\alpha z^{-1}) \quad (3.9)$$

Expanding both sides of Eqn. 3.9 and comparing the coefficients gives

$$\begin{bmatrix} 1 & 0 & \cdot & 0 & b_1 & 0 & \cdot & 0 \\ a_1 & 1 & \cdot & 0 & b_2 & b_1 & \cdot & 0 \\ \cdot & a_1 & \cdot & \cdot & \cdot & b_2 & \cdot & \cdot \\ a_{n_a} & \cdot & \cdot & 1 & b_{n_b} & \cdot & \cdot & b_1 \\ 0 & a_{n_a} & \cdot & a_1 & 0 & b_{n_b} & \cdot & b_2 \\ \cdot & 0 & \cdot & \cdot & \cdot & 0 & \cdot & \cdot \\ \cdot & \cdot & \cdot & \cdot & \cdot & \cdot & \cdot & \cdot \\ 0 & 0 & \cdot & a_{n_a} & 0 & 0 & \cdot & b_{n_b} \end{bmatrix} \begin{bmatrix} f_1 \\ \cdot \\ \cdot \\ f_{n_f} \\ g_o \\ \cdot \\ \cdot \\ g_{n_g} \end{bmatrix} = \begin{bmatrix} a_1(\alpha - 1) \\ a_2(\alpha^2 - 1) \\ \cdot \\ \cdot \\ a_{n_a}(\alpha^{n_a} - 1) \\ 0 \\ \cdot \\ 0 \end{bmatrix} \quad (3.10)$$

or in a matrix form

$$M.w(\alpha) = L(\alpha) \quad (3.11)$$

Since the system parameters a_i and b_i are determined by the on-line identifier, the control parameters f_i and g_i can be solved in order to calculate the control signal $u(i)$ if the

shifting factor α is fixed. In this case, the pole shifting control algorithm falls into a special case of the pole assignment control algorithm [73]. It is evident that the rule determining the pole shifting factor is very important. It is desirable, for optimum performance, to modify the pole shifting factor on-line according to the operating conditions of the controlled system.

It is clear from Eqn. 3.10 that the control signal $u(t)$ at time t is a function of the pole shifting factor α at that time. Expanding Eqn 3.4 and using Eqn 3.11, the control signal as a function in t and α can be written as:

$$u(t, \alpha) = \mathbf{X}_c^T(t) \mathbf{w}(\alpha_t) = \mathbf{X}_c^T(t) \mathbf{M}^{-1} \mathbf{L}(\alpha) \quad (3.12)$$

where

$$\mathbf{X}_c(t) = \begin{bmatrix} -u(t-1) & \dots & -u(t-n_f) & -y(t) & -y(t-1) & \dots & -y(t-n_g) \end{bmatrix}^T \quad (3.13)$$

is the measurement variable vector.

3.2.3 Taylor Series Expansion of Control Signal $u(t)$ in Terms of α

The control signal $u(t, \alpha)$, can be expressed in a Taylor series in terms of the factor α as

$$u(t, \alpha) = u(t, \alpha_o) + \sum_{i=1}^{\infty} \frac{1}{i!} \left[\frac{\partial^i u(t, \alpha)}{\partial \alpha^i} \right]_{\alpha=\alpha_o} (\alpha - \alpha_o)^i \quad (3.14)$$

The i^{th} order differential of $u(t, \alpha)$ with respect to α becomes

$$\left[\frac{\partial^i \mathbf{u}(t, \alpha)}{\partial \alpha^i} \right]_{\alpha=\alpha_o} = \mathbf{X}_c^T(t) \mathbf{M}^{-1} \left[\frac{\partial^i \mathbf{L}(\alpha)}{\partial \alpha^i} \right]_{\alpha=\alpha_o} = \mathbf{X}_c^T(t) \mathbf{M}^{-1} \mathbf{L}^{(i)}(\alpha_o) \quad (3.15)$$

From Eqn. 3.11 and for simplicity, let $\alpha_o = 0$, $\mathbf{L}^{(i)}(0)$ becomes

$$\mathbf{L}^{(i)}(0) = [0 \quad \dots \quad 0 \quad i!a_i \quad 0 \quad \dots \quad 0]^T \quad i \leq n_a \quad (3.16)$$

where $i!a_i$ is the i th term, and

$$\mathbf{L}^{(i)}(0) = [0 \quad \dots \quad 0]^T \quad i > n_a \quad (3.17)$$

Defining the i th order sensitivity constant s_i as

$$s_i = \frac{1}{i!} \left[\frac{\partial^i \mathbf{u}(t, \alpha)}{\partial \alpha^i} \right]_{\alpha=\alpha_o} = \frac{1}{i!} \mathbf{X}_c^T(t) \mathbf{M}^{-1} \mathbf{L}^{(i)}(0) = p_i a_i \quad i \leq n_a \quad (3.18)$$

where p_i is the i th term of the row vector $\mathbf{X}_c^T(t) \mathbf{M}^{-1}$, Eqn. 3.14 can be written in a simpler form as

$$\mathbf{u}(t, \alpha) = \mathbf{u}(t, 0) + \sum_{i=1}^{n_a} s_i \alpha^i \quad (3.19)$$

3.2.4 System Output Prediction, $\hat{\mathbf{y}}(t+1)$

At time t , the predicted system output $\hat{\mathbf{y}}(t+1)$ at time $(t+1)$ can be obtained if it is assumed that the control $\mathbf{u}(t, \alpha)$ at time t is known.

The explicit form of $\hat{\mathbf{y}}(t+1)$ is:

$$\hat{y}(t+1) = \mathbf{X}_i^T(t)\boldsymbol{\beta} + b_1 u(t, \alpha) + b_1 U_{ref} \quad (3.20)$$

where

$$\mathbf{X}_i(t) = [-u_i(t-1) \quad \dots \quad -u_i(t-n_f) \quad -y(t) \quad -y(t-1) \quad \dots \quad -y(t-n_g)]^T \quad (3.21)$$

is the measurement vector, $u_i(t-j)$ is the system input, $y(t-j)$ is the system output,

$$\boldsymbol{\beta} = [-b_2 \quad -b_3 \quad \dots \quad -b_{n_b} \quad a_1 \quad a_2 \quad \dots \quad a_{n_a}]^T \quad (3.22)$$

is an identified parameter vector, and U_{ref} is the steady state system input reference.

Substituting Eqn. 3.19 into Eqn. 3.20, system output predicted value $\hat{y}(t+1)$ can be expressed as a function of α as given below:

$$\hat{y}(t+1) = \mathbf{X}_i^T(t)\boldsymbol{\beta} + b_1 [u(t,0) + \sum_{i=1}^{n_a} s_i \alpha^i + U_{ref}] \quad (3.23)$$

3.2.5 Performance Index and Constraints

Taking the idea of MV control, the performance index is expressed as

$$\min_{\alpha} J(t+1, \alpha) = E \left[\hat{y}(t+1) - y_{ref}(t+1) \right]^2 \quad (3.24)$$

where $y_{ref}(t+1)$ is the system output reference.

Substituting Eqn. 3.23 into Eqn. 3.24 and considering the independence between the white noise and other variables, the minimization of $J(t+1, \alpha)$ in terms of $u(t, \alpha)$ is:

$$\min_{\alpha} \hat{J}(t+1, \alpha) = \left[X_i^T(t) \beta + b_1 \left\{ u(t, 0) + \sum_{i=1}^{n_a} s_i \alpha^i + U_{ref} \right\} - y_{ref}(t+1) \right]^2 \quad (3.25)$$

or equivalent to the minimization problem of a quadratic function:

$$\min_{u(t, \alpha)} \hat{J}(t+1, u(t, \alpha)) = \left[X_i^T(t) \beta + b_1 U_{ref} + b_1 u(t, \alpha) - y_{ref}(t+1) \right]^2 \quad (3.26)$$

In order to get a reasonable controller, when minimizing $\hat{J}(t+1, \alpha)$ with respect to α , it should be noted that α would be subject to some constraints. First of all, the controller should keep the closed-loop system stable. It implies that all roots of the closed loop polynomial $T(z^{-1}) = A(\alpha z^{-1})$ should be within the unit circle in the z -domain. Supposing λ_c is the absolute value of the largest characteristic root of $A(z^{-1})$, then $\alpha \lambda_c$ is the absolute value of the largest characteristic root of $T(z^{-1})$. To assure the stability of the closed-loop system α ought to satisfy the following inequality (stability constraint):

$$-\frac{1}{\lambda_c} < \alpha < \frac{1}{\lambda_c} \quad (3.27)$$

Another constraint that should be taken into account in controller design is the control limit. If u_{min} and u_{max} are the lower and upper control limits respectively, the optimal solution of α should also satisfy the following inequality (control constraint):

$$u_{min} \leq u(t, 0) + \sum_{i=1}^{n_a} s_i \alpha^i \leq u_{max} \quad (3.28)$$

Equations 3.23, 3.24 and 3.25 constitute the optimization of PS-control algorithm.

The optimization idea is schematically illustrated in Fig. 3.2.

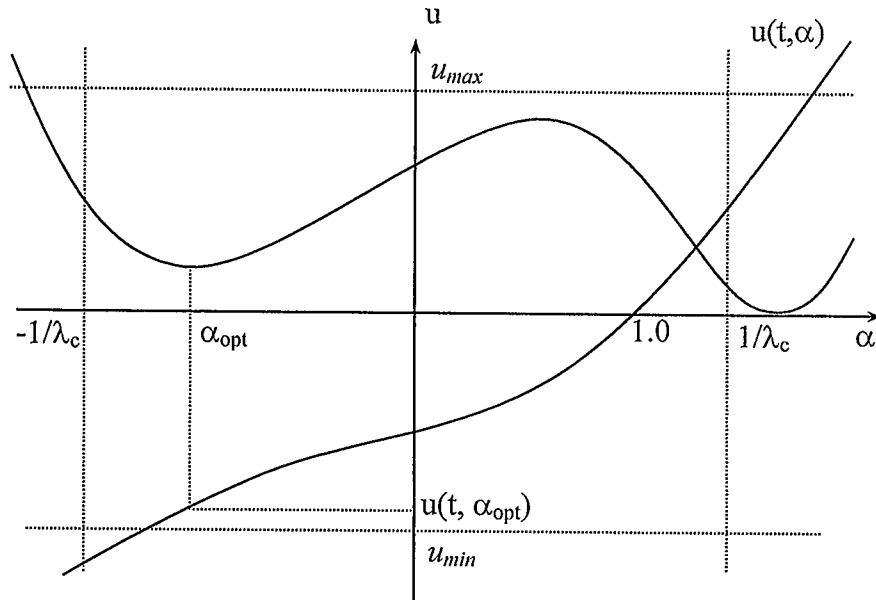


Fig. 3.2 Schematic diagram of optimization

3.2.6 Properties of the PS Algorithm

References [34, 73, 74] describe the properties of the PS-control algorithm in detail. Some of the key issues are highlighted here.

3.2.6.1 Pole-Shift Factor, α

Figure 3.3 shows the pole-shifting process. The essence of the PS-control algorithm lies in the fact that the nearer the closed-loop poles are moved to the center of the unit circle in the z -plan, the more stable is the system. The pole shift factor α achieves this goal, i.e., in closed-loop the open-loop poles are shifted radially towards the center of

the unit circle without violating the control limits.

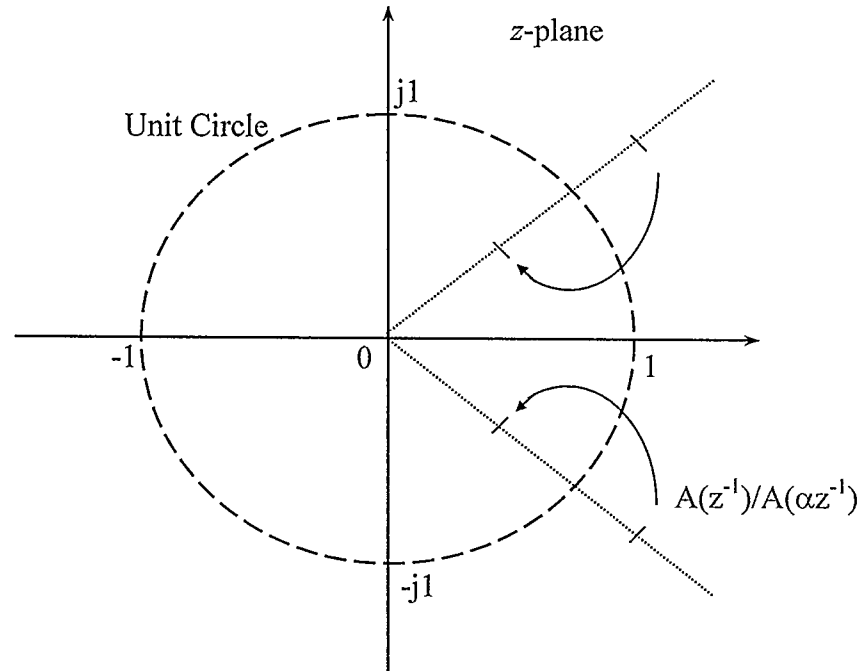


Fig. 3.3 Pole-shifting process

In the PS algorithm, the varying range of the pole-shifting factor α is $(-1/\lambda_c, 1/\lambda_c)$.

For different conditions, it acts in the following way:

- The open-loop system is unstable ($\lambda_c > 1$). When this control strategy is applied, it first behaves as a PA controller, places the largest closed-loop poles within the unit circle to assure closed-loop stability and then optimizes its performance.
- The open-loop system is stable ($\lambda_c < 1$). The range of $(-1/\lambda_c, 1/\lambda_c)$ is larger than $(0, 1)$. It thus provides a more feasible area for performance optimization. Theoretically, it will result in a better performance.

3.2.6.2 Optimization Function

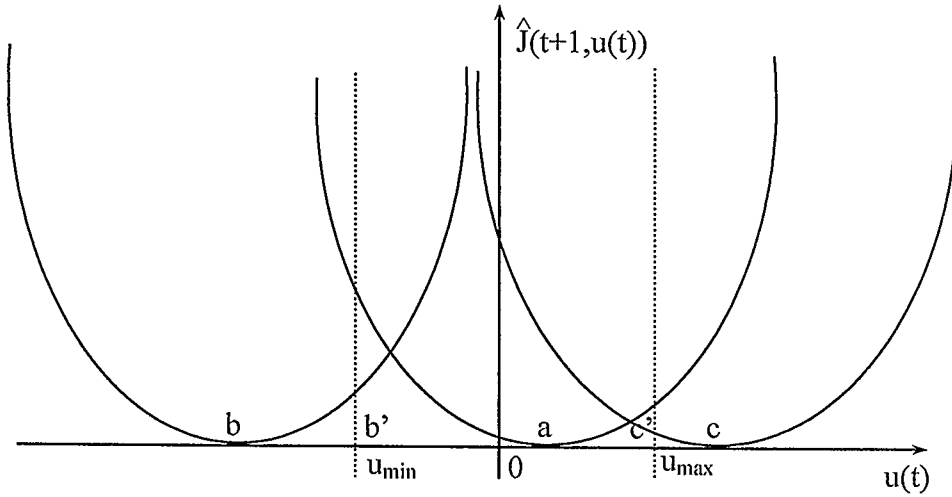


Fig. 3.4 Illustration of performance index

The performance index, i.e., $\hat{J}[t+1, u(t, \alpha)]$, Eqn. 3.26 is a quadratic function of the control $u(t, \alpha)$. There are only three possible locations for the control obtained by optimizing $\hat{J}[t+1, u(t, \alpha)]$ with only the stability constraint, for instance, points a , b , c shown in Fig. 3.4. When the control constraint is considered, the control at point a is within the control limits and thus can be applied to the controlled system directly. But the controls at points b and c are outside the control limits and cannot be achieved by the controller. It is also evident from Fig. 3.4 that the controls at points $b'(u_{min})$ and $c'(u_{max})$ are the optimal substitutions for the controls at points b and c respectively.

A set of control versus pole-shifting factor curves at different sampling times is shown in Fig. 3.5. All control curves pass the α -axis at the point of $\alpha = 1.0$ where the control is zero, which indicates the fact of no pole shifting and thus no control signal. Consider that the open-loop system is stable ($1/\lambda_c > 1.0$) and no optimal value of the pole

shifting factor α_{opt} is obtained by optimizing $\hat{J}[t+1, u(t, \alpha)]$ with the stability constraint only (obviously $-1/\lambda_c < \alpha_{opt} < 1.0$ or $1.0 < \alpha_{opt} < 1/\lambda_c$). If the control $u(t, \alpha_{opt})$ is outside the limits $[u(t, \alpha_{opt}) < u_{min} < 0$ or $0 < u_{max} < u(t, \alpha_{opt})]$, when the control limit (u_{min} or u_{max}) is applied to the system there must be a pole-shifting factor α_{limit} corresponding to the control. From Eqn. 3.19 the control $u(t, \alpha)$ is a continuous, single-valued function in terms of the pole-shifting factor α . With the mean-value theorem of continuous functions, α_{limit} must satisfy

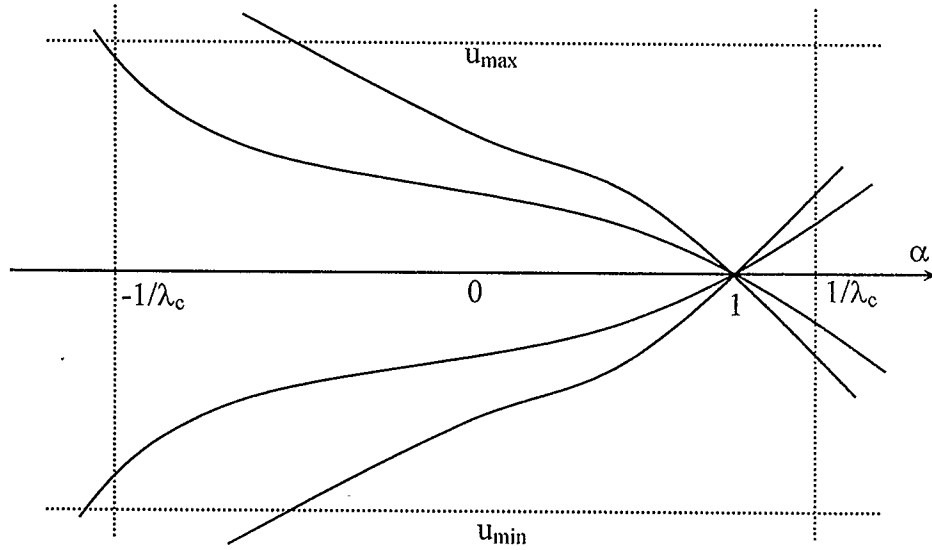


Fig. 3.5 Illustration of control signal

$$-\frac{1}{\lambda_c} < \alpha_{opt} < \alpha_{limit} < 1.0 \text{ or } 1.0 < \alpha_{limit} < \alpha_{opt} < \frac{1}{\lambda_c} \quad (3.29)$$

which indicates that α_{limit} is within the range $(-1/\lambda_c, 1/\lambda_c)$ and thus assures the closed-loop stability of the controlled system. The explanation is the same for the case of unstable open-loop system except that there needs to be a basic control effort to move the unstable

poles into the unit circle in the z -domain and the control limits must be larger than this basic control effort.

The above strategy simplifies the optimization scheme and reduces the optimization time. It indicates that if the control signal has to reach its limit, the best control signal for this situation is the control limit itself and more importantly the closed-loop system will not lose its stability under this condition.

Chapter 4

APPLICATION OF SAPSS IN A SINGLE-MACHINE INFINITE-BUS SYSTEM

4.1 Introduction

Power systems are non-linear systems and operate over a wide range. They are subject to random load changes that can be considered as a white noise disturbance. It is desired to develop a stabilizer that has the ability to adjust its own parameters on-line according to the environment it works in to yield satisfactory control performance. For a successful use of an adaptive stabilizer in power systems, the flexibility of the controller is a major advantage as it determines its applicability to different conditions. It is also desirable that dependence on the outside interference in its execution be kept to the minimum. The larger the number of controller coefficients that need to be tuned manually, the more difficult it is to apply to practical situations.

In this chapter, the proposed SVC adaptive power system stabilizer (SAPSS) employing a self-optimizing pole-shifting control strategy and its application to a Single-Machine Infinite-Bus power system is described. Based on an identified model of the system, the control is computed by an algorithm that shifts the closed loop poles of the system to some optimal locations inside the unit circle in the z -domain. The amount of the shift is determined by a pole-shifting factor calculated on line to minimize a given performance criterion. If the system parameters are identified accurately, there will be no need for any coefficients to be tuned manually.

System's parameters identification is very important for the successful application

of the adaptive controller. Fast parameter tracking ability is preferred especially for time-varying systems. In this dissertation, a comparative study of the RLS-Identifier with a variable forgetting factor and the KF as parameters estimator is used to show the performance of each identifier to track the system parameters. A comparison is made between them in order to employ the most suitable identification technique to track the system parameters and update a controller using a self-optimizing pole-shifting control strategy to damp the oscillations.

The traditional PSS is also used to design a SVC conventional power system stabilizer (SCPSS) to control the output of the SVC. A comparison of the damping effectiveness of the proposed SAPSS and the SCPSS is made for different operating conditions.

4.2 Self-Tuning Control

Self-tuning concepts have received much attention in recent years. Based on the certainty equivalence principle, the set of system parameters is identified as shown in Fig. 4.1 and the control is calculated using a pre-selected strategy [77].

Different identification techniques can be used for system parameter identification. For simplicity, the recursive least squares (RLS) identification technique is commonly used in an identification routine. To improve the parameter identification, the old data is discounted by a forgetting factor. For small variations in operating point its value should be almost unity but for large excursions, as during transients, it should be less than one. For improved tracking of system operating conditions, the identification

routine used in this study incorporates a varying forgetting factor.

The kalman filter identification technique can also be considered an optimal solution to solve the problem of determining the optimal estimate for parameters vector when the measurement vector is given [64]. Kalman filter as parameters estimator minimizes the expected value of the squared estimation error.

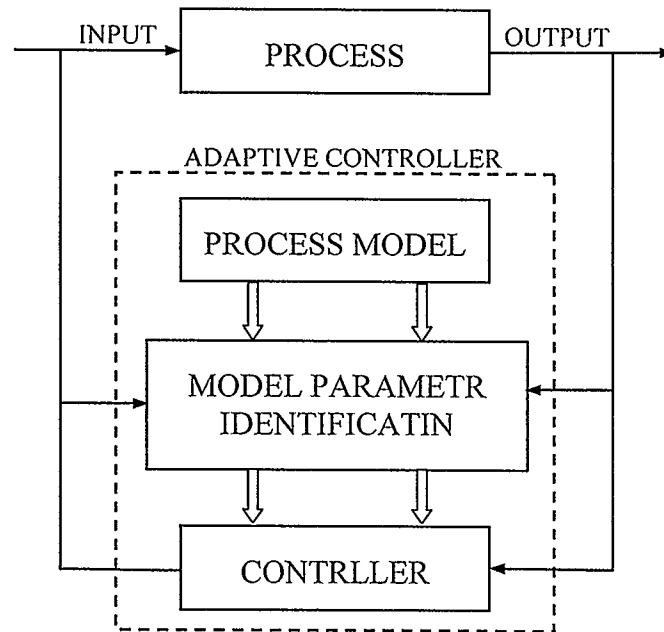


Fig. 4.1 Block diagram of a self-tuning adaptive controller

A self-tuning controller based on pole-zero assignment is very simple, and produces a smooth control action. Pole-shifting control simplifies the calculation algorithm. Instead of considering both the poles and the zeros of the system, pole-shifting control considers only the poles of the system and allows the zeros to be configured according to design algorithm. This simplification is very significant for on-line implementation [78].

In the pole-shifting control strategy, the closed-loop poles of the system are shifted radially towards the center of the unit circle in the z -domain by a factor less than one. Selection of a suitable value for the pole-shifting factor α , has been a problem because of its dependence on the operating condition. Under dynamic conditions, pole-shifting factor can be close to zero, i.e., the poles can be shifted very close to the center. However, under transient conditions this factor can not be taken so small because of the practical limits on the control. Therefore, the value of this factor is chosen such that it achieves the best compromise between small and large system disturbances [79].

The full procedure is carried out during each sampling interval such that various steps of the complete algorithm can be written as [10]:

- (i) Sample plant input and output signals.
- (ii) Update system parameter estimates in a model of the plant using a recursive algorithm. Employ latest input and output signals in addition to a certain number of previous sampled values of the input and output signals.
- (iii) Obtain a set of new controller values based on the updated plant-model synthesis.
- (iv) Calculate and apply the new control input based on the new controller values.
- (v) Prepare for the next recursion.
- (vi) Wait for the next sampling clock pulse before cycling to the first step.

4.3 System Configuration and Model

To study the performance of the self-tuning regulator as a supplementary controller to the SVC, this study has been performed on a single machine connected to a constant voltage bus through a long ac transmission line, with SVC at the middle of the line as shown in Fig. 4.2. The machine is equipped with IEEE type 1 excitation system. Static VAR compensator is modeled by a susceptance in the same manner as for power flow calculation, but varying within limits depending on the control provided by the voltage regulator of the SVC.

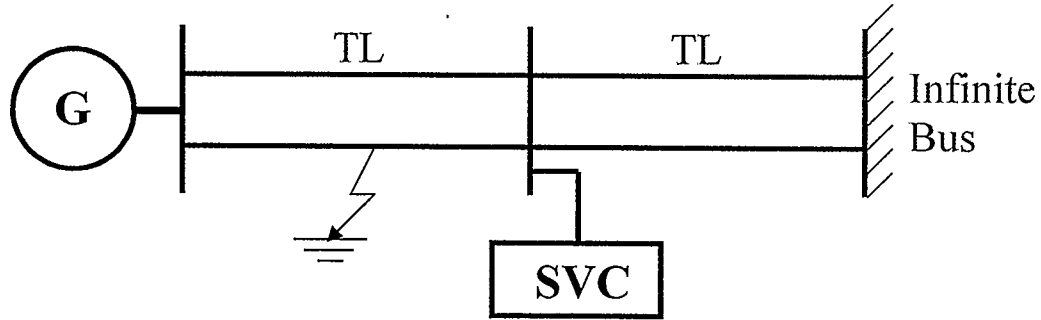


Fig. 4.2. System model

A supplementary adaptive stabilizer is connected to the summing junction of the voltage regulator of the SVC, with transient signals derived from the system. The variable susceptance B_{svc} is used to update the admittance matrix. The voltage of the controlled bus is measured and compared with its reference value, which is assumed to be its value at time zero minus. The voltage error is amplified and used to change the susceptance of a reactor unit at the controlling bus [79].

Parameters of the generator, governor, exciter, AVR, transmission line and SVC,

equations and all operating conditions of the system are given in Appendix A.

Simulation of the system model including the SVC is done using Matlab Simulink toolbox. The system model is identified as a third order discrete model of the form:

$$A(z^{-1})y(t) = B(z^{-1})u(t) + \zeta(t) \quad (4.1)$$

where $A(z^{-1})$ and $B(z^{-1})$ are polynomials in the backward shift operator z^{-1} and are defined as

$$A(z^{-1}) = 1 + a_1 z^{-1} + a_2 z^{-2} + a_3 z^{-3} \quad (4.2)$$

$$B(z^{-1}) = b_1 z^{-1} + b_2 z^{-2} + b_3 z^{-3} \quad (4.3)$$

and the variables $y(t)$, $u(t)$ and $\zeta(t)$ are the system output, system input and white noise, respectively.

The continual re-estimation of the plant model parameters, a_i and b_i , is called recursive parameter estimation such that, at the commencement of each sampling interval, the estimations obtained during the previous recursion are made available and form a startup point ready to be updated.

The SVC with firing control system is represented, for simplicity, by a first order model, characterized by a gain and a time constant as shown in Fig. 4.3. The dynamic equations representing SVC action for variation in the SVC susceptance are given by [79]:

$$B_{svc} = (K_{svc} / T_{svc}) \cdot (V_{svc(ref)} - V_{svc} + V_{aux}) - (1 / T_{svc}) \cdot \Delta B_{svc} \quad (4.4)$$

$$\Delta B_{svc} = B_{svc} - B_{svc(ref)} \quad (4.5)$$

$$V_{aux} = u(t) \quad (4.6)$$

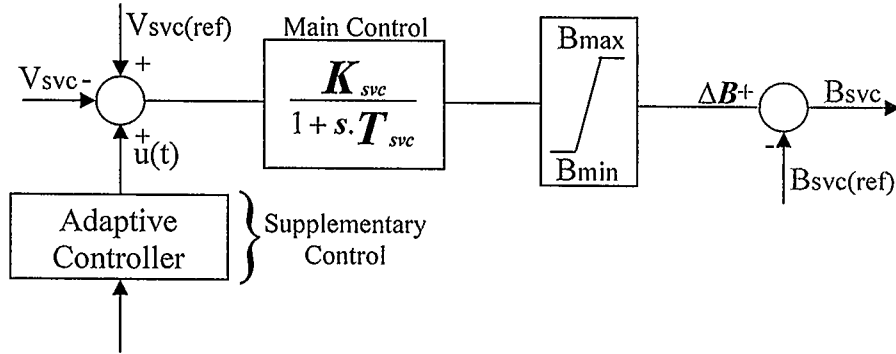


Fig. 4.3 Block diagram of SVC with adaptive control

The discretization interval used for the computations is 1 ms. The mathematical model and parameters of the generating unit, AVR, governor, transmission line, SVC and operating conditions are given in Appendix A.

4.4 System Identification

Control is computed based on the identified model parameters. Thus, to compute the control appropriate to the operating conditions, system parameters have to be estimated on-line. Correctness of the identification determines the preciseness of the identified model that tries to reflect the system. For a time-varying system, good tracking ability of the identification method is very desirable.

Several methods of identification can be used to obtain an estimate for the model parameters. In this work, two commonly techniques, RLS-Identifier and KF-Identifier, are used to achieve the continuous tracking of the system behaviour.

Rewrite Eqn. 4.1 in the following form suitable for identification:

$$y(t) = \theta^T(t)\varphi(t) + \zeta(t) \quad (4.7)$$

$$\theta(t) = [a_1 \quad a_2 \quad a_3 \quad b_1 \quad b_2 \quad b_3]^T \quad (4.8)$$

$$\varphi(t) = [-y(t-1) \quad -y(t-2) \quad -y(t-3) \quad u(t-1) \quad u(t-2) \quad u(t-3)]^T \quad (4.9)$$

where $\theta(t)$ is the parameter vector and $\varphi(t)$ is the measurement vector.

The system parameter vector $\theta(t)$ is calculated by using one of the recursive methods described in Chapter 2.

Simulation studies of the identified system using the two identification techniques are given in the following sections.

4.4.1 On-line Identification Using RLS Algorithm

In this study, the RLS-Identifier is applied to the plant to track the parameters and the output of the system. For a sampling rate of 20 Hz, the response of the RLS-Identifier is compared to the actual system output for various disturbances under different operation conditions.

Figures 4.4 through 4.7 show typical curves for the identification output signal tracking the output of the system, the convergence of the identified A and B parameters and forgetting factor variation when the generator with only a CPSS applied to the governor, shown in Fig. 4.2 operating at power of 0.7p.u. 0.9 power factor lag, undergoes a three phase to ground short circuit applied at the middle of one transmission line

between the generator and the SVC bus at time 0.5s and cleared 100ms later by disconnection of the faulted line. The line is successfully reclosed after 6.5s. It can be seen that the RLS identifier can not only track the dynamic response of the system, but it can also track the transient response of the system very well.

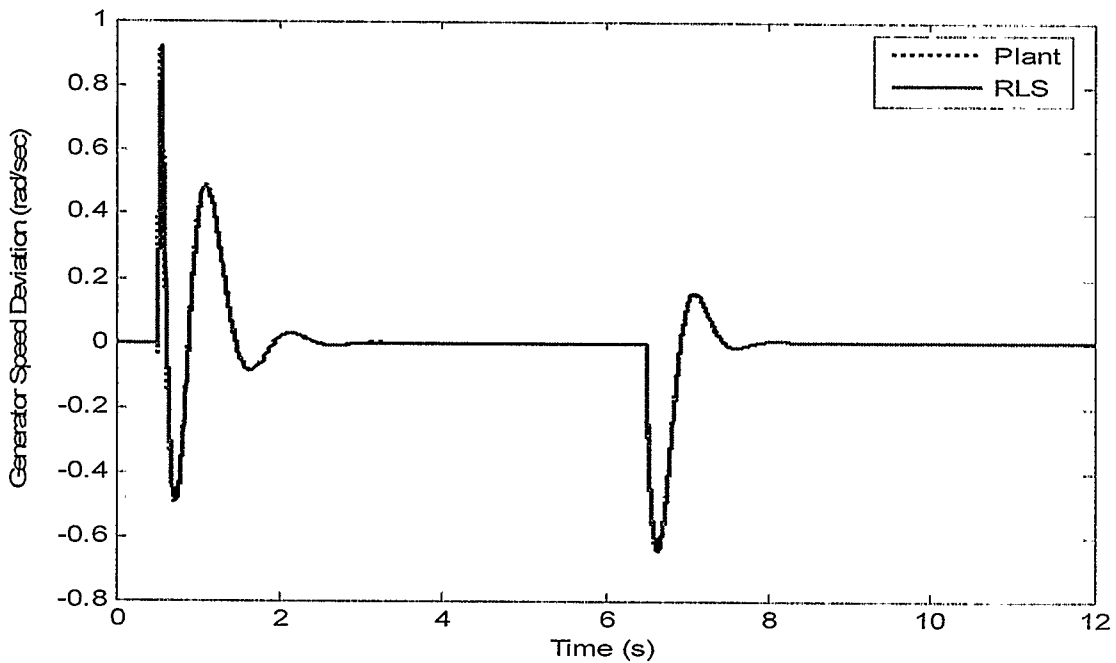


Fig. 4.4 Generator angular speed deviation and RLS output

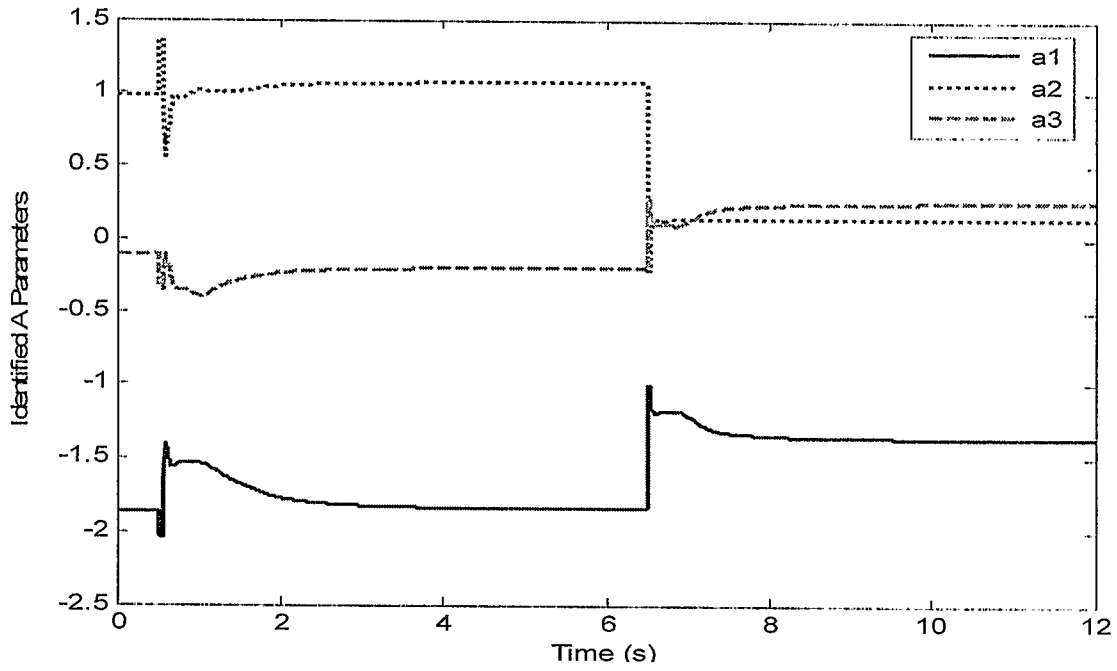


Fig. 4.5 Variation of A parameters on-line

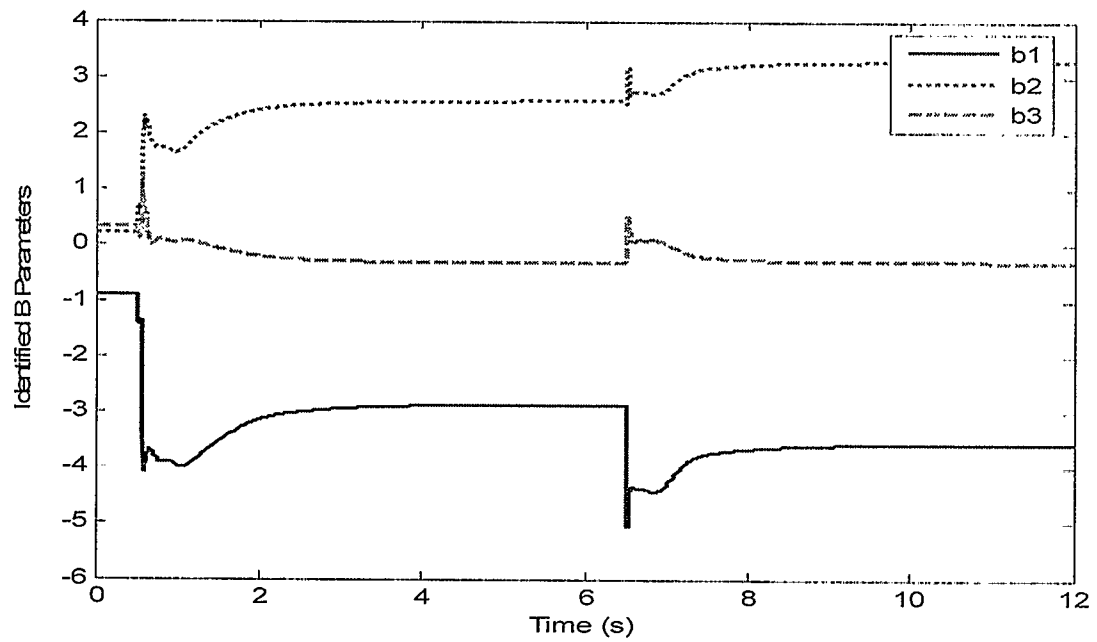


Fig. 4.6 Variation of B parameters on-line

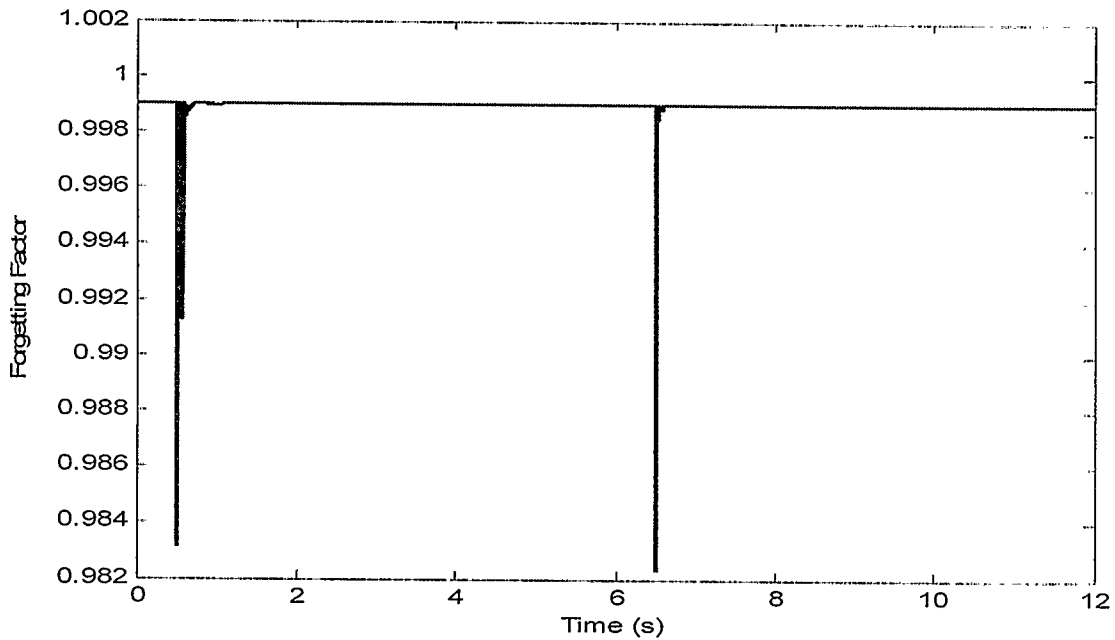


Fig. 4.7 Forgetting factor variation

4.4.2 On-line Identification Using KF Algorithm

In this sub-section, the KF identification technique is applied to the model of the system shown in Fig. 4.2 as parameters estimator, and then tested for the same system operating initial conditions and the same types of disturbances as used with the tests of the RLS identifier. The output of the estimator is compared to the output of the system.

Figures 4.8 through 4.10 show typical curves for the identification output signal tracking the output of the system and the convergence of the identified A and B parameters when system model shown in Fig. 4.2 undergoes a three phase to ground short circuit applied at the middle of one transmission line between the generator and the SVC bus at time 0.5s and cleared 100ms later by disconnection of the faulted line. The line is

successfully reclosed after 6.5s. The results show perfect tracking is accomplished using the KF-Identifier.

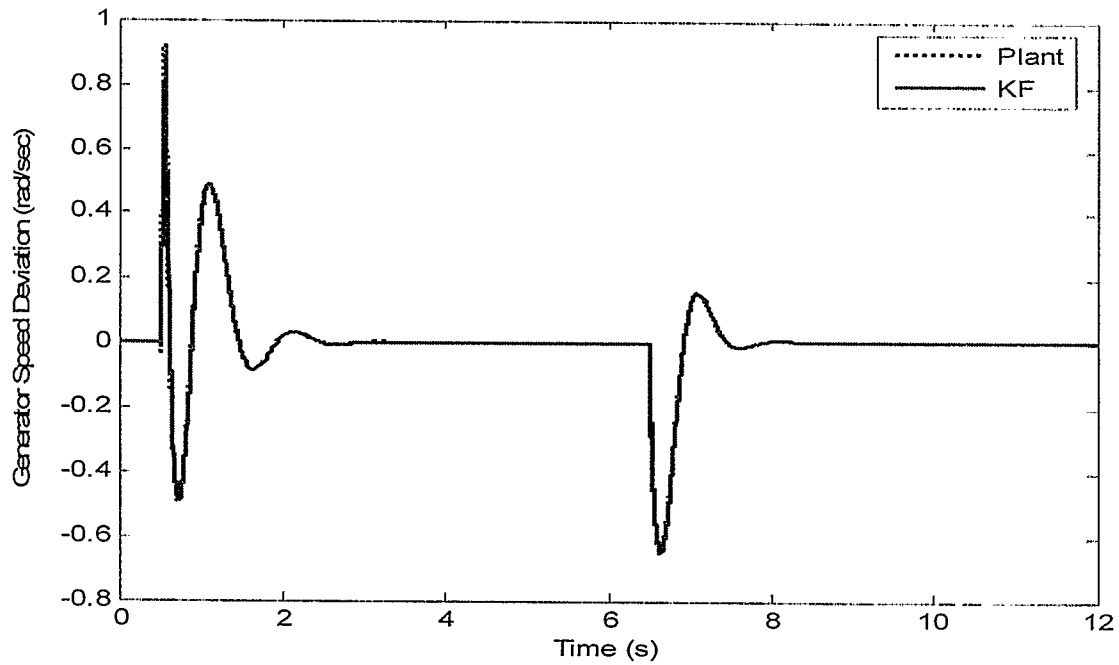


Fig. 4.8 Generator angular speed deviation and KF output

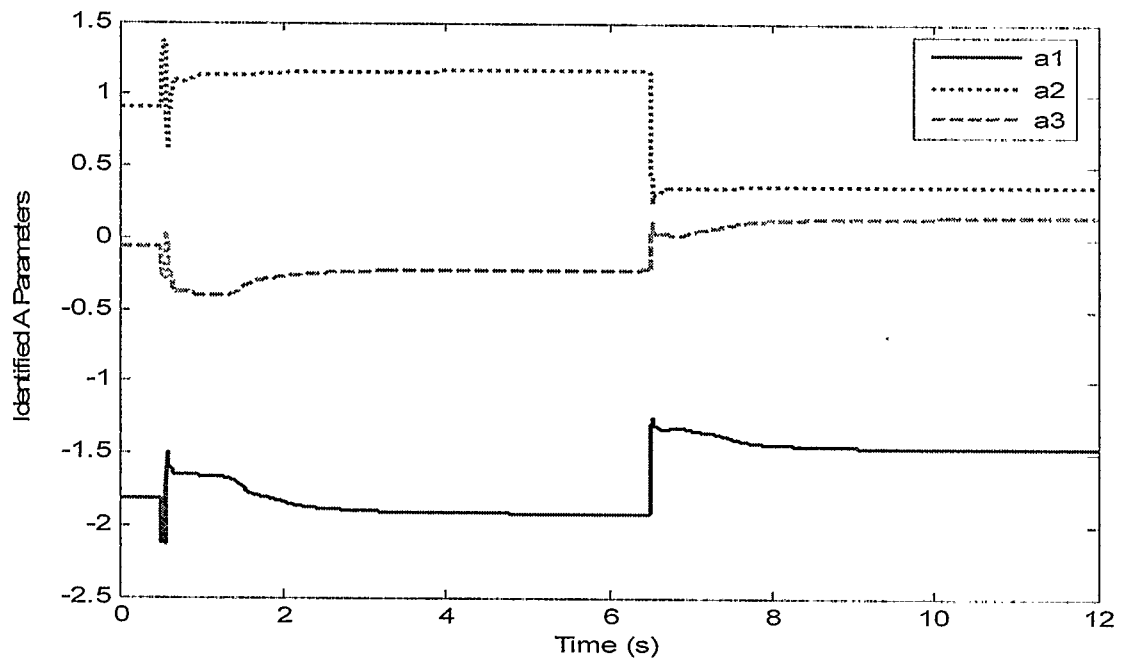


Fig. 4.9 Variation of A parameters on-line

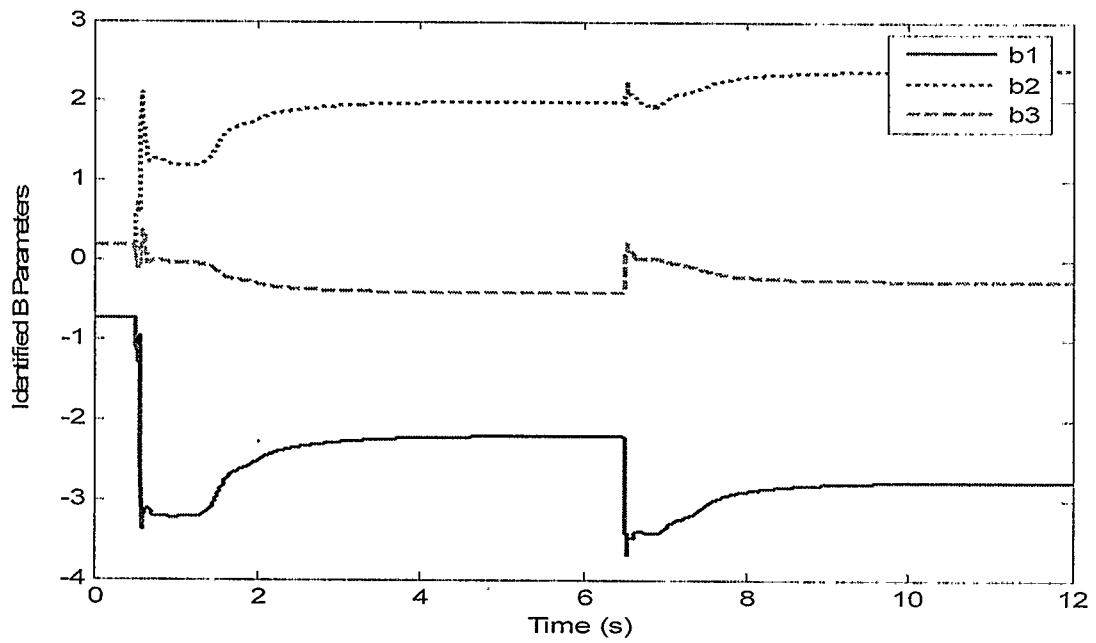


Fig. 4.10 Variation B parameters on-line

4.4.3 Discussion

In order to find the differences and similarities between the methods of RLS-Identifier and KF-Identifier to estimate the parameters of the system, many simulation studies have been conducted for different operating conditions and different disturbances. The results show that the RLS and KF identifiers provide high quality tracking properties for the parameters of the system. Both techniques are suitable for on-line estimation and have the same performance and level of accuracy when their outputs are compared to the output of the actual system. In addition, both of them have relatively simple structures that make them desirable to be applied in practice.

In order to know which of the two identifiers used in the simulation has the smallest convergence time, an additional test is made to find the mean square error of multiple runs for each identifier while the white noise is the input of the system.

It can be seen from Fig. 4.1 that the parameters of the RLS-Identifier converge in only 6 samples which means its convergence time is 0.006 s. while Fig. 4.12 shows that the parameters of the KF-Identifier converge at time 0.017 s. According to analysis of the convergence time of each identifier, it can be seen that the parameters convergence time with the RLS-Identifier is much less than the parameters convergence time with the KF-Identifier. It leaves more time for performing other functions. Therefore, the RLS-Identifier has been used to update the controller described in the following sections.

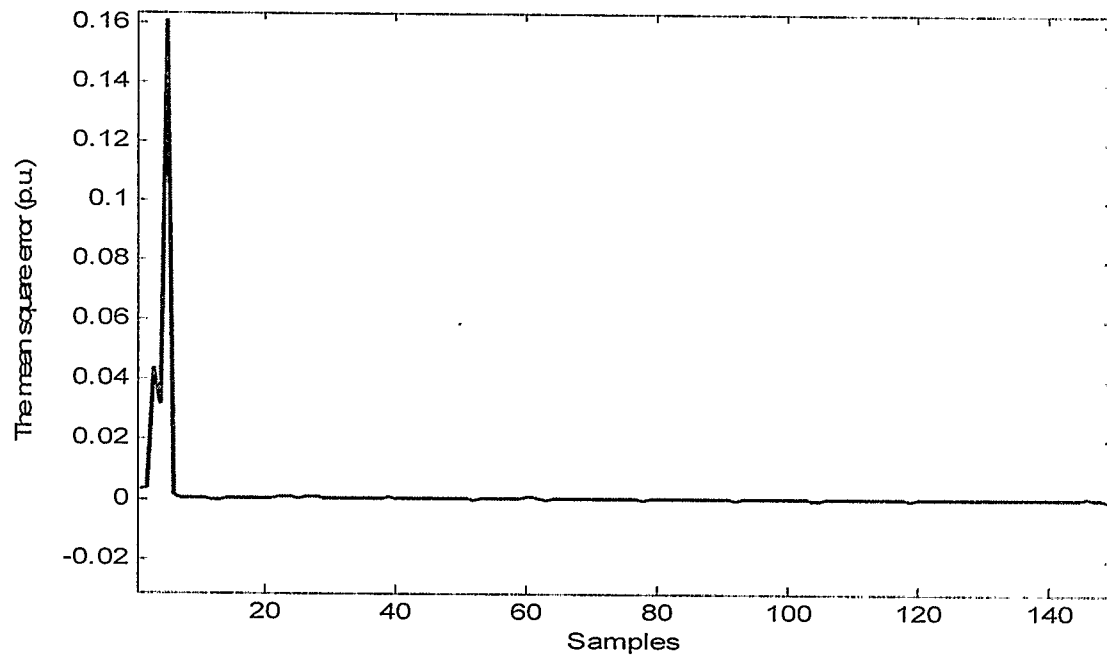


Fig. 4.11 Mean square error for the RLS-identifier

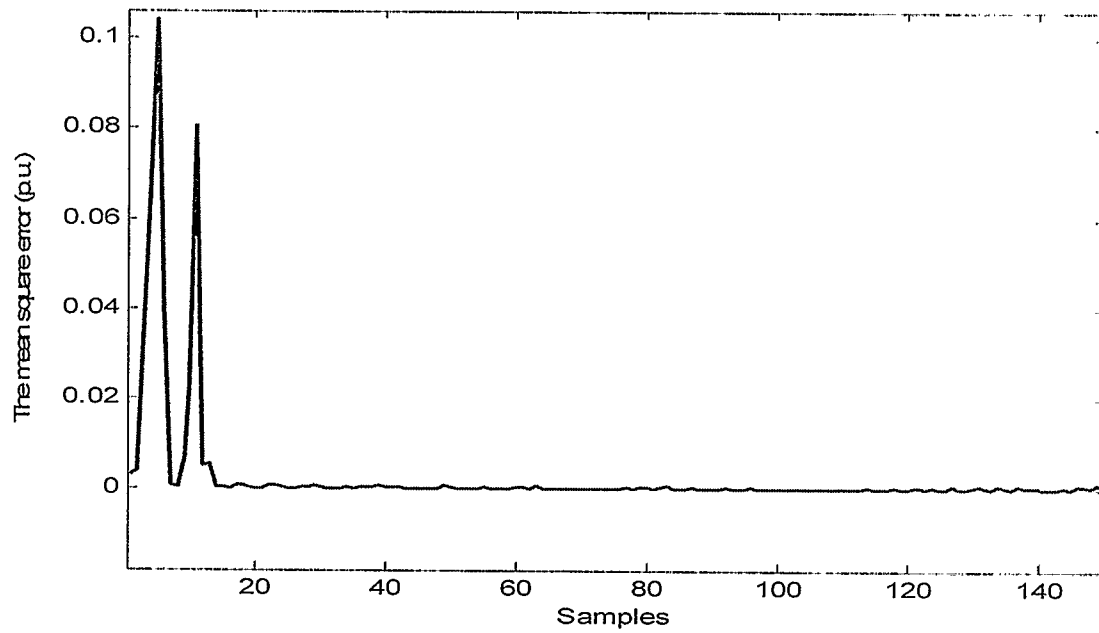


Fig. 4.12 Mean square error for the KF-identifier

4.5 Control Strategy

Once the system model parameters are identified, the control signal can be calculated based on the discrete model shown in Eqn. 4.1. Assume the feedback loop has the form

$$\frac{u(t)}{y(t)} = -\frac{G(z^{-1})}{F(z^{-1})} \quad (4.10)$$

where

$$F(z^{-1}) = 1 + f_1 z^{-1} + f_2 z^{-2} \quad (4.11)$$

$$G(z^{-1}) = g_0 + g_1 z^{-1} + g_2 z^{-2} \quad (4.12)$$

In the PS control algorithm, the characteristic polynomial of the closed-loop system is assumed to have the same form as that of the open-loop system. Also in the closed-loop, the open-loop poles are shifted radially towards the center of the unit circle in the z -plane by a factor α . This implies the use of the following equation:

$$T(z^{-1}) = A(z^{-1})F(z^{-1}) + B(z^{-1})G(z^{-1}) = A(\alpha z^{-1}) \quad (4.13)$$

Expanding both sides of Eqn. 4.13 and comparing the coefficients gives [34]:

$$\begin{bmatrix} 1 & 0 & b_1 & 0 & 0 \\ a_1 & 1 & b_2 & b_1 & 0 \\ a_2 & a_1 & b_3 & b_2 & b_1 \\ a_3 & a_2 & 0 & b_3 & b_2 \\ 0 & a_3 & 0 & 0 & b_3 \end{bmatrix} \begin{bmatrix} f_1 \\ f_2 \\ g_0 \\ g_1 \\ g_2 \end{bmatrix} = \begin{bmatrix} a_1(\alpha - 1) \\ a_2(\alpha^2 - 1) \\ a_3(\alpha^3 - 1) \\ 0 \\ 0 \end{bmatrix} \quad (4.14)$$

or in matrix form

$$M.w(\alpha) = L(\alpha) \quad (4.15)$$

If the pole-shift factor α is fixed, the PS control algorithm degenerates into a special case of the pole-assignment control algorithm. It is evident that the rule determining the pole-shifting factor is very important. For optimum performance α is modified on-line according to the operating conditions of the controlled system.

From Eqns. 4.10 and 4.15, the control signal $u(t)$ can be expressed as a function of the pole-shifting factor α as:

$$u(t) = X^T(t)w(\alpha) = X^T(t)M^{-1}L(\alpha) \quad (4.16)$$

where

$$X(t) = [-u(t-1) \quad -u(t-2) \quad -y(t) \quad -y(t-1) \quad -y(t-2)]^T \quad (4.17)$$

Full details of the control technique in addition to its properties and constraints are given in Chapter 3.

4.5.1 Controller Start-Up:

New control is computed each sampling interval on the assumption that the updated system parameter estimate obtained by the system identifier is ‘accurate’. This is carried out in the same way as an off-line procedure. However, in a self-tuning controller it is carried out recursively on-line [10]. This means that while the model parameter estimates are good, the controller output is good, whereas if the model parameter estimates are bad then almost surely the computed control will be bad. This point is particularly important on controller start-up, in that the self-tuning control algorithm will work even if fairly arbitrary initial estimates are entered for the model parameter estimates. This may provide pretty violent control; however, the estimates will converge to their true values in a short space of time.

4.6 Simulation Studies

To illustrate the above, some studies were performed on the system given in Fig. 4.2. A self-tuning controller with an identifier and variable pole-shifting control was applied to an SVC connected to the middle bus of the transmission, Fig. 4.2.

The active angular speed deviation $\Delta\omega(t)$ is sampled at the rate of 50Hz for parameter identification and control computation. Sampling frequencies above 100Hz provide no practical benefit and the performance deteriorates for sampling rates under 20Hz. A sampling period of 20ms is chosen to make sure that there is enough time available for updating the RLS algorithm and control computation [10]. The absolute limits for the control output are limited to $\pm 0.1 p.u.$ and the absolute limits for the SVC

output are limited to $\pm 0.15 p.u.$ [80].

4.6.1 Normal Load Conditions

The normal operating condition of the single machine power system is set at $P=0.7$ p.u., power factor 0.9 lag. In the simulation, a 0.15 step increase in the mechanical torque of the generator is applied at 0.5 s. To clarify the behaviour of the system, comparison is done between the proposed SVC adaptive power system stabilizer (SAPSS), the SVC conventional power system stabilizer (SCPSS) and without any supplementary control on the SVC (NO SPSS). Response of the angular speed deviation of the generator, the output of the SVC controller, the voltage variation at the middle bus and the voltage variation of the generator bus are shown in Figs. 4.8 – 4.11, respectively. Outputs of the supplementary controllers are shown in Fig. 4.12.

It can be seen from Fig. 4.8 that the proposed SVC controller can effectively damp the system oscillations. Although there is no difference between the three cases, NO SPSS, SCPSS and SAPSS in the first peak, it can be seen that, after the first peak, the SVC adaptive controller damps out the oscillations more effectively. For example, the generator speed deviation in the subsequent swing with SAPSS is -0.065 rad/sec, with SCPSS is -0.085 and with no PSS is -1.15 rad/sec. In contrast, the voltage of the system without using SCPSS or SAPSS is almost constant, especially at the middle bus. However, the voltage variation with the SAPSS is the largest compared to the voltage variation with the SCPSS as demonstrated in Figs 4.10, 4.11.

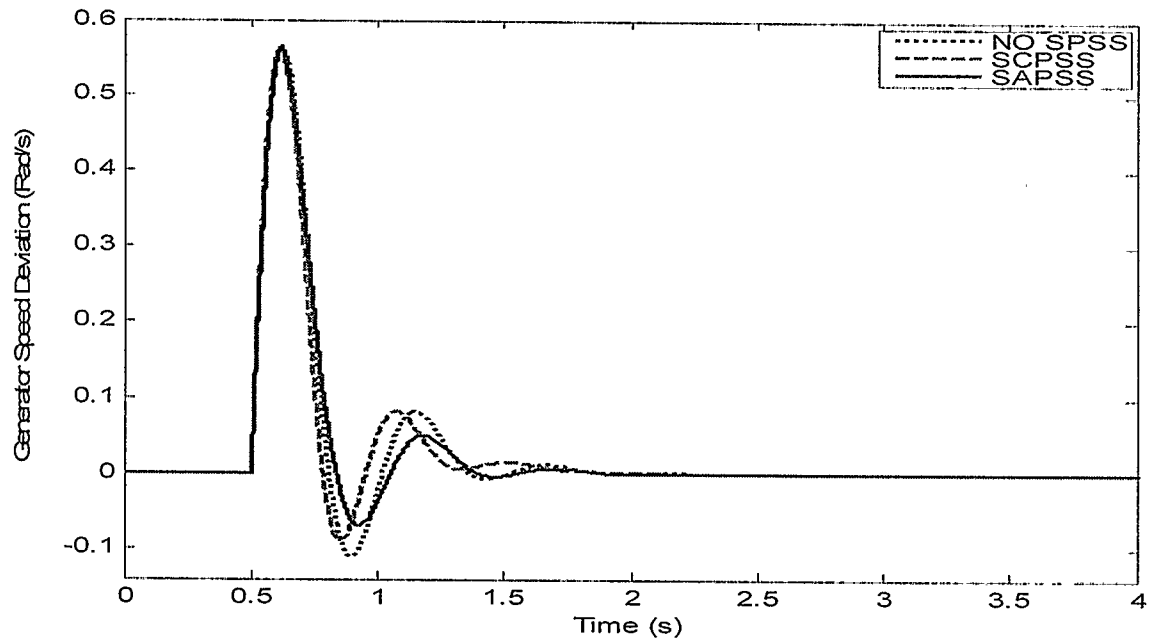


Fig. 4.8 Generator angular speed deviation in response to a 0.15 p.u. step increase in mechanical torque at 0.5 s. initial condition, $P=0.7$ p.u., p.f.= 0.9 lag.

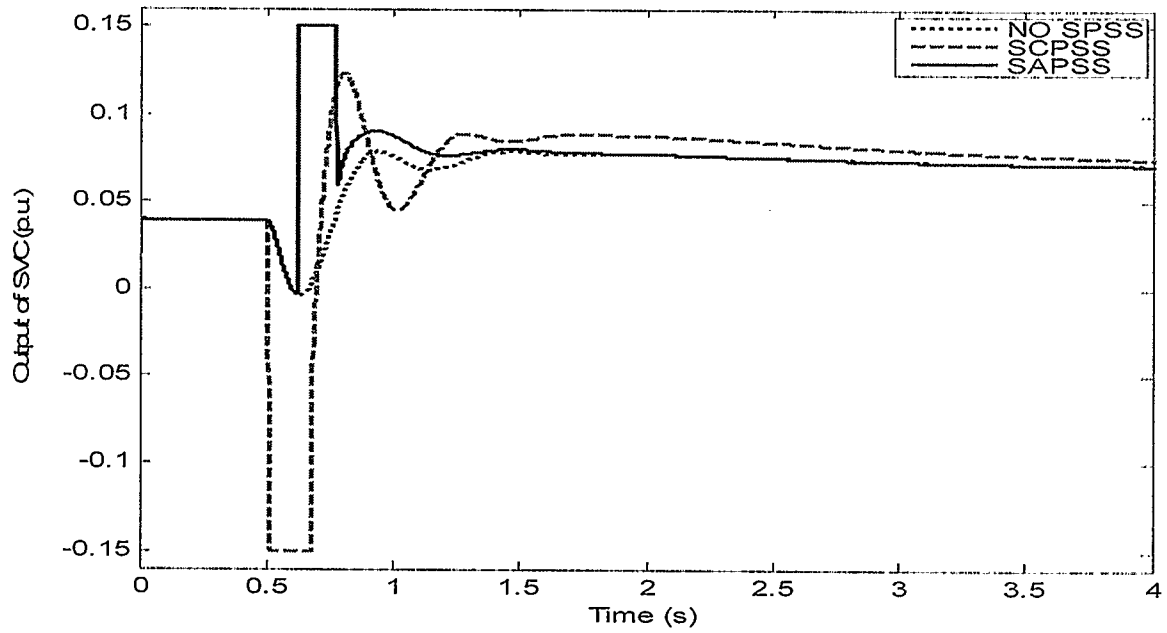


Fig. 4.9 SVC controller output in response to a 0.15 step increase in mechanical torque.

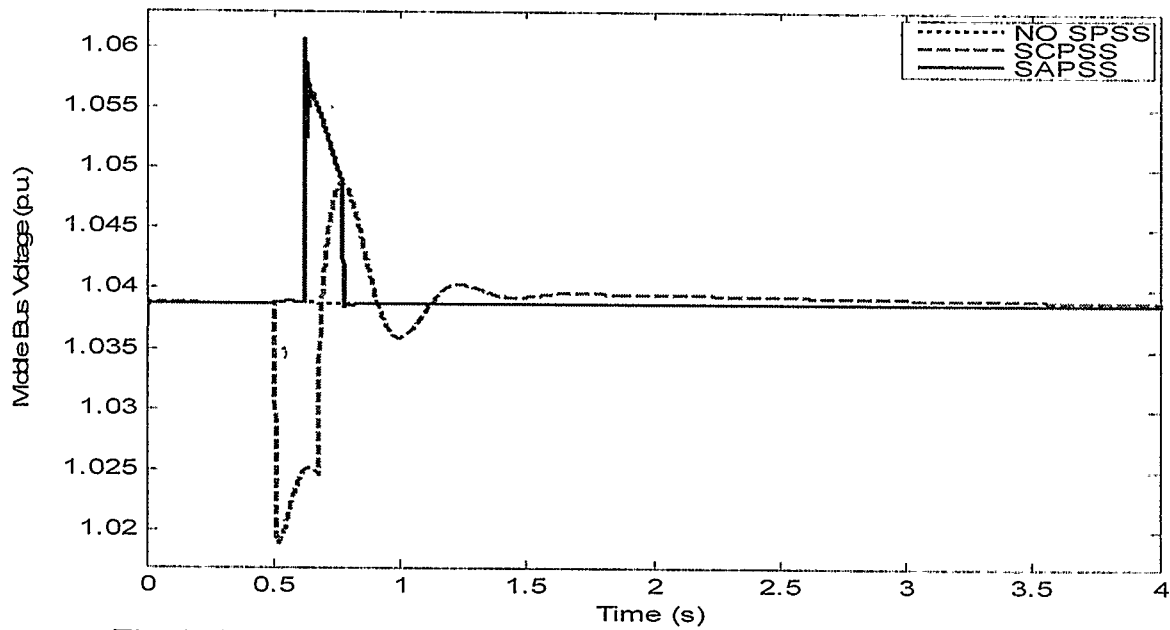


Fig. 4.10 Middle bus voltage in response to a 0.15 p.u. step increase in mechanical torque.

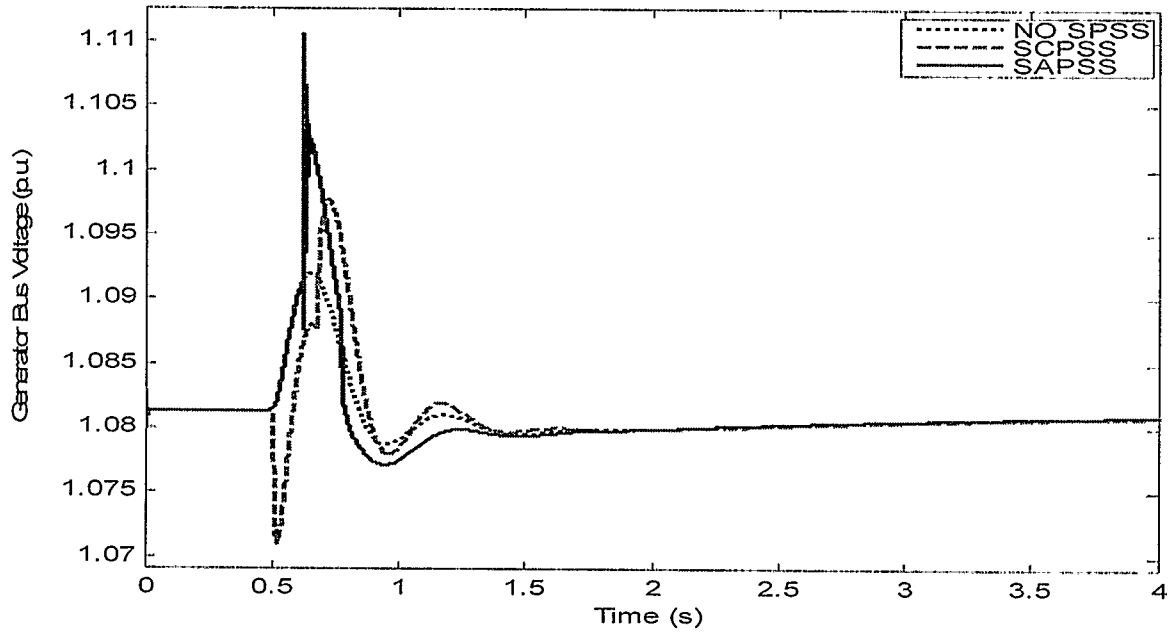


Fig. 4.11 Generator terminal voltage in response to a 0.15 p.u. step increase in mechanical torque.

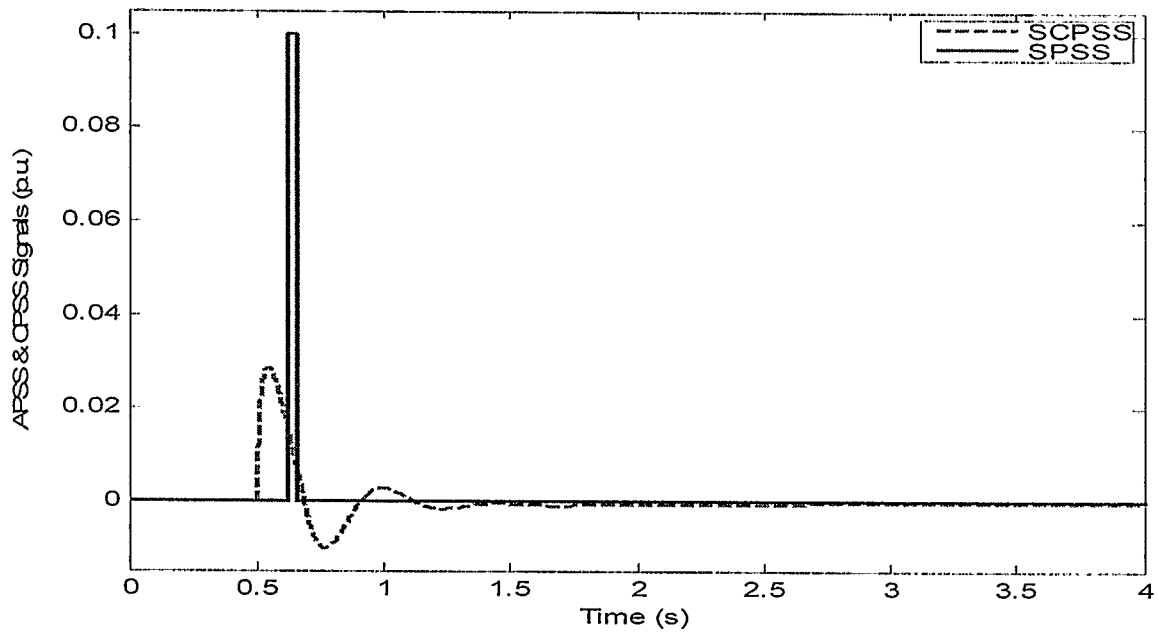


Fig. 4.12 Controls output of SAPSS & SCPSS in response to a 0.15 p.u. step increase in mechanical torque.

4.6.2 Light Load Conditions

At light load initial conditions, $P = 0.2$ p.u. and 0.8 power factor lag, a disturbance of 0.15 p.u. step increase in input torque is applied at 0.5 s. The system response is shown in Figs. 4.13 – 4.15.

From the response of the generator angular speed deviation in Fig. 4.13 it is again seen that starting with second swing the proposed SVC controller provides better damping of the system oscillations.

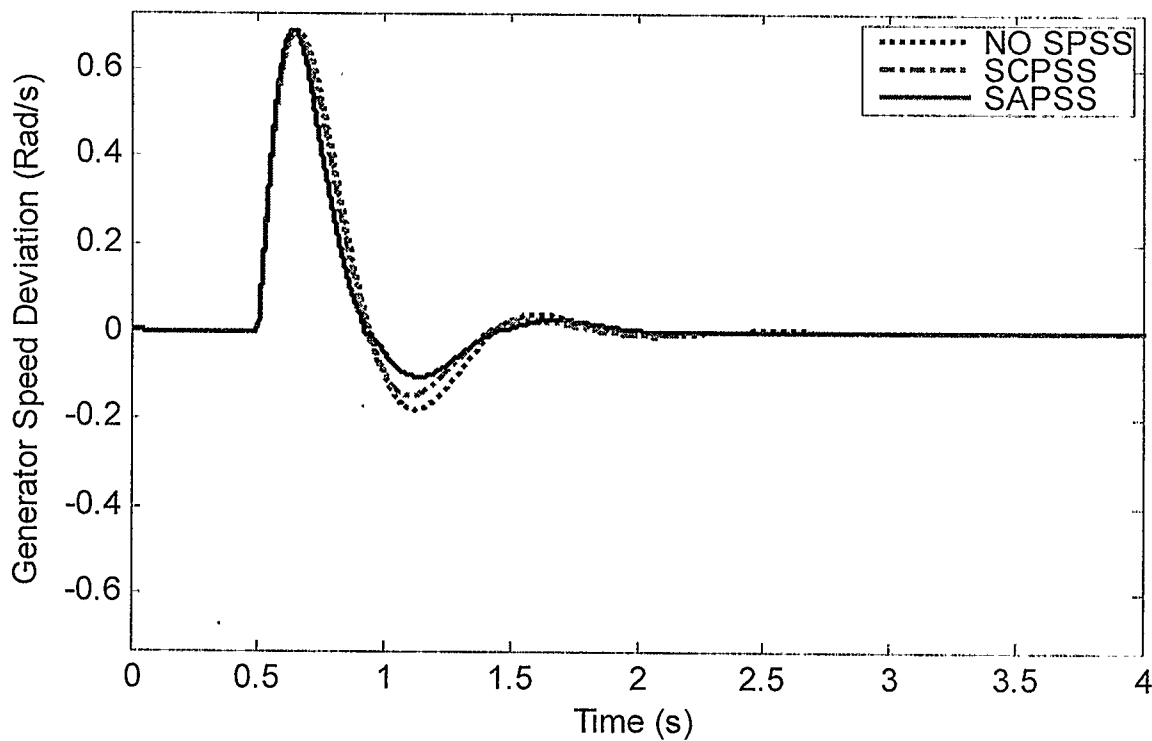


Fig. 4.13 Generator angular speed deviation in response to a 0.15 p.u. step increase in mechanical torque at 0.5 s., initial condition $P = 0.2$ p.u., p.f. = 0.8 lag

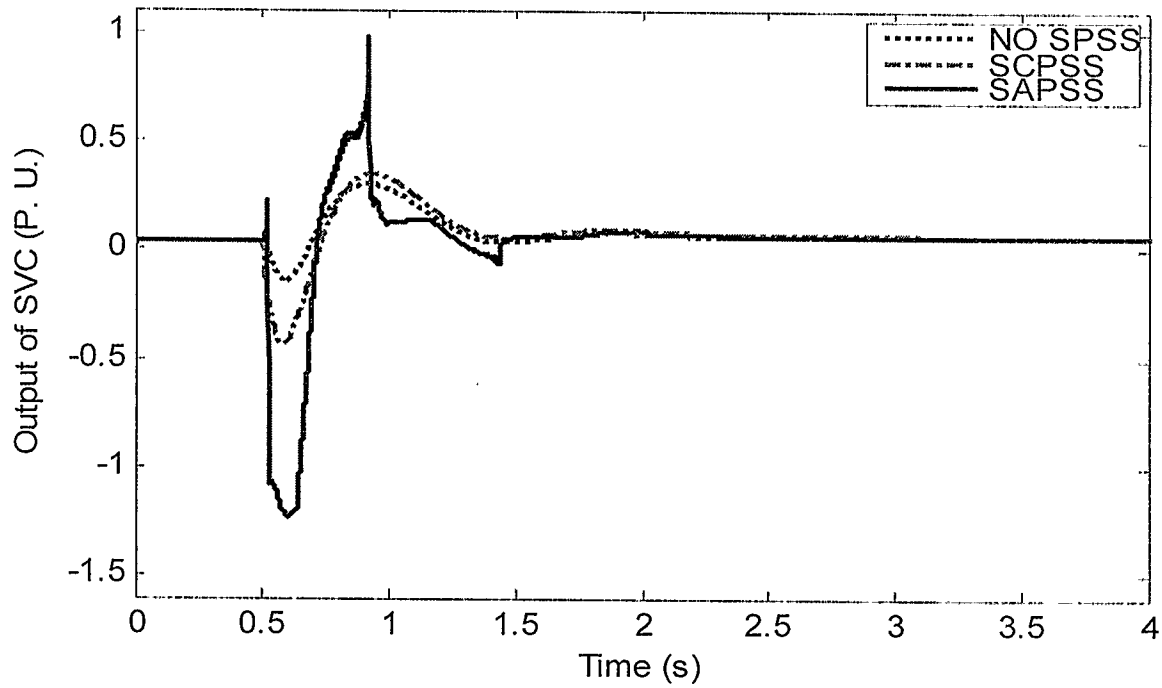


Fig. 4.14 SVC controller output in response to a 0.15 p.u. step increase in mechanical torque.

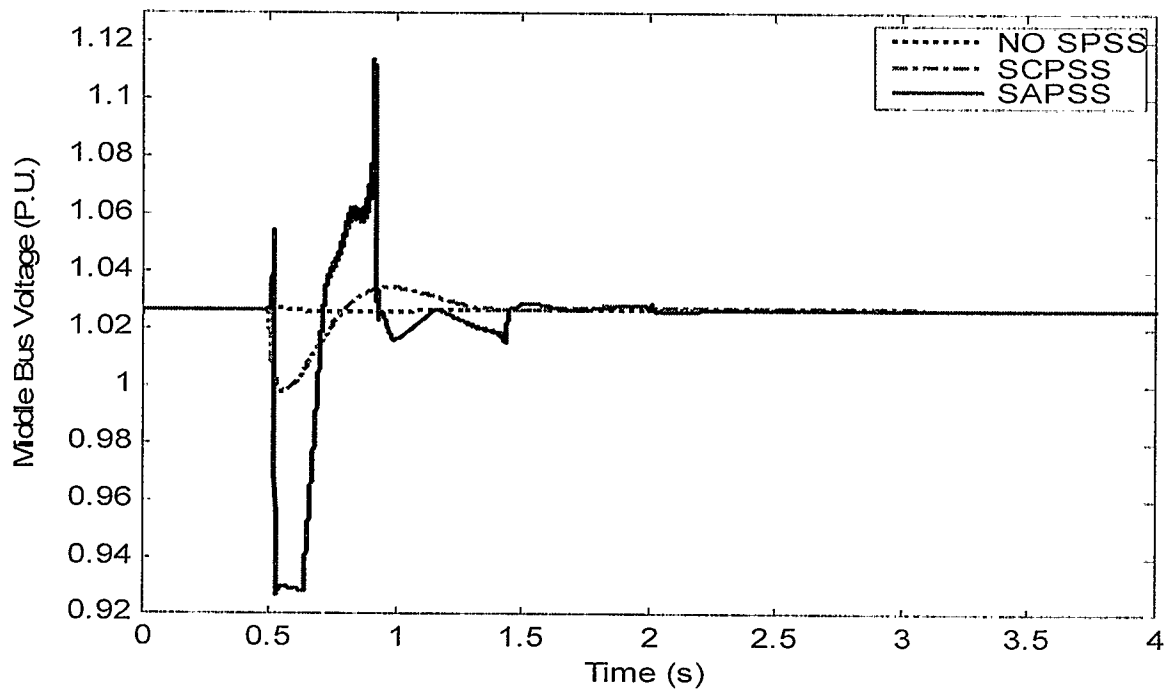


Fig. 4.15 Middle bus voltage in response to a 0.15 p.u. step increase in mechanical torque.

4.6.3 Leading Power Factor Load Conditions

The situation with system operating at a leading power factor load condition is much more difficult because the stability margin is reduced [81]. However, in order to absorb the capacitive charging current in high voltage power system, it might become necessary to sometimes operate the generator at a leading power factor. The behavior of the system in this situation is shown in Figs. 4.16 - 4.18 when the initial operating conditions are $P = 0.7$ p.u. and 0.9 lead power factor and a 0.15 p.u. step increase in the input torque reference of the generator is applied at time 0.5 s.

The results in Fig. 4.16 show the effectiveness of the proposed SVC controller to damp the system oscillations. The generator speed does not settle faster with SAPSS.

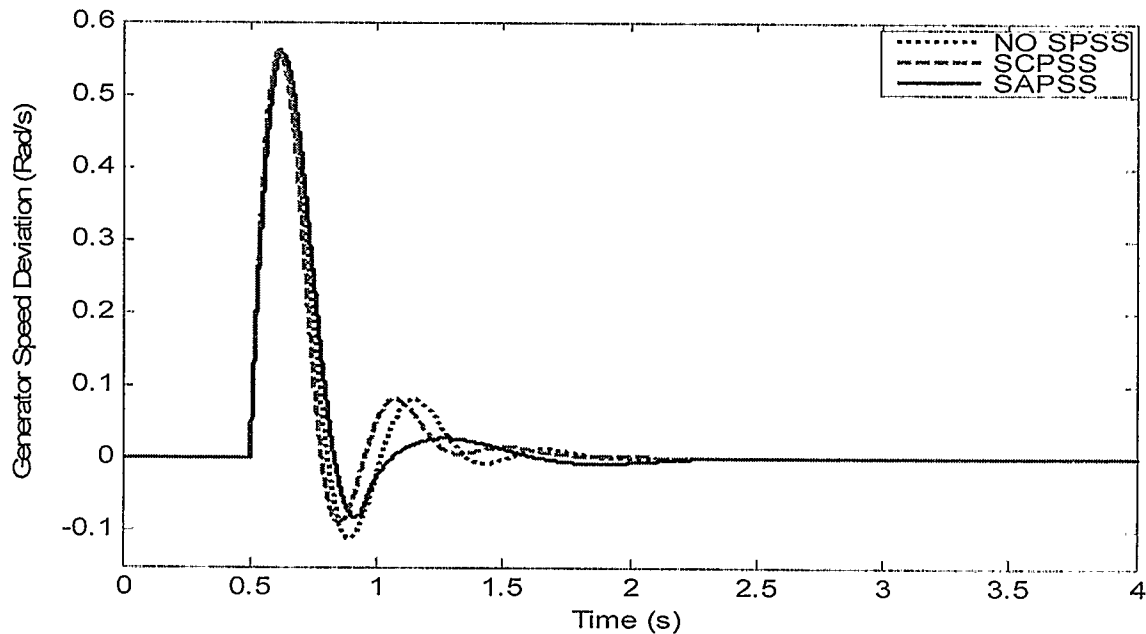


Fig. 4.16 Angular speed deviation in response to a 0.15 p.u. step increase in mechanical torque at time 0.5 s., initial condition $P = 0.7$ p.u., p.f. = 0.9 lead

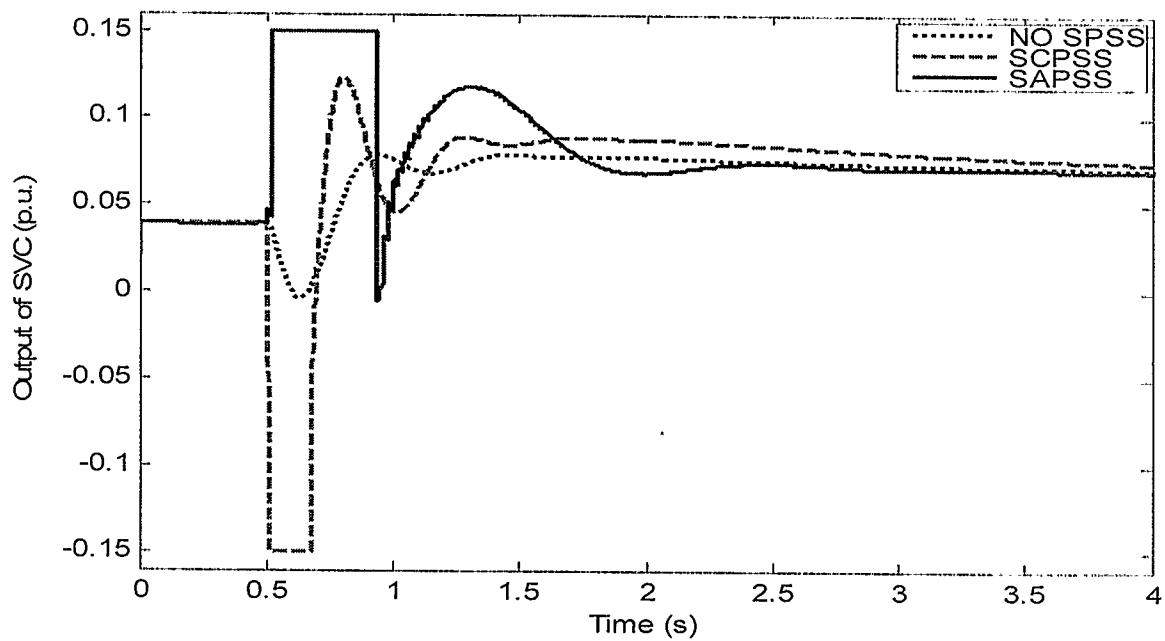


Fig. 4.17 SVC controller output in response to a 0.15 p.u. step increase in mechanical torque

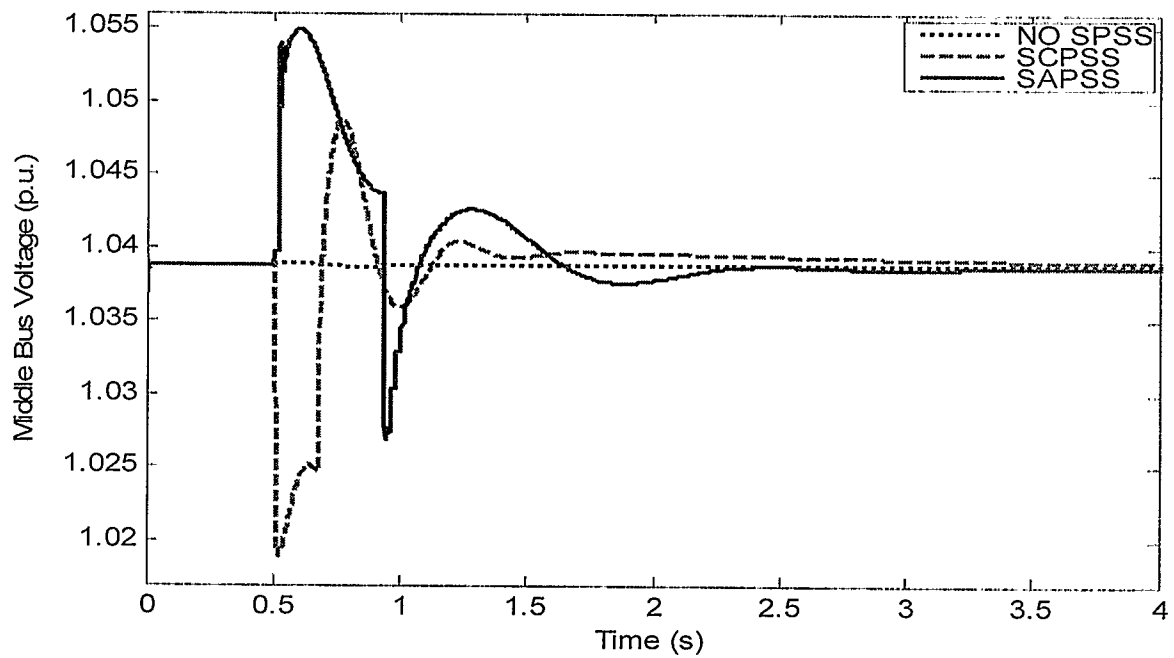


Fig. 4.18 Middle bus voltage in response to a 0.15 p.u. step increase in mechanical torque

4.6.4 Change in Voltage Reference of the Generator Bus

In this test, a 5% step increase in the generator voltage reference is applied at 0.5 s when the system is operating at normal load operating condition of $P = 0.7$ p.u. and 0.9 power factor lag and then back again to the initial condition at 6.5 s. Behaviour of the system is shown in Figs. 4.19 through 4.21..

The response of the generator angular speed variation in Fig 4.19 shows that both the SCPSS and the SAPSS have the same ability to improve the system stability, because the disturbance in this test is not considered as a major disturbance, but it can be seen that the proposed SVC controller provides slightly improved damping when the system returns again to its initial operating conditions. With the SAPSS, the generator speed deviation goes to zero in about 7.5 s, whereas with the SCPSS and no PSS it goes to zero at about 8.0 s. Middle bus voltage settles to the new value with SAPSS almost immediately and earlier than with SCPSS and no PSS. On return to the initial conditions, middle bus voltage with the SAPSS also settles almost 2 s earlier than with the SCPSS.

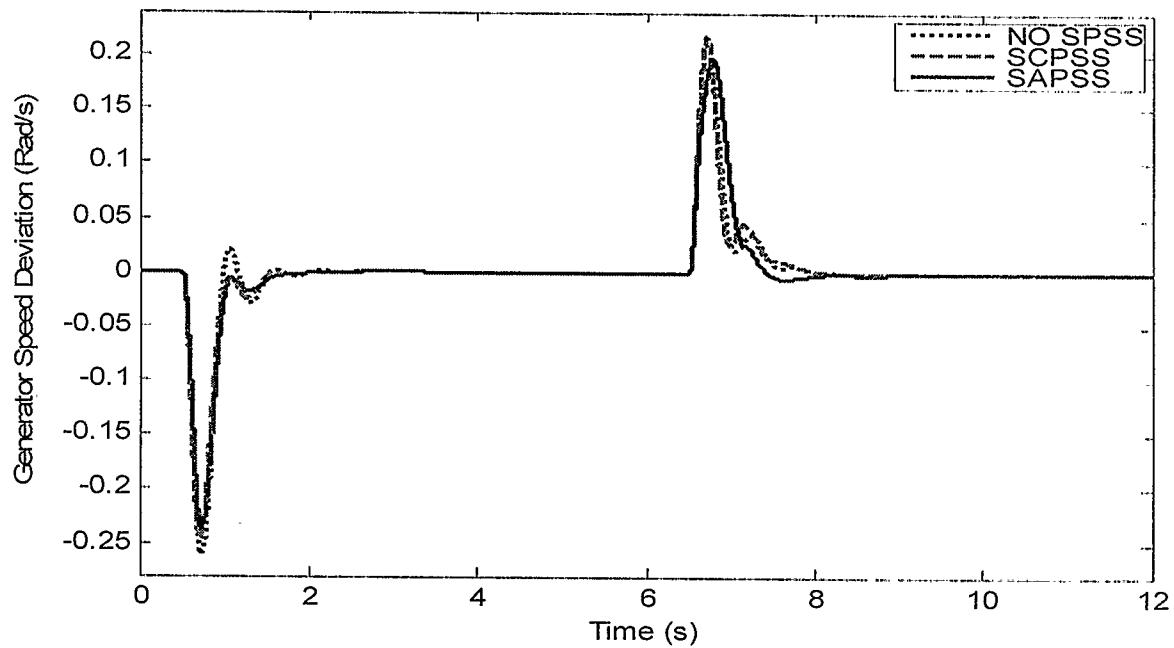


Fig. 4.19 Angular speed deviation in response to a 5% step increase in the generator terminal voltage reference and back to the initial condition

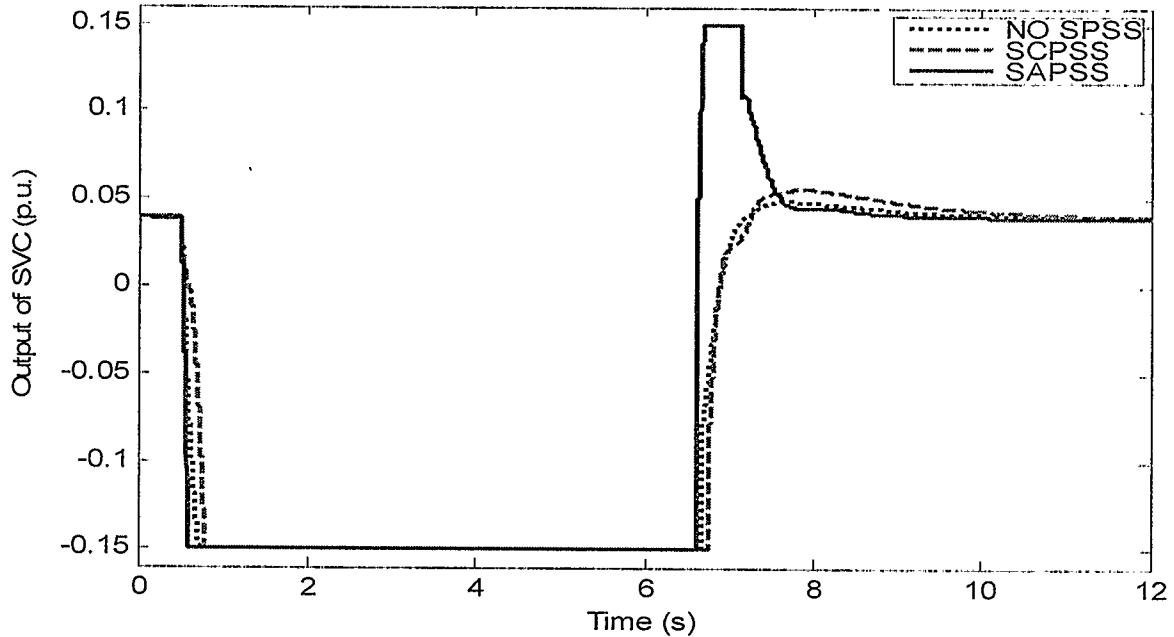


Fig. 4.20 SVC controller output in response to a 5% step increase in the terminal voltage reference and back to the initial condition

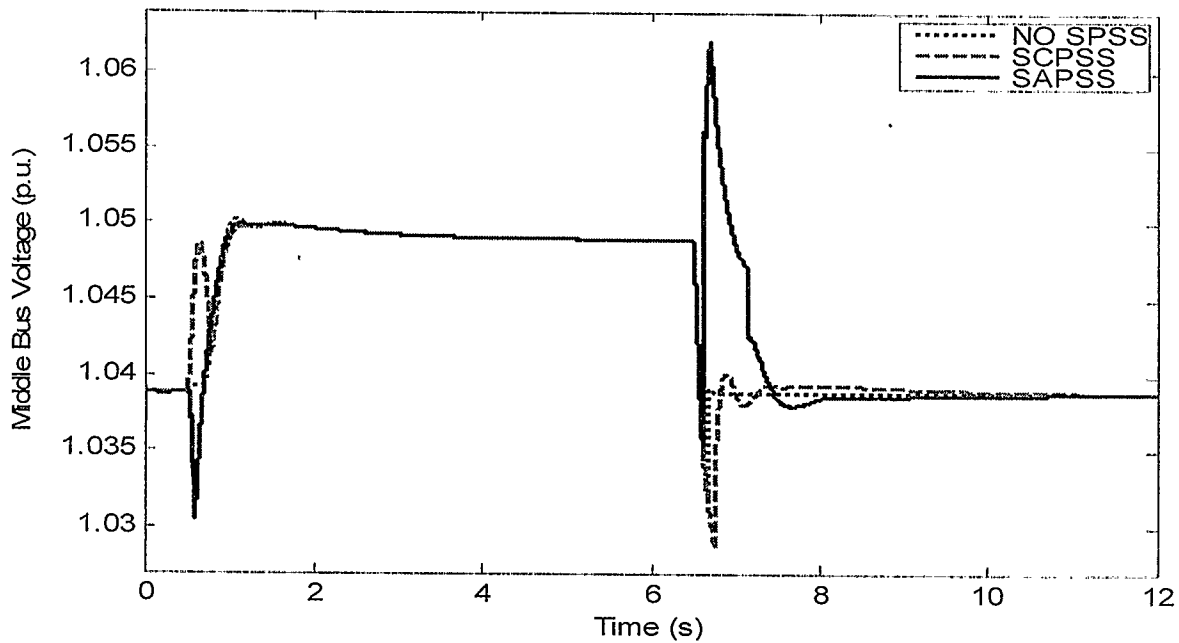


Fig. 4.21 Middle bus voltage in response to a 5% step increase in the terminal voltage reference and back to the initial condition

4.6.5 Voltage Reference Change of the Middle Bus

When the system is operating at normal load operating conditions $P = 0.7$ p.u. and 0.9 power factor lag, a 5% step increase in the middle bus voltage reference is applied at 0.5 s and then back again to the initial condition at 6.5 s. The responses in this case are shown in Figs. 4.22 through 4.24.

It can be seen from Fig. 4.22 that the proposed SVC controller damps the system oscillations and reduces the overshoot of the angular speed deviation much better than the conventional one, 0.034 versus 0.042 pu. Furthermore, it can be seen there is not much difference in the middle bus voltage at the time of applying the step increase.

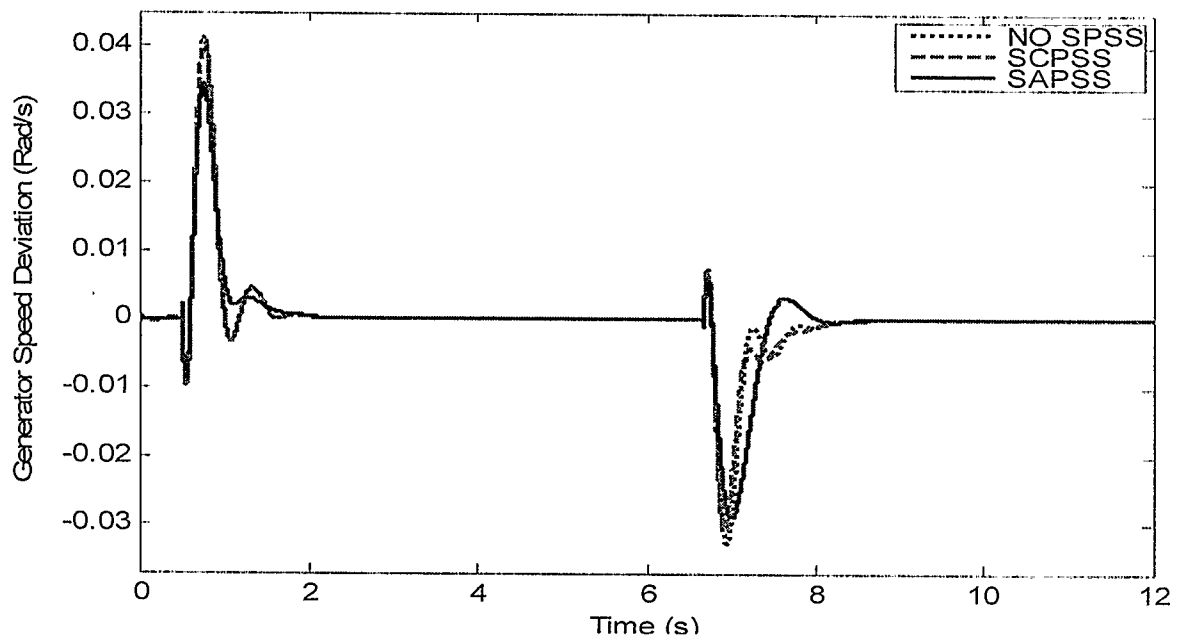


Fig. 4.22 Angular speed deviation in response to a 5% step increase in the middle bus voltage reference and back to the initial condition

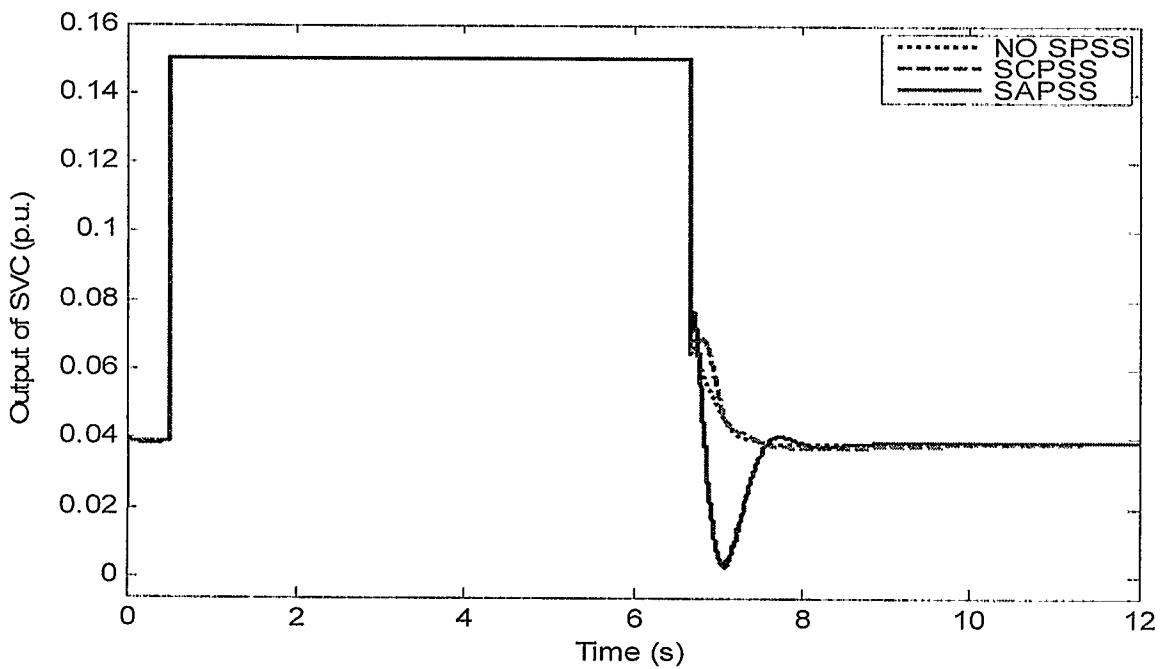


Fig. 4.23 SVC controller output in response to a 5% step increase in the terminal voltage reference and back to the initial condition

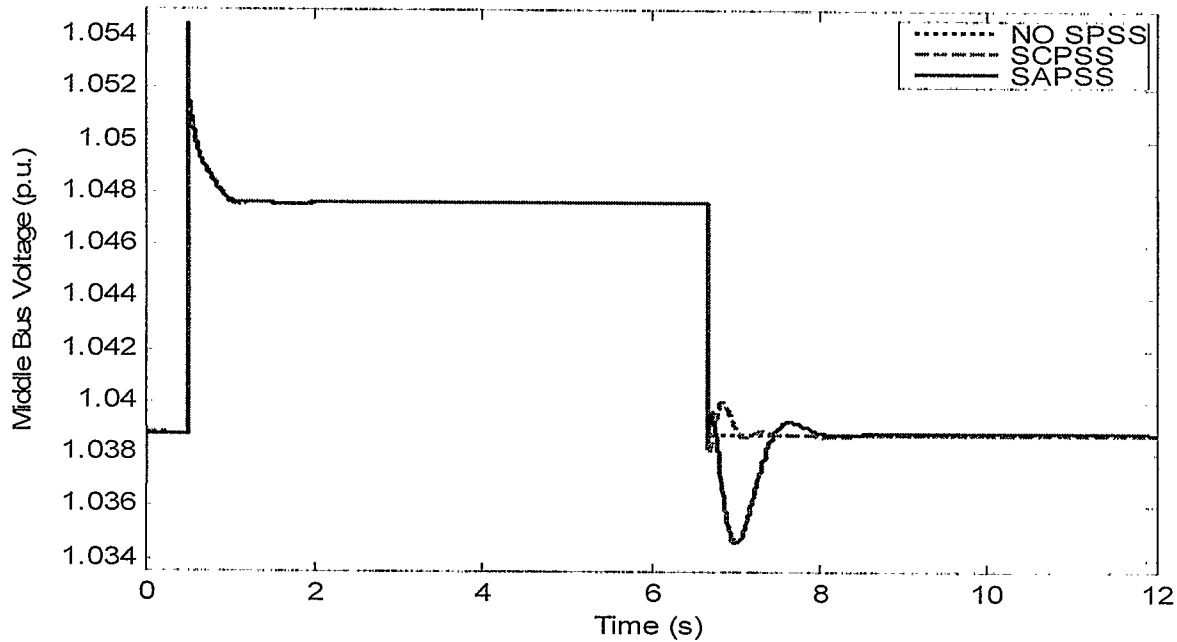


Fig. 4.24 Middle bus voltage in response to a 5% step increase in the terminal voltage reference and back to the initial condition

4.6.6 The Effectiveness of Changing the Sampling Rate and Test of the Coordination with the Generator PSS

In order to compare the system behaviour to the same disturbance, three different sampling periods for controller and identifier, 10 ms, 20 ms and 50 ms, have been used with the adaptive PSS applied in the following three configurations:

- APSS applied on the generator automatic voltage regulator (GAVR).
- APSS applied on the SVC.
- APSS applied on both locations, i.e. GAVR and SVC at the same time.

At the normal operating condition of the single machine system, $P = 0.7$ p.u. and

0.9 lag power factor, a 0.15 p.u. step increase in the torque reference is applied at time 0.5 s. and then return back to the initial condition at 6.5s .The system responses are shown in Figs. 4.25 – 4.27.

Sampling time less than 10ms provides no practical benefit and the performance deteriorates for sampling time above 100ms [10]. From the results of this test, it can be seen that 20 ms of sampling time is the best one and it gives good results with SVC and generator. Furthermore, it can be seen from Fig 4.27 that the proposed controller can coordinate with another PSS on the generator in the system and work together to make the system oscillation damping more efficient.

Another conclusion that can be drawn from this test is that generator speed deviation can be damped much more effectively by applying the APSS on the SVC than on the generator.

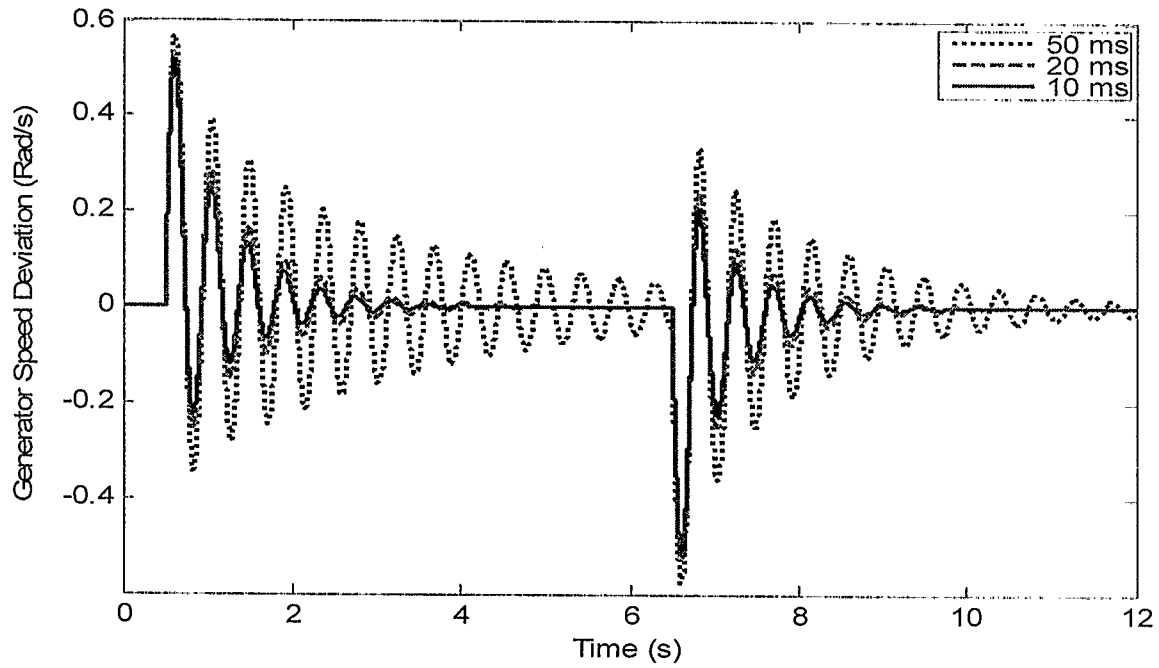


Fig. 4.25 Angular speed deviation in response to a 0.15 p.u. step increase in mechanical torque at 0.5 s. and back to initial condition, $P=0.7$ p.u., $p.f.=0.9$ lag, for different sampling periods and the APSS on the generator only

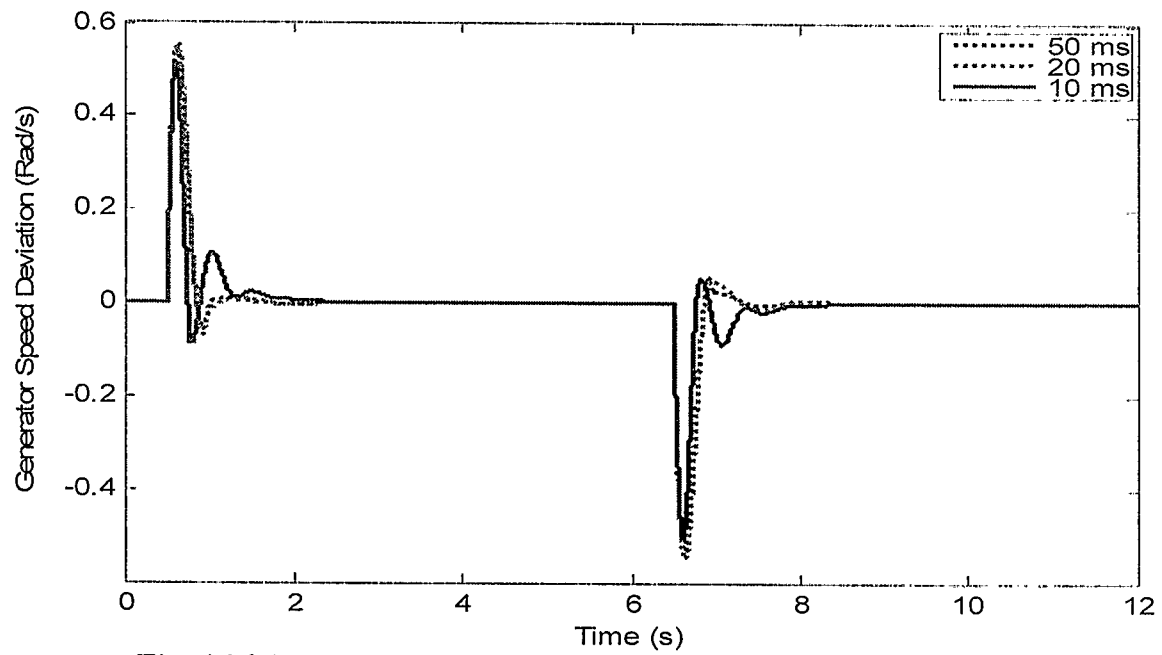


Fig. 4.26 Angular speed deviation in response to a 0.15 p.u. step increase in mechanical torque at 0.5 s, initial condition, $P = 0.7$ p.u., p.f. = 0.9 lag, for different sampling periods and the APSS on the SVC only

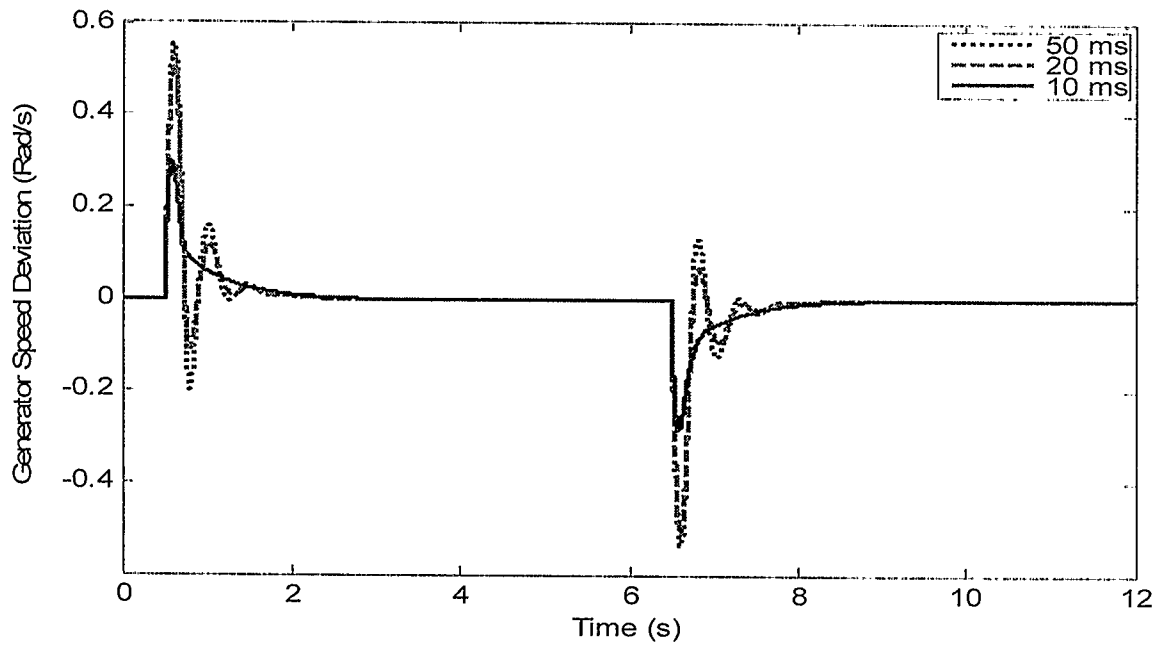


Fig. 4.27 Angular speed deviation in response to a 0.15 p.u. step increase in mechanical torque at 0.5 s, initial condition, $P = 0.7$ p.u., $p.f. = 0.9$ lag, for different sampling periods and the APSS on the generator and SVC

4.6.7 Three-Phase to Ground Short Circuit

To verify the behaviour of the proposed SVC adaptive controller under transient conditions, a three phase to ground short circuit is applied with the system operating at normal operating condition $P = 0.7$ p.u. and 0.9 power factor lag. The fault is applied at 0.5 s to the middle of one transmission line between the generator and the SVC bus and cleared 50 ms later by disconnection of the faulted line and successful reclosure at 6.5 s. The response of this test is shown in Figs. 4.28 – 4.30.

Results in Fig. 4.28 show that the performance of the proposed SVC controller to damp the system oscillation quickly is still the best after the first peak.

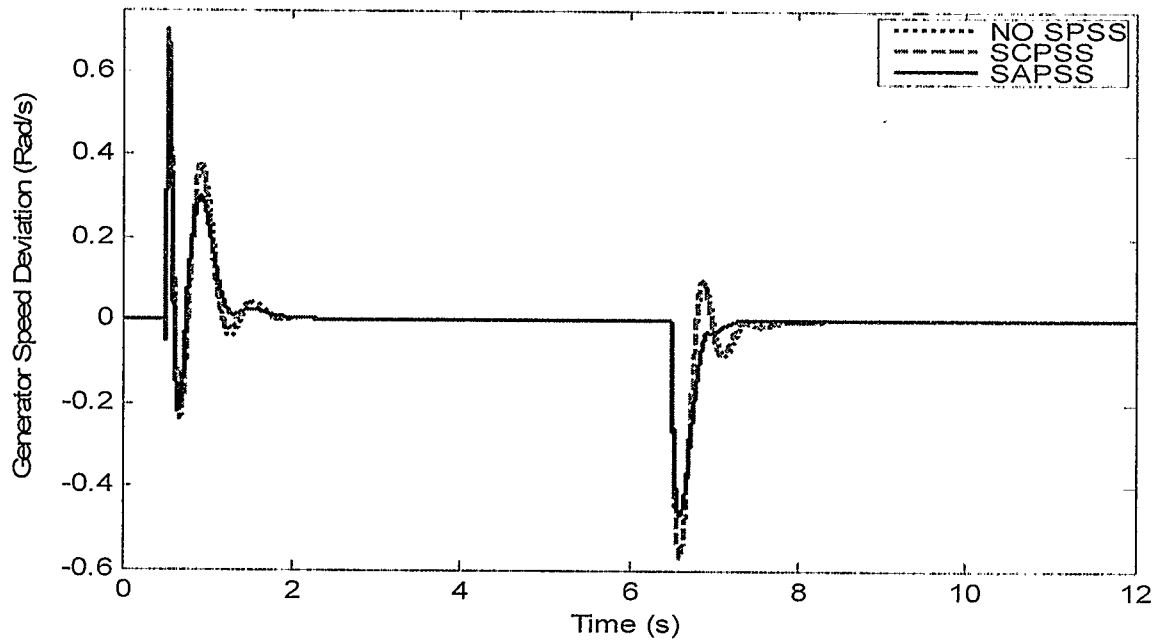


Fig. 4.28 Angular speed deviation in response to a three phase to ground fault at the middle of one transmission line and successful reclosure

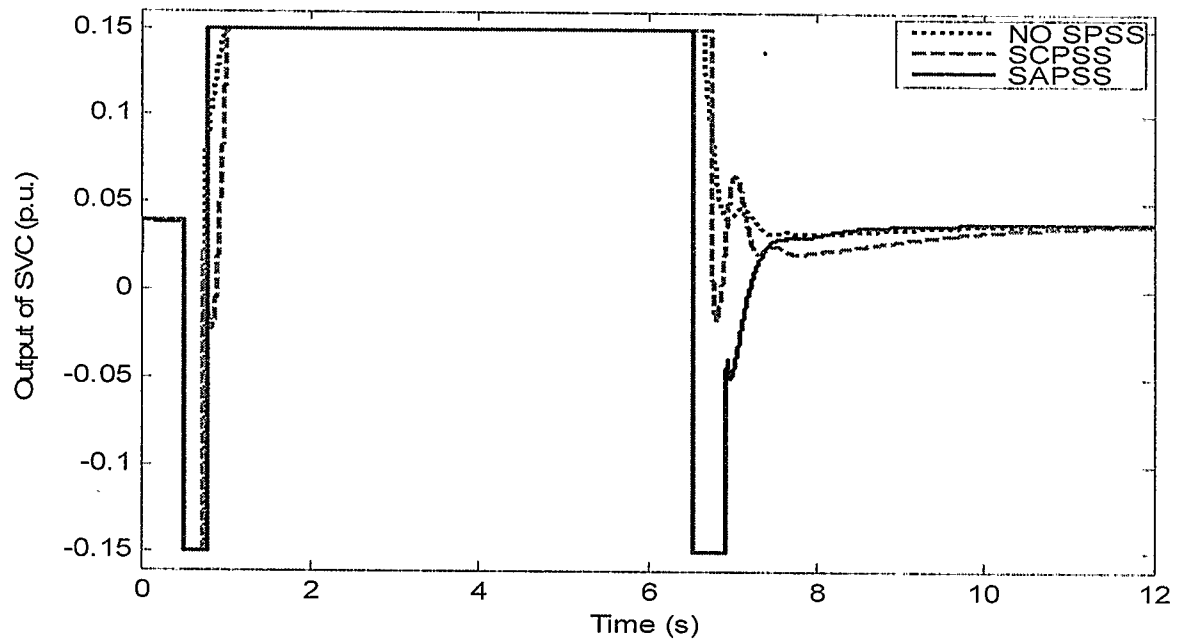


Fig. 4.29 SVC controller output in response to a three phase to ground fault at the middle of one transmission line and successful reclosure

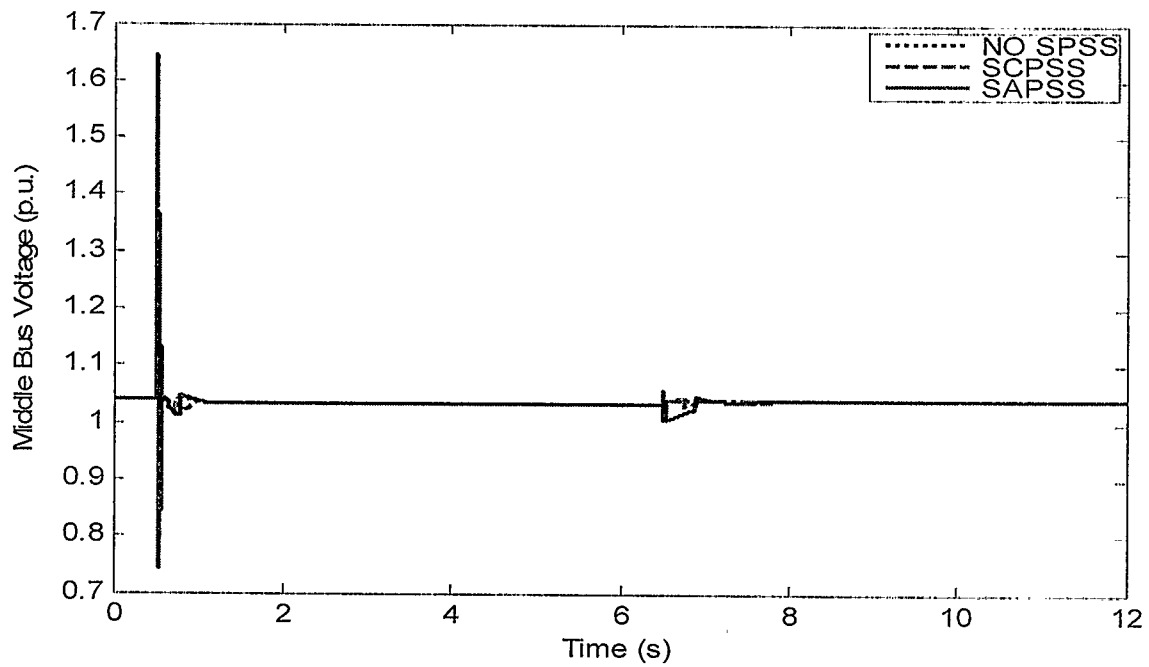


Fig. 4.30 Middle bus voltage in response to a three phase to ground fault at the middle of one transmission line and successful reclosure

4.6.8 Comparison between Using the Output of SVC (Bsvc) and the Generator Speed Deviation as Supplementary Stabilizing Signal to the Identifier and the Controller

In order to verify the best supplementary stabilizing signal to be used as input signal to the SAPSS to improve the damping of the system oscillations, this test provides a comparison between two different input signals to the proposed SAPSS. The output of the SVC signal (Bsvc) and the signal of the generator angular speed deviation ($\Delta\omega$) are supplied as input to the APSS and their response is compared to the system response in case of only the CPSS applied on the generator. At the normal operating condition of the single machine power system, $P=0.7$ p.u. and power factor 0.9 lag, a 0.15 step increase in the mechanical torque of the generator is applied at 0.5 s. It can be seen from Fig. 4.31 that to get the best damping of the system oscillations, the generator speed deviation as the input to the APSS provides the best results.

4.6.9 Dynamic Stability

In this test the system is initially working at 1.5 p.u. power at a unity power factor. A ramp of $1e^{-3}$ p.u. slope is added to the mechanical torque reference at 0s. Response of the generator speed deviation is shown in Fig. 4.32. The three lines in Fig. 4.32 indicate the time at which the generator loses synchronism in the three cases. As shown in Table 4.1, the proposed SVC adaptive controller (SAPSS) enhances the stability margin of the system by approximately 0.35 pu power over the SCPSS.

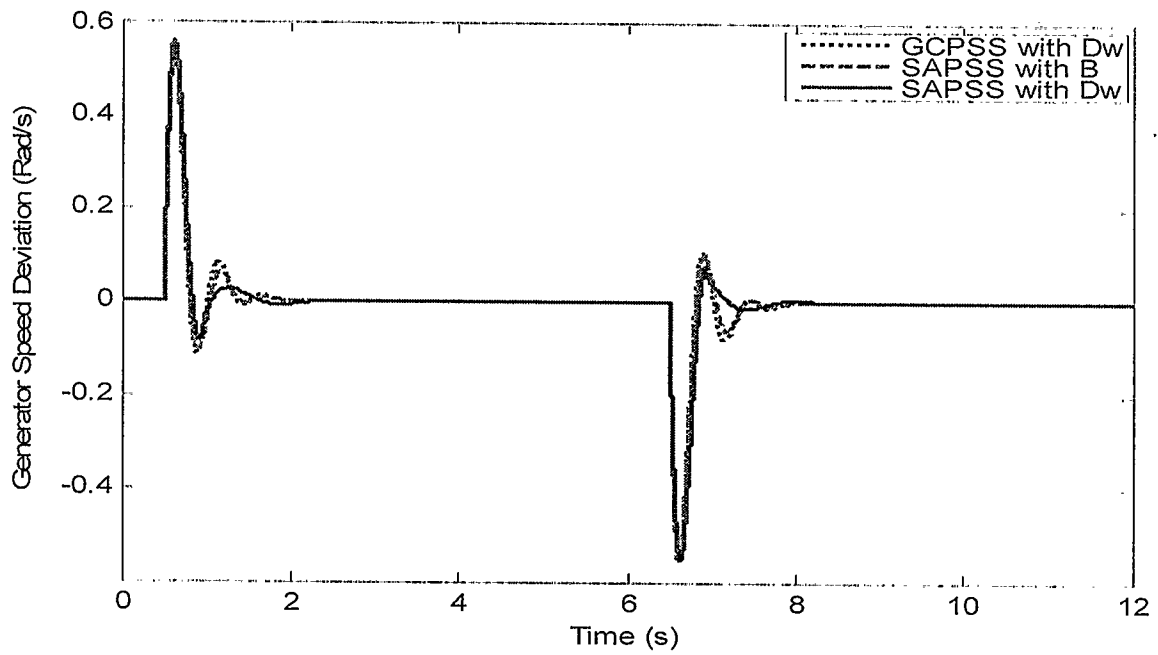


Fig. 4.31 Response of the angular speed deviation to different input signals

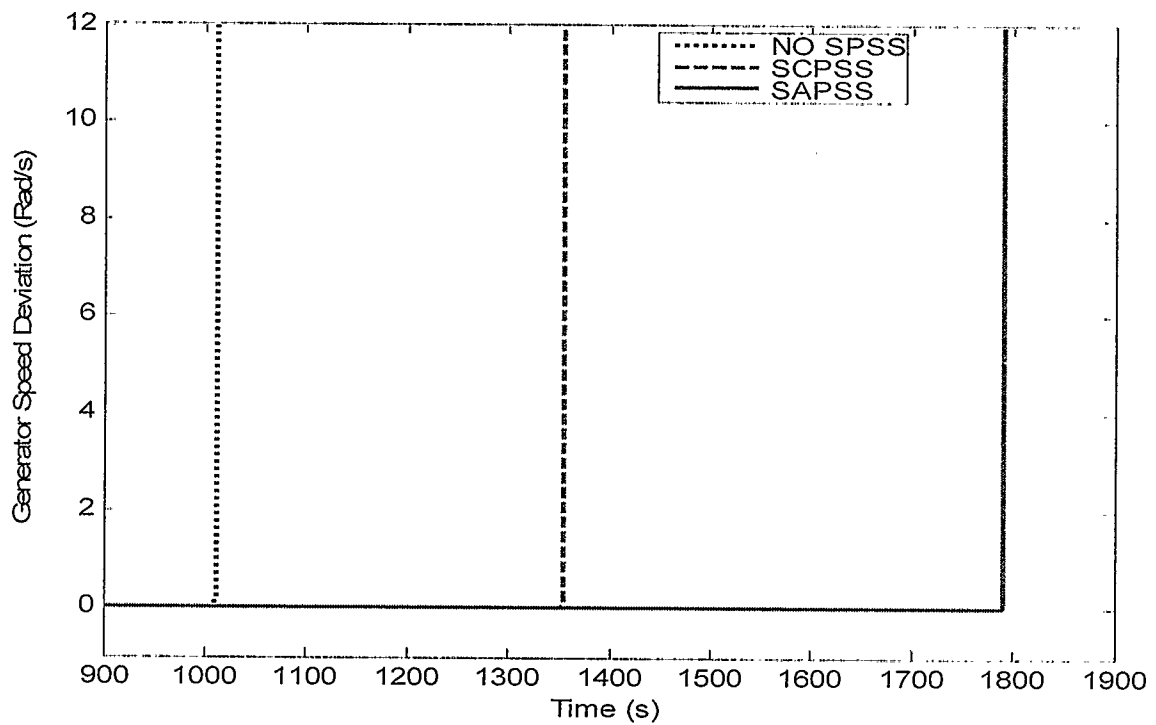


Fig. 4.32 Loss of synchronism in the stability margin test

Table 4.1 Maximum values of the torque applied to the system in the stability margin test

Test case	NO SPSS	SCPSS	SAPSS
Torque (p.u.)	3.0111	3.3558	3.7912

4.7 Summary

A comparison between the RLS-Identifier and the KF-Identifier is made in this Chapter in order to choose a suitable identifier that gives better performance of parameters estimation and updating the controller to develop an adaptive controller. The proposed SVC adaptive controller employing a self-optimizing pole-shifting control strategy and its application to a Single-Machine Infinite-Bus power system is described. The following conclusions can be drawn from the results. For real-time control, use of a third order system model to represent the controlled system is acceptable. In order to track the controlled system, using a varying forgetting factor in parameter identification is recommended. The proposed control strategy based on a pole-shifting approach combines the advantages of pole-assignment control algorithm and minimum variance control algorithm. Test results of various conditions show that the proposed SVC adaptive controller can provide good damping over a wide range and improve the dynamic performance of the power system. It is preferable to apply the SAPSS on the SVC than on the generator. The dynamic and transient stability margin is also increased with the proposed SAPSS.

Chapter 5

APPLICATION OF SAPSS IN A MULTI-MACHINE SYSTEM

5.1 Introduction

Multi-modal oscillations appear in a multi-machine power system in which the interconnected generating units have quite different inertia constants and are weakly connected by transmission lines. These oscillations are generally analyzed in three main oscillation modes, i.e. local, inter-area and inter-machine modes. Depending upon their location in the system, some generators participate in only one oscillation mode, while others participate in more than one mode [82].

Advances in power electronics have enabled the introduction of powerful tools namely, FACTS devices. Although originally FACTS devices were introduced to improve power system operation, such as transmission line loading, voltage control, etc., they can also help in improving power system dynamic stability and damping low frequency oscillations if provided a suitable supplementary control.

One of the important FACTS devices is the SVC. Angular speed deviation, frequency deviation, transmission line active and reactive power deviation are used as supplementary signals to improve damping through the SVC control concept [83]. In this chapter, the proposed SAPSS is used to provide an auxiliary power deviation signal to the SVC to damp multi-mode oscillations in a multi-machine system.

5.2 System Configuration and Model

A five machine power system without infinite bus, shown in Fig. 5.1, is used to evaluate the performance of the proposed SAPSS in the multi-machine system. Five generating units are connected through a transmission network. Generators G_1 , G_2 and G_4 have much larger capacities than G_3 and G_5 . All generators are equipped with governors, exciters, AVR and governors include CPSSs.

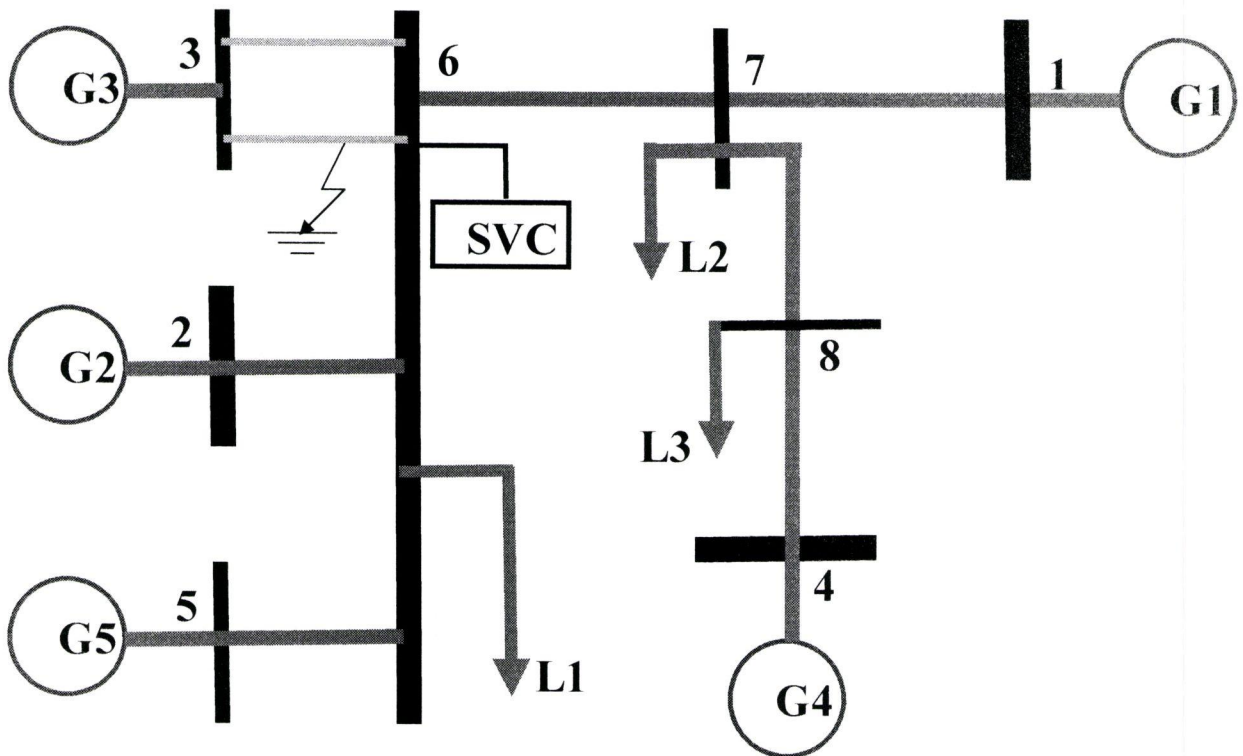


Fig. 5.1 A five machine power system model including the SVC

The generating units are modeled by five first order differential equations. Generators G_2 , G_3 and G_5 may be considered to form one area and generators G_1 and G_4 a second area. The two areas are connected through a tie-line connecting buses #6 and #7. Under normal conditions, each area serves its own load and is almost fully loaded with a small load flow over the tie-line [10].

Stabilizer is modeled as described in Chapter 4. Figure 4.3 in chapter 4 shows the block diagram of the SVC with the supplementary Adaptive Control and Eqns 4.4 – 4-6 represent the dynamic SVC action for variation in the SVC susceptance. Parameters of all generators, governors, exciters, AVRs, transmission lines, SVC, loads and operating conditions are given in Appendix B.

The simulation of the system model containing the SVC is done using Matlab's Simulink toolbox. The system model is identified as a third order discrete model of the form described in Eqns 4.1- 4.3 in Chapter 4.

5.2.1 Placement of SVC

Allocating the SVC in the multi-machine system plays an important role for low frequency oscillation damping. Literature [84] describes several steps for a technique to determine the best location for the SVC to have a good damping performance. It describes an approach developed to define SVC location for small signal stability enhancement.

In this study, by observation of the results of an extensive series of tests performed on the system model, it has been found that, to get good damping, the best choice is to install the static VAr compensator at bus #6 of the multi-machine system.

The comparison is done between all buses in the system, but performance for only the best three buses, 6, 7, and 8 for the location of the SVC is shown in Fig. 5.2. This figure shows that bus #6 is the best location for the SVC in the multi-machine model system. Speed deviation of generator #3 and the deviation of power flow of the tie line 6-

7 are used as alternate input signals to the damping loop of the SVC controller, and their performance is compared.

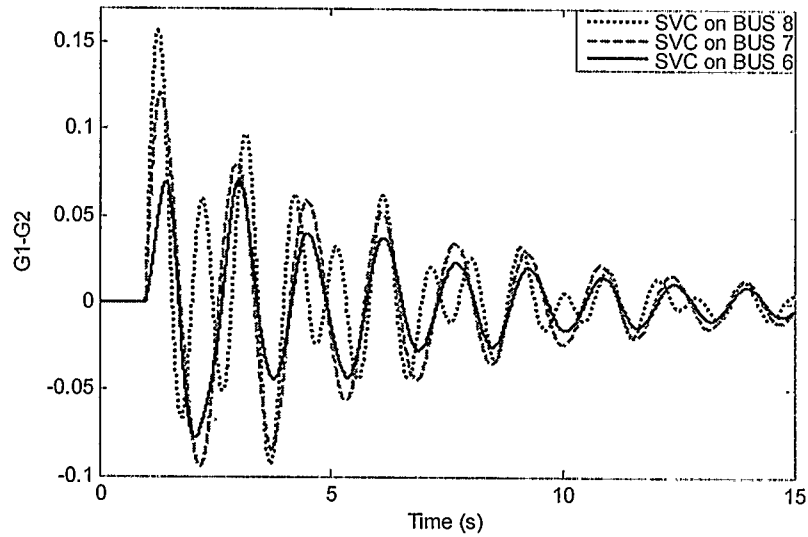


Fig. 5.2 Response of speed deviation of G1-G2

5.3 System Identification

The recursive least squares identification method, described in chapters 2 and 4 with varying forgetting factor, is also used for the design of the self-tuning controller for application on the multi-machine system.

In order to verify the performance of the RLS identification algorithm during a large disturbance, a three- phase line to ground short circuit was applied at the middle of one of the transmission lines between bus #3 and bus #6 of the multi- machine system at 1s, while the system was operating at the operating point given in Appendix B without any PSS. The fault was cleared 50 ms later by the disconnection of the faulted line and it was successfully reclosed after 16s. Figures 5.3 through 5.6 show typical curves for the

identification output signal tracking the output of the system, the forgetting factor variation, and the convergence of the identified A and B parameters of the system given in Fig. 5.1 when the supplementary stabilizing signal to the identifier and the controller is the speed deviation of generator #3. Figures 5.7 through 5.10 show typical curves for the identification output signal tracking the output of the system, the forgetting factor variation, and the convergence of the identified A and B parameters of the system given in Fig. 5.1 when the power deviation of the tie-line 6-7 is the supplementary stabilizing signal to the identifier and the controller.

It can be seen from the results in Figs. 5.3 through 5.10 that the use of power deviation of the tie-line 6-7 as the signal to track the output of the system is much better than the use of the speed deviation of generator #3.

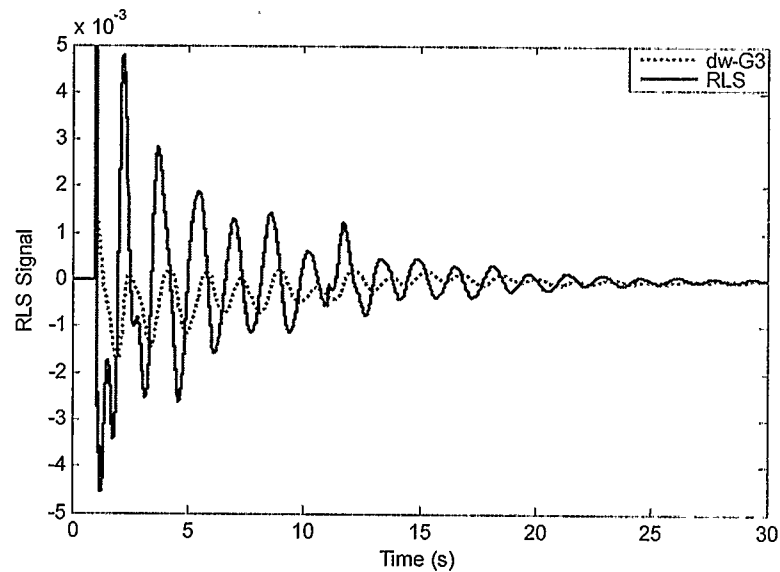


Fig. 5.3 Response of the angular speed deviation of G3 and RLS output

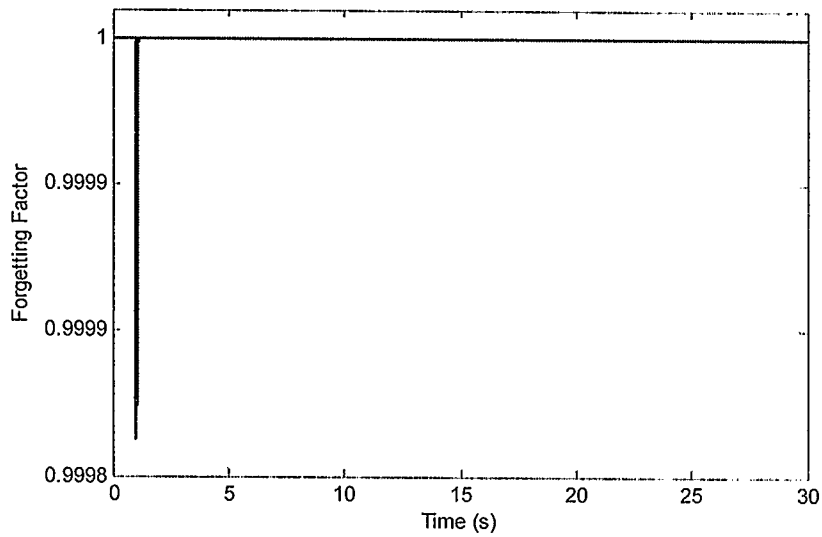


Fig. 5.4 Forgetting factor variation

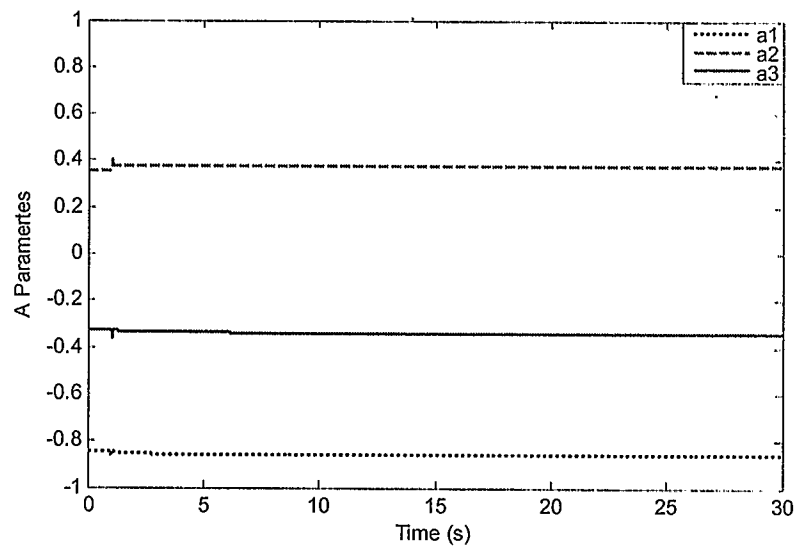


Fig. 5.5 Response of A parameters on-line variation

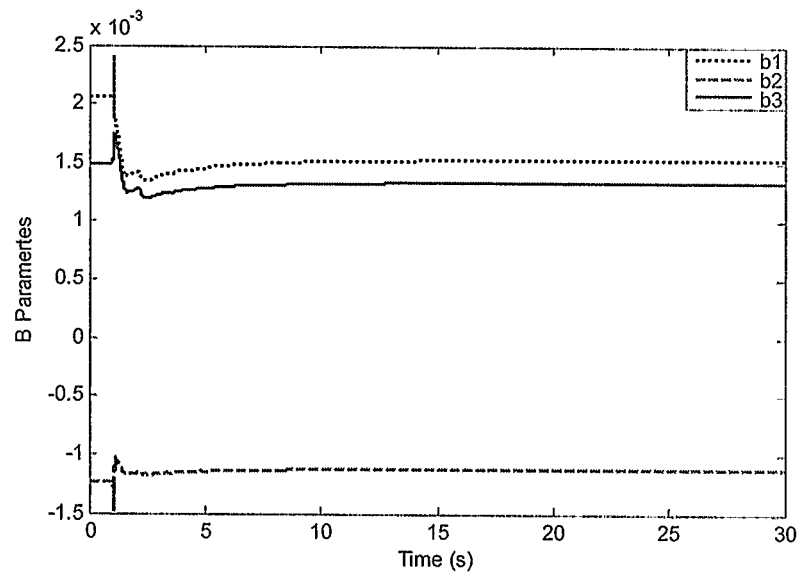


Fig. 5.6 Response of B parameters on-line variation

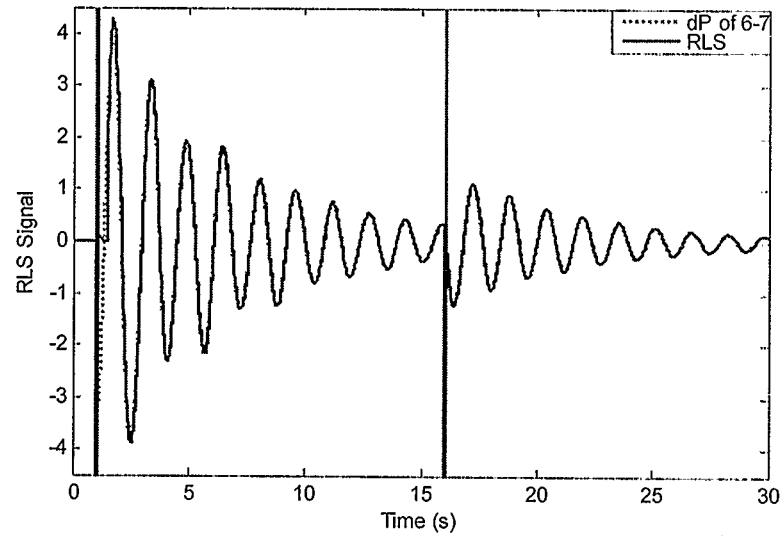


Fig. 5.7 Response of power deviation of tie-line 6-7 and RLS output

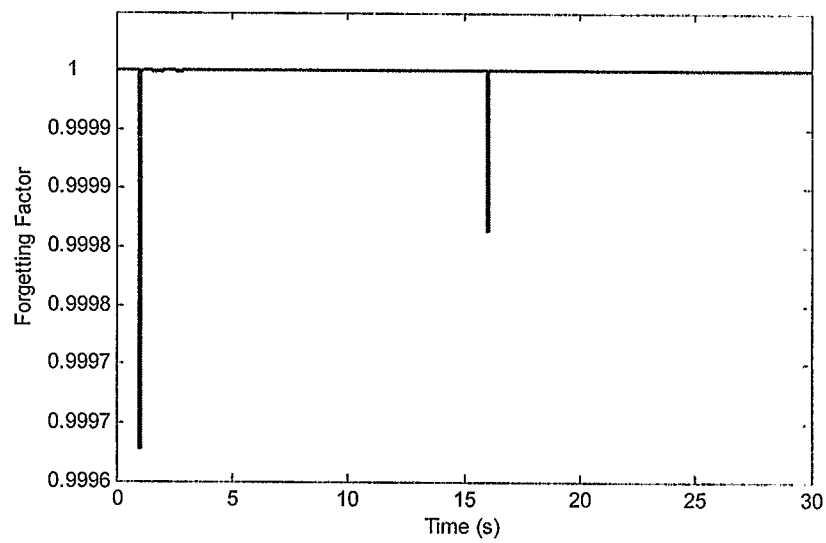


Fig. 5.8 Forgetting factor variation

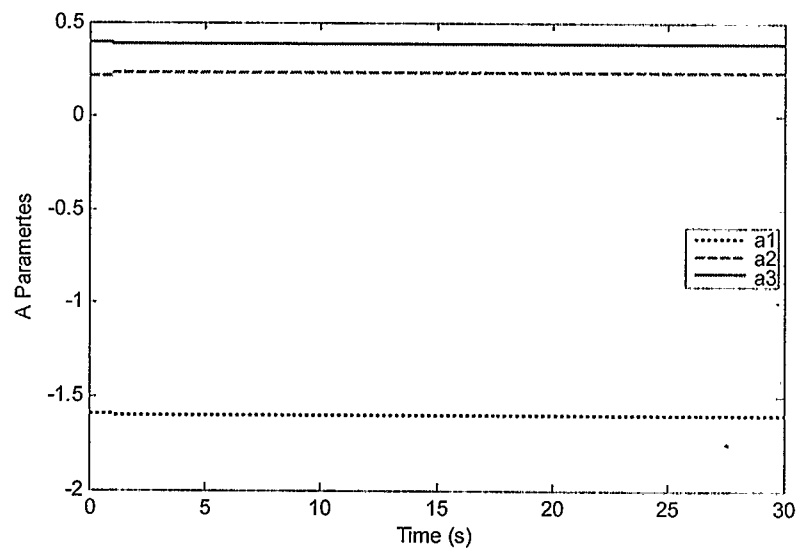


Fig. 5.9 Response of A parameters on-line variation

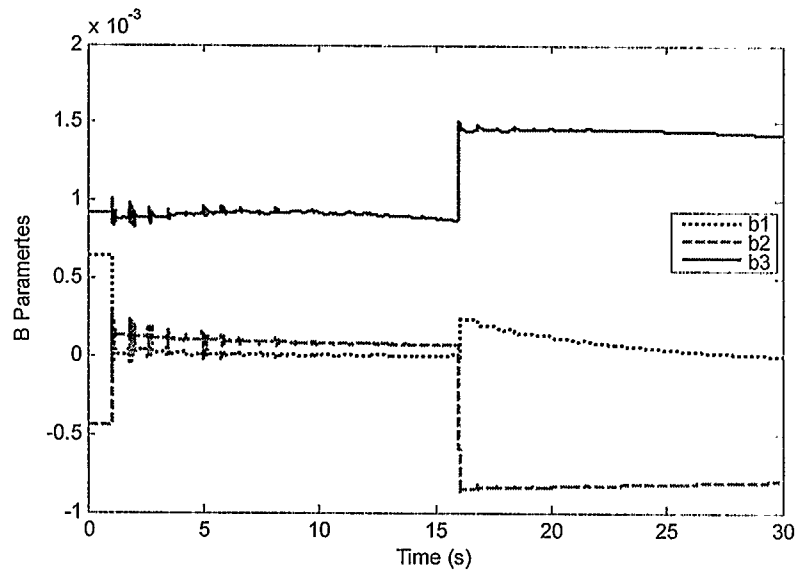


Fig. 5.10 Response of B parameters on-line variation

5.4 Control Strategy

As mentioned before, the control strategy designed for the self-tuning control is based on the assumption that the parameters of the system model are known. Once the system model is identified, the control signal can be calculated based on the identified model. In this study, the pole-shifting control algorithm is employed in the SVC controller and applied on the multi-machine system to increase the damping of the system oscillation.

The characteristics and equations that explain the algorithm of the PS control are described in chapters 3 and 4.

5.5 Simulation Studies

A non-linear fifth-order model is used to simulate the dynamic behavior of the multi-machine power system. The differential equations used to simulate the synchronous generators and the parameters used in simulation studies are given in Appendix B. The AVR/Exciter and CPSS refer to IEEE Standard 421.5 Type ST1A AVR and Exciter Model and an IEEE Standard 421.5 PSS1A Type CPSS [85]. Active dynamic signal from the system sampled at the rate of 50Hz is used as the input for the identification and control computation. Most of the tests in this study are done using the power deviation of the tie-line 6-7. The absolute limits for the control output are set at $\pm 0.1 p.u.$ and the absolute limits for the SVC output are set at $\pm 0.15 p.u.$ [80].

Due to the different sizes of the generators and system configuration, multi-mode oscillations occur when the system experiences a disturbance. In order to observe this fact, a three phase to ground fault was applied at the middle of one transmission line between buses 3 and 6 at 1s, while the system was operating without any PSS at the operating point given in Appendix B, and cleared 50ms later by removing the faulted line. At 16s, the faulted transmission line was restored successfully and the system returned to its initial condition.

Oscillations in Figs.5.11- 5-13 show the local and the inter-area modes. These two frequencies differ significantly due to the large difference in the inertias of the generators. The response of speed difference between G_1 and G_2 in Fig. 5.11 shows the inter-area

mode oscillations, while the response of speed difference between G_2 and G_3 in Fig. 5.12 exhibits mainly the local mode oscillations in the first part.

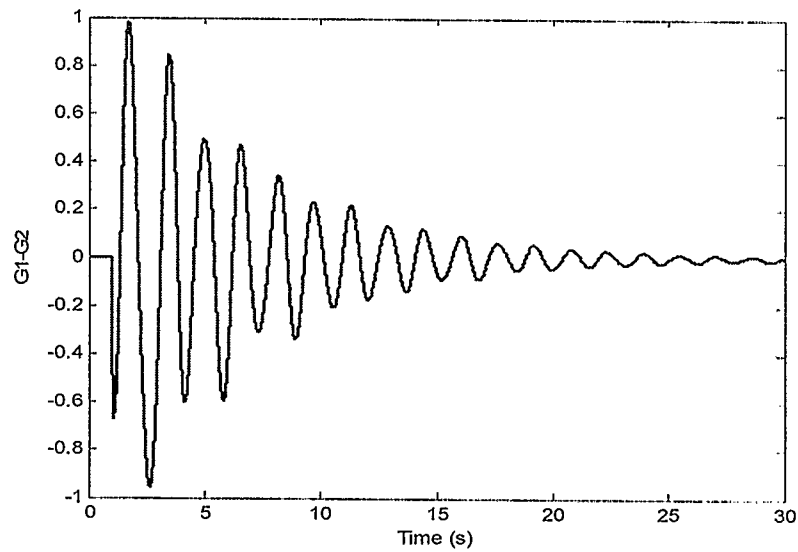


Fig. 5.11 Response of speed deviation of G1-G2

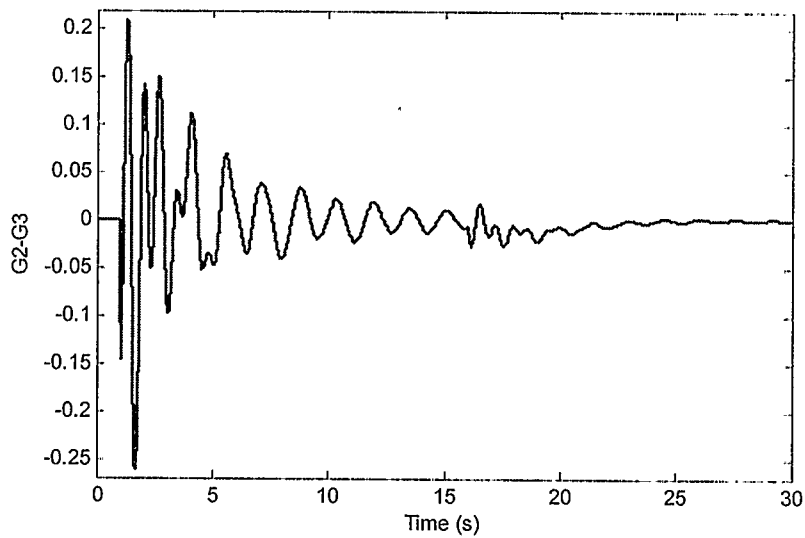


Fig. 5.12 Response of speed deviation of G2-G3

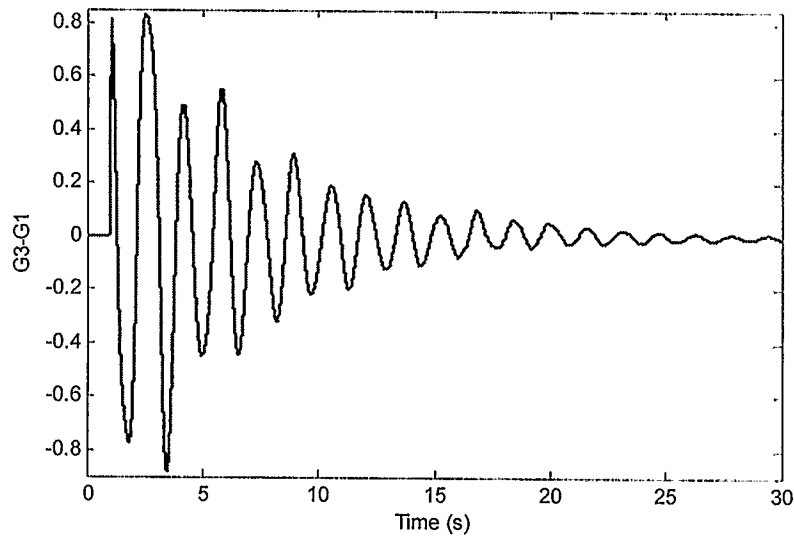


Fig. 5.13 Response of speed deviation of G3-G1

5.5.1 Change of the Input Reference Torque

5.5.1.1 Speed Deviation of Generator #3 as Supplementary Stabilizing Signal

In order to verify the performance of the proposed SAPSS during disturbances on the multi-machine system when the identification and controller use the speed deviation of generator #3 as the supplementary stabilizing signal, a 0.1pu step decrease in input torque reference of G_3 is applied at 1s with the system working at the operating point given in Appendix B. From the results shown in Figs 5.14 through 5.16, it can be seen that the SAPSS damps out the inter-area mode oscillations in Fig 5.14, but there is hardly any effect on the local mode oscillations, Fig. 1.15.

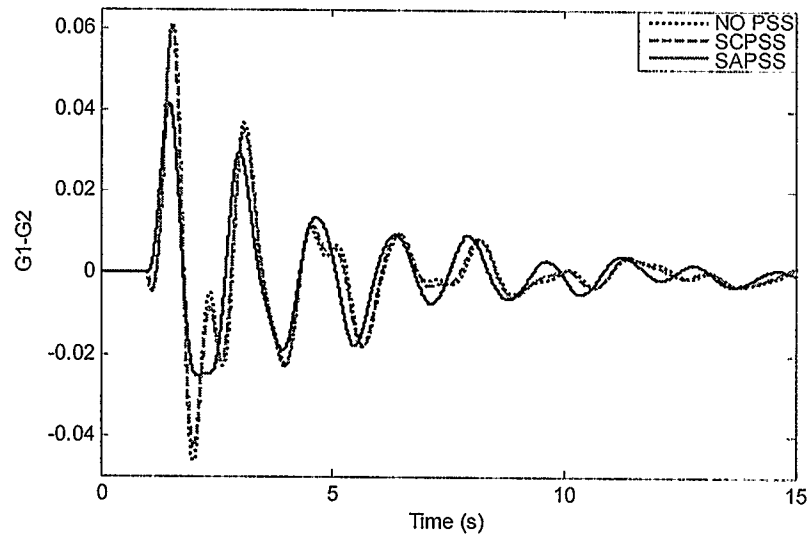


Fig. 5.14 Response of speed deviation of G1-G2

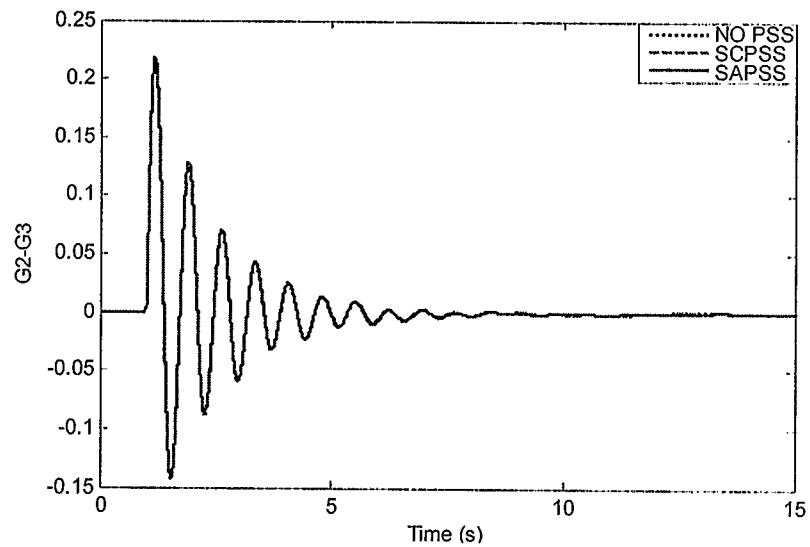


Fig. 5.15 Response of speed deviation of G2-G3

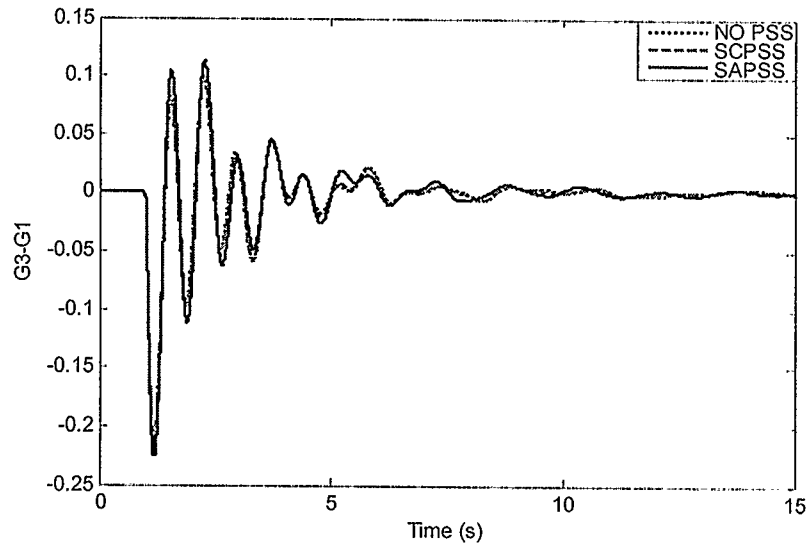


Fig. 5.16 Response of speed deviation of G3-G1

5.5.1.2 Power Deviation of the Tie-Line 6-7 as Supplementary Stabilizing Signal

In order to verify the performance of the proposed SAPSS during disturbances on the multi-machine system when the identification and controller use the power deviation of tie-line 6-7 as the supplementary stabilizing signal, a 0.1pu step decrease in input torque reference of G_3 is applied at 1s while the system was working at the operating point given in Appendix B. As shown in Figs 5.17 through 5.19, the proposed SAPSS damps out the inter-area mode oscillations effectively, Fig 5.17, than in Fig. 5.14 with speed deviation as input signal. However, the same influence on the local mode oscillations as seen in Fig 5.18 is still negligible. This is because the supplementary stabilizing signal is derived from the power oscillations in the line between buses 6 and 7 connecting the two areas.

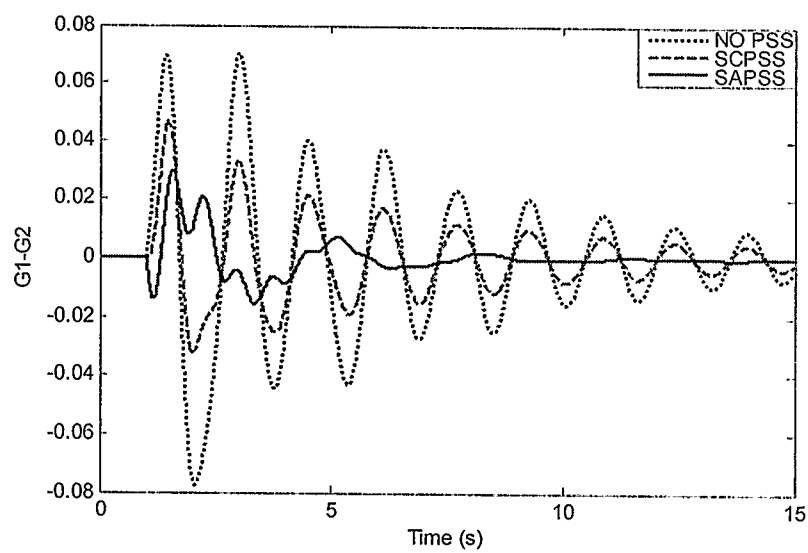


Fig. 5.17 Response of speed deviation of G1-G2

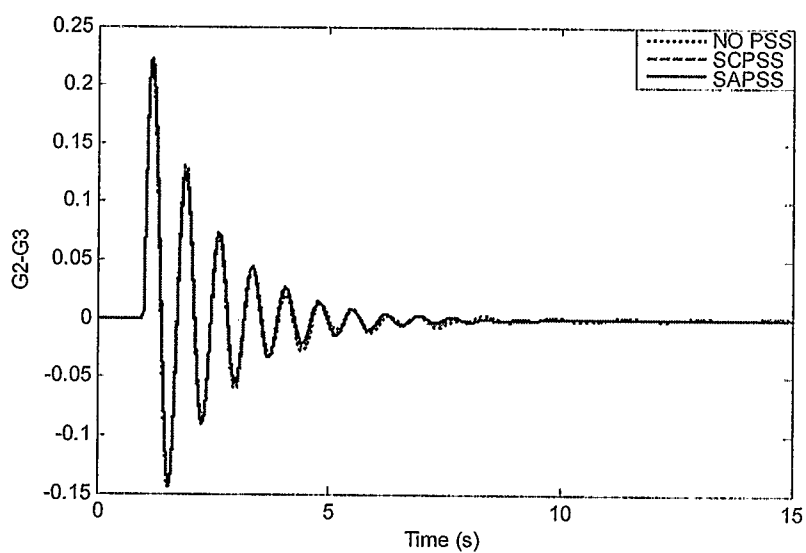


Fig. 5.18 Response of speed deviation of G2-G3

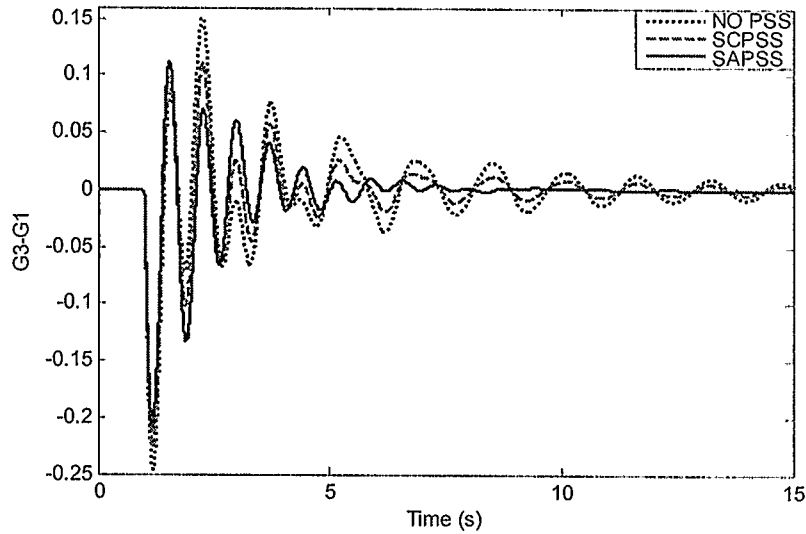


Fig. 5.19 Response of speed deviation of G3-G1

5.5.2 Three-Phase to Ground Short Circuit

With the power system operating at the same operating conditions, a three phase to ground fault was applied at the middle of one transmission line between buses 3 and 6 at 1s and cleared 50ms later by removing the faulted line. At 16s, the faulted transmission line was restored successfully. Response of the system under this large disturbance with NO PSS, with SCPSS and with the proposed SAPSS, using power deviation of the tie-line 6-7 as the supplementary stabilizing signal, is shown in Figs 5.20 - 5-22. It can be seen that the proposed SAPSS damps out the oscillations effectively.

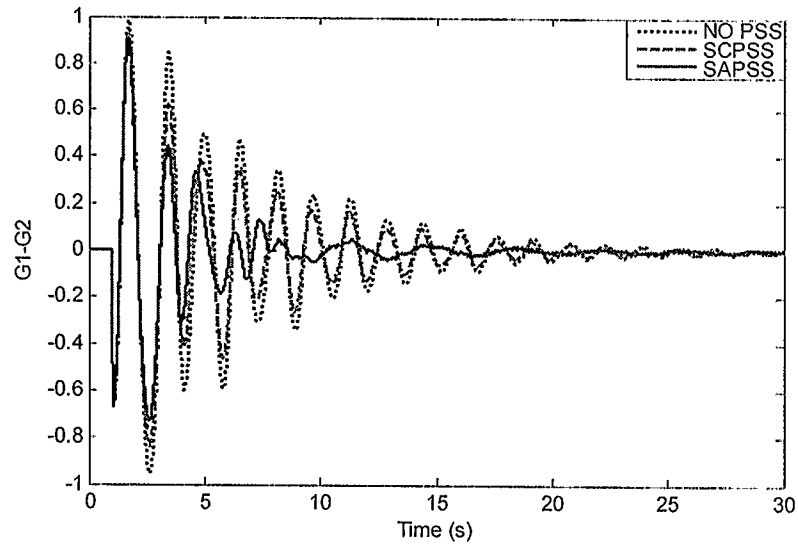


Fig. 5.20 Response of speed deviation of G1-G2

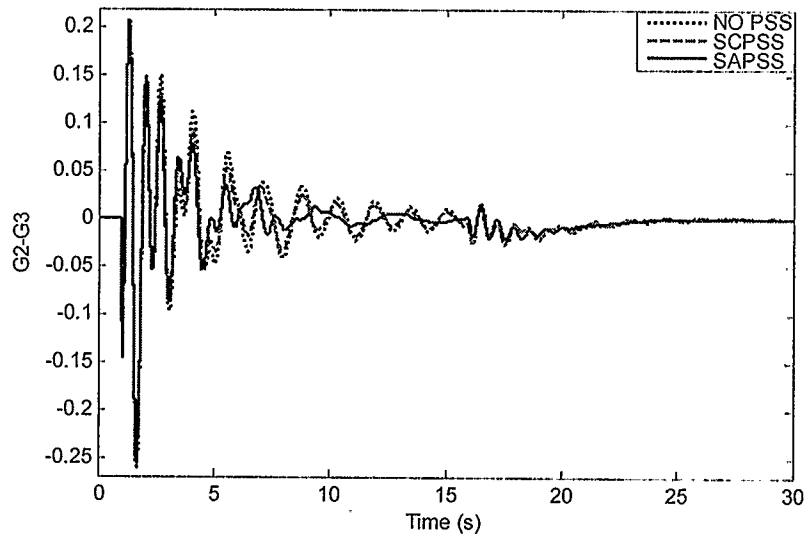


Fig. 5.21 Response of speed deviation of G2-G3

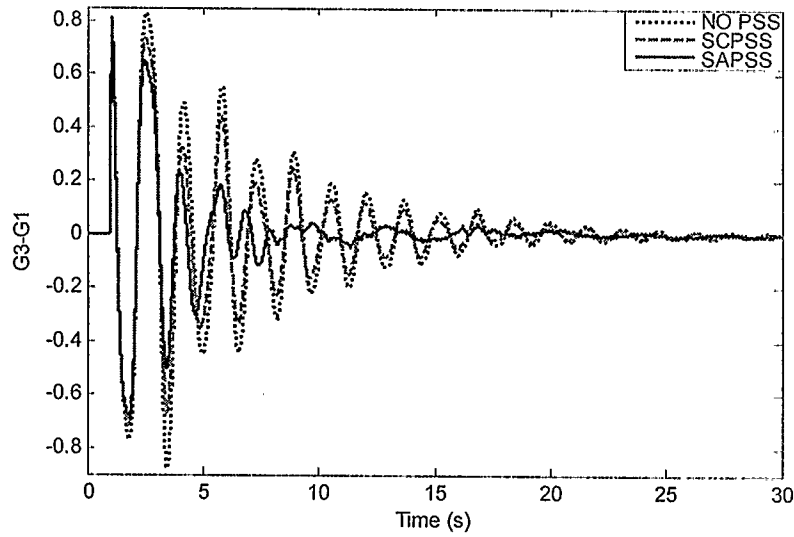


Fig. 5.22 Response of speed deviation of G3-G1

5.6 Summary

This chapter has demonstrated the effectiveness of the proposed SAPSS in damping the inter-area mode of oscillation in multi-machine power system. The test results indicate that the proposed SAPSS using the supplementary stabilizing signal derived from the power oscillations in the line between buses 6 and 7 has more influence on damping the system oscillations, especially on damping the inter-area mode oscillations, than the SAPSS using the supplementary stabilizing signal from the speed deviation of generator #3. That is because the power deviation signal is derived from the point where the inter-area oscillations mode appear. It affects the response of the system much better than the generator #3 speed deviation in general.

Chapter 6

CONCLUSIONS

6.1 Conclusions

It has been proven early that power system stabilizers are very effectiveness in enhancing the stability of the power system. Numerous theoretical studies and experimental tests have been conducted to better understand the behaviour of the PSS and to make it more applicable in practice.

The flexible ac transmission system (FACTS) is one of two main systems used to damp system oscillations. It also demonstrates good performance in damping oscillations for a wide rang of operating conditions. The most commonly used of the FACTS devices is static var compensator (SVC). It was almost the first kind of reactive power and voltage control device. It is especially suitable for voltage control of long distance bulk power transmission lines, but can also be used to improve the dynamic and transient stability of power systems. To enhance the performance of an SVC, in addition to the voltage control, a supplementary control, either conventional or adaptive, is required. The importance of using different types of PSSs in power systems is discussed in Chapter 1.

Due to the nonlinear time varying characteristics of the power system, the conventional fixed-parameter controllers (CPSSs) pose operational challenges to the operator. The performance of a CPSS is inadequate at different operating conditions. The power quality and stability margin is sacrificed when the CPSS is not able to improve the

performance at all operating conditions. This indicates the need for some type of adaptive stabilizer that tracks the operating conditions of the system.

This dissertation focuses on the following primary issues:

1. First, investigate the development of a controller that can draw the attention in the control engineering area. Control engineers are often faced with conflicting issues. The conventional controllers are inadequate in terms of performance and the required manual tuning of the parameters. This issue has been addressed in this study by choosing a compromise solution such as applying the self-tuning concept that employs a recursive identification method for obtaining a model of the plant to the level necessary and applies a PS-Control as a linear feedback controller [34, 57, 73] because of its simplicity and acceptance.
2. Second, focusing on determining a suitable identification technique to represent the dynamic characteristics of the power system. Although the techniques for on line adaptation are becoming fairly standard, in a real power system environment the demands placed upon adaptive estimation and control techniques can be extremely severe. Based on a comparison of the performance of the two identification techniques, RLS and KF, it has been found that the RLS with variable forgetting factor is more appropriate for this application.
3. Third, focusing on the PS-Control algorithm. A pole-shift factor α is introduced in the closed-loop polynomial. The optimal value of α is found

based on performance index minimization. The upper and lower bounds on α are also found by restricting the closed-loop poles within the unit circle in the z -domain for stability. Once the value of α is realized based on the above two criteria, it is substituted in the feedback control equations to find the control signal to be applied as a supplementary control signal every sampling interval. The number of coefficients required to be tuned in the PS-control is nil. Hence the self-tuning property is achieved to its fullest extent [73].

4. Fourth, apply the proposed adaptive SVC controller with its supplementary adaptive control signal in the single-machine power system and multi-machine power system to verify the performance of the proposed SAPSS on the two systems under different operating conditions. The simulation results show that the proposed SAPSS has high effectiveness for damping the system oscillations on both systems. The self-coordination ability of the proposed SAPSS with other SCPSS is also demonstrated.

6.2 Future Work

Power system stability still requires much work in order to achieve the suitable threshold of operating systems. This study opens lots of new ways that need to be investigated in the area of self-tuning control. However, the following points are suggested for further research in the near future:

1. The proposed SVC adaptive controller is required to be realized physically first in a laboratory environment to verify the effectiveness of the identification and the

control theories on a physical system.

2. Replace the SVC with one of the new brand of FACTS devices and design a self-tuning controller to damp system oscillations, for example, Thyristor-Controlled Series Capacitor (TCSC), or Unified Power Flow Controller (UPFC).
3. Apply another identification algorithm instead of the RLS to make comparison between them in identifying and tracking the system parameters, such as genetic algorithm or fuzzy logic.
4. Apply another control technique instead of the PS to make comparison between them in damping the system oscillations, for example, neural networks.

REFERENCES

- [1] C. W. Taylor, "Improving grid behavior ," IEEE Spectrum, vol. 36, no. 6, 1999, pp. 40-45.
- [2] M. Klien, G. J. Rogers, and P. Kundur, "A fundamental study in interarea oscillations in power systems," IEEE Trans. On power system, vol. 6, no. 3, August 1991, pp. 914-921.
- [3] E. V. Larsen, J. J. Sanchez-Gasca, and J. H. Chow, "Concepts for design of FACTS controllers to damp power swings," IEEE Trans. On power systems, vol. 10, no. 2, May 1995, pp. 948-955.
- [4] P.M. Anderson and A.A. Fouad, "Power System Control and Stability", IEEE Press, Piscataway, NJ, 1994.
- [5] W.A. Wittelstadt, "Four Methods of Power System Damping", IEEE Trans. on Power Apparatus and Systems, vol. PAS-88, Jan. 1969, pp. 28-35.
- [6] P.K. Dash, B. Puthal, O.P. Malik and G.S. Hope, "Transient Stability and Optimal Control of Parallel AC-DC Power Systems", IEEE Trans. on Power Apparatus and Systems, vol. PAS-95, March 1976, pp. 811-820.
- [7] S.N. Iyer and B.J. Cory, "Optimal Control of a Turbo-Generator including an Exciter and Governor", IEEE Trans. on Power Apparatus and Systems, vol. 11, no. 2, June 1971, pp. 2142-2149.
- [8] J.A. Dineley, A.J. Morries and C. Preece, "Optimal Transient Stability from Excitation Control of Synchronous Generators", IEEE Trans. on Power Apparatus and Systems, vol. PAS-87, Aug. 1968, pp. 1696-1705.

- [9] O.P. Malik, G.S. Hope and S.J. Cheng, "Design and Test Results of a Software Based Digital AVR", IEEE Trans. on Power Apparatus and Systems, vol. PAS-89, no. 5, 1976, pp. 634-642.
- [10] Wael Hussien, "Studies on a Duplicate Adaptive PSS", Master of Science Thesis, Department of Electrical Engineering, University of Calgary, Canada, 2002.
- [11] N.A. Vovos and G.D. Galanos, "Enhancement of the Transient Stability of Integrated AC/DC Systems Using Active and Reactive Power Modulation", IEEE Trans. on Power Apparatus and Systems, vol. 104, 1985, pp. 1696-1702.
- [12] T. Smed and G. Anderson, "Utilizing HVDC to Damp Power Oscillations", IEEE Trans. on Power Delivery, vol. 8, no. 2, 1993, pp. 620-625.
- [13] E.Lerch, D. Povh and X. Lu, "vanced SVC Control for Damping Power System Oscillations", IEEE Trans. on Power Systems, vol. 6, no. 2, 1991, pp. 524-531.
- [14] P.S. Dolan, J.R. Smith and W.A. Wittelstadt, "A Study of TCSC Optimal Damping Control Parameters for Different Operating Conditions", IEEE Trans. on Power Systems, vol. 10, no. 4, 1995, pp. 1972-1977.
- [15] Narain G. Hingorani, "Flexible AC Transmission", IEEE Spectrum, vol. 30, no. 4, April 1993, pp. 40-45.
- [16] F.P. De-Mello and C.A. Arnold, "Concepts of Synchronous Machine Stability as Affected by Excitation Control", IEEE Trans. on Power Apparatus and Systems, vol. PAS-88, no. 4, April 1969, pp. 316-329.
- [17] E.V. Larsen and D.A Swann, "Applying Power System Stabilizers, Part I-III", IEEE Trans. on Power Apparatus and Systems, vol. PAS-100, June 1981, pp. 3017-3046.

- [18] Yao-Nan Yu, "Electric Power System Dynamics", Academic Press 1983.
- [19] C. Raczkowski, "Complex Root Compensator – A New Concept for Dynamic Stability Improvement", IEEE Trans. on Power Apparatus and Systems, vol. PAS-93, Sept. 1974, pp. 1842-1848.
- [20] P. Kundur, D.C. Lee and H.M. Zein El-Din, "Power System Stabilizers for Thermal Units: Analytical Techniques and On-Site Validation", IEEE Trans. on Power Apparatus and Systems, vol. PAS-100, no. 1, Jan. 1981, pp. 81-95.
- [21] W. Watson and G. Manchur, "Experience With Supplementary Damping Signal for Generator Static Excitation Systems", IEEE Trans. on Power Apparatus and Systems, vol. PAS-92, 1973, pp. 199-211.
- [22] R.W. Farmer, "State-of-the-art Technique for System Stabilizer Tuning", IEEE Trans. on Power Apparatus and Systems, vol. PAS-102, 1983, pp. 699-709.
- [23] K. Bollinger, A. Laha, R. Hamilton and T. Harras, "Power Stabilizer Design Using Root Locus Method", IEEE Trans. on Power Apparatus and Systems, vol. PAS-94, 1975, pp. 1484-1488.
- [24] A. Doi and S. Abe, "Coordinated Synthesis of Power System Stabilizer in Multi-Machine Power System", IEEE Trans. on Power Apparatus and Systems, vol. PAS-103, no. 6, June 1984, pp. 1473-1479.
- [25] R.J. Fleming, M.A. Mohan and K. Parvatisam, "Selection of Parameters of Stabilizers in Multi-Machine Power System", IEEE Trans. on Power Apparatus and Systems, vol. PAS-100, no. 5, May 1981, pp. 2329-2333.

- [26] W.C. Chan and Y.Y. Hsu, "An Optimal Variable Structure Stabilizer for Power System Stabilization", IEEE Trans. on Power Apparatus and Systems, vol. PAS-102, 1983, pp. 1738-1746.
- [27] D.A. Pierre, "A Perspective on Adaptive Control of Power Systems", IEEE Trans. on Power Systems, vol. PWRS-2, no. 5, Sep. 1987, pp. 387-396.
- [28] K.J. Astrom and W. Watson, "On Self-Tuning Regulators", Automatica, vol. 9, 1973, pp. 185-199.
- [29] I.D. Landau, "A Survey of Model Reference Adaptive Techniques: Theory and Application", Automatica, vol. 10, 1974, pp. 353-379.
- [30] K.J. Astrom and B. Wittenmark, "Adaptive Control", Addison Wesley Publishing Company, Reading, MA, 1995.
- [31] I.D. Landau, R. Lozano and M. M'Saad, "Adaptive Control", Springer, London, 1995.
- [32] V. Strejc, "Least Squares Parameter Estimation", Automatica, vol. 16, no. 1980, pp. 535-550.
- [33] E. Irving, J.P. Barret, C. Charcossey and J.P. Monvillf, "Improving Power Network Stability and Units Stress with Adaptive Generator Control", Automatica, vol. 15, 1979, pp. 31-46.
- [34] A. Ghosh, G. Ledwich, O.P. Malik and G.S. Hope, "Power System Stabilizer Based on Adaptive Control Techniques", IEEE Trans. on Power Apparatus and Systems, vol. PAS-103, Aug. 1984, pp. 1983-1986.
- [35] L. Ljung, "System Identification – Theory for User", Prentice Hall, Englewood Cliffs, NJ, 1987.

- [36] T.R. Fortescue, L.S. Kershenbaum and B.E. Ydstie, "Implementation of Self-Tuning Regulators with Variable Forgetting Factors", *Automatica*, vol. 17, no. 6, 1981, pp. 831-835.
- [37] P.S. Sanoff and P.E. Wellstead, "Comments on Implementation of Self-Tuning Regulators with Variable Forgetting Factors", *Automatica*, vol. 19, 1983, pp. 345-346.
- [38] M.B Zarrop, "Variable Forgetting Factors in Parameter Estimation", *Automatica*, vol. 19, 1983, pp. 295-298.
- [39] T. Soderstrom, L. Ljung and I. Gustavsson, "A Theoretical Analysis of Recursive Identification Method", *Automatica*, vol. 20, 1984, pp. 231-244.
- [40] G.C. Goodwin and R.L. Payne, "Dynamic System Identification: Experiment Design and Data Analysis", Academic Press, New York, San Fransisco, U.S.A., 1977.
- [41] K.J. Astrom, U. Borisson, L. Ljung and B. Wittenmark, "Theory and Applications of Self-Tuning Regulators", *Automatica*, vol. 13, 1977, pp. 457-476.
- [42] D.W. Clark and P.J. Gawthrop, "A Self-Tuning Controller", *IEE Proceedings*, vol. 122, 1975, pp. 929-934.
- [43] B. Wittenmark and K.J. Astrom, "Practical Issues in the Implementation of Self-Tuning Control", *Automatica*, vol. 20, no. 5, 1984, pp. 595-605.
- [44] U. Borrisson and R. Syding, "Self-Tuning Control of an Ore Crusher", *Automatica*, vol. 12, 1976, pp. 1-7.
- [45] P.E. Wellstead, D. Prager and P. Zanker, "Pole Assignment Self-Tuning Regulator", *IEE Proceedings*. Vol. 126, no. 8, Aug. 1979, pp. 781-787.

- [46] D.W. Clark, "Model Following and Pole-Placement Self-Tuners", Optimization Control and Applied Mathematics, vol. 3, 1982, pp. 323-335.
- [47] A. Ghosh, G. Ledwich, O.P. Malik, G.S. Hope, "An Adaptive Synchronous Machine Stabilizer", IEEE Trans. on Power Apparatus and Systems, vol. PWRS-1, no. 3, 1986, pp. 101-109.
- [48] O.P. Malik, G.P. Chen, G.S. Hope, Y.H. Qin and G.Y. Xu, "An Adaptive Self-Optimizing Pole-Shifting Control Algorithm", IEE Proceedings Part-D, vol. 139, no. 5, 1992, pp. 429-438.
- [49] Xuechun Yu, "Robustness Analysis and Controller Design for Static VAR Compensator in Power System", Ph. D. Thesis, Electrical Engineering, Iowa State University, U.S.A., 2000.
- [50] S. Chen, S.A. Billings and P.M. Grant, "Non-linear Systems Identification Using Neural Networks", Int. J. Control, vol. 51, 1990, pp. 1191-1214.
- [51] S. Chen, S.A. Billings and P.M. Grant, "Recursive Hybrid Algorithm for Non-Linear System Identification Using Radial Basis Function Networks", Int. J. Control, vol. 55, no. 5, 1992, pp. 1051-1070.
- [52] T.Soderstrom, L. Ljung and I. Gustavsson, "A Theoretical Analysis of Recursive Identification Method" Automatica, Vol. 14, 1978 pp 231-244.
- [53] L. Ljung and T.Soderstrom, "Theory and Practice of Recursive Identification", The MIT Press Cambridge, Massachusetts London, England, 1983.
- [54] V. Strejc "Trends in Identification" Automatica vol. 17 1981 pp 7-21.
- [55] A.P. Sage and J.A. Melsa, "System Identification", Academic Press, New York and London, 1971.

- [56] P. Eykhoff, "System Identification – A Survey", Wiley London, 1974.
- [57] Shi-Jie Cheng, "A Self-Tuning Power System Stabilizer", Ph. D. Thesis, Department of Electrical Engineering, University of Calgary, Canada, 1986.
- [58] K. J Astrom and P. Eykhoff "System Identification – A survey" *Automatica* vol. 17 1971 pp 123-162.
- [59] V. S. Levadi "Design of input signals for Parameter Estimation" *IEEE Trans.* Vol. AC-11 1966 pp 205-211.
- [60] Y.S. Chow, "A Micro Processor Based Stabilizer", M.Sc. Thesis, Department of Electrical Engineering, University of Calgary, Canada, 1985.
- [61] J. Gertter and Cz. Banfasz, "A Recursive (on-line) Maximum likelihood Identification Method" *IEEE Trans. Aut. Control* vol. AC-19 1974 pp 816-820.
- [62] V. Peterka, "Bsyesian System Identification" *Automatica* vol. 17 1981 pp 41-53.
- [63] G. J. Bierman, "Factorization Method for Discrete Sequential Estimation" Academic Press New York 1977.
- [64] Toresten Soerstorm, " System Identification", Prentice Hall International, 1989.
- [65] R. Lezano, "Independent Tracking and Regulation Adaptive Control with Forgetting Factor", *Automatica* vol. 18. 1982 pp 455-459.
- [66] B. Wittenmark and KJ. Astrom, "Practical Issues in the Implementation of Self-Tuning Control", *Automatica*, Vol.20, 1984, pp. 595-605.
- [67] P.E. Wellstead and S.P. Sanoff, "Extended Self-Tuning Algorithm", *Int. J. Control*, Vol. 34, No. 3, 1981, pp. 433-456.
- [68] R.G. Cheetham, "A Turbo-Generator Self-Tuning Voltage Regulator" *Int. J. Control*, Vol. 36, 1982, pp. 127-142.

- [69] K. Latawiec and M. Chyra, "On Low Frequency and Long-Run Effects in Self-Tuning Control" *Automatica* Vol.19 1983 pp419-424.
- [70] S.J. Cheng, Y.S. Chow, O.P. Malik, G.S. Hope, "An Adaptive Synchronous Machine Stabilizer", *IEEE Trans. on Power Systems*, vol. PWRS-1, no. 3, 1986, pp. 101-109.
- [71] G.P. Chen and O.P. Malik and G.S. Hope and Y.H. Qin and G.Y. Xu, "An Adaptive Power System Stabilizer Based on the Self-Optimizing Pole Shifting Control Strategy", *IEEE Trans. on Energy Conversion*, vol. EC-8, Dec. 1993, pp. 639-646.
- [72] A. Y. Allidina, and F .M. Hughes, "Generalized Self-Tuning Controller with Pole-Assignment", *IEE Proceedings*, vol. 127, 1980, pp. 13-18.
- [73] G.P. Chen, "An Adaptive Self-Optimizing Power System Stabilizer", Ph.D. Dissertation, The University of Calgary, Calgary, Canada, February 1994.
- [74] Ramakrishna Gokaraju, "Beyond Gain-Type Scheduling Controllers: New Tools for Identification and Control for Adaptive PSS", Ph.D. Dissertation, The University of Calgary, Calgary, Canada, May 2000.
- [75] E. Swidenbank and S. McLoone and D. Flynn and G.W. Irwin and M.D. Brown and B. W. Hogg, "Neural Network Based Control for Synchronous Generators", *IEEE Trans. on Energy Conversion*, vol. 14, no. 4, Dec. 1999, pp. 1673-1679.
- [76] A.Y. Zomaya P.M. Mills and M.O. Tade, "Neuro-Adaptive Process Control- A Practical Approach", John Wiley & Sons, NY, U.S.A., 1996.
- [77] C. J. Harris and S. A. Billings, "Self-Tuing and Adaptive Control", *Inst. Of Electrical Engineers, Control Engineering Series*, 15, London 1981.

- [78] Shi-Jie Cheng, Y. S. Chow, O. P. Malik and G. S. Hope, "An Adaptive Synchronous Machine Stabilizer", IEEE Trans on Power Apparatus and Systems, vol. PWRS-1(3), pp 101-109 1986.
- [79] P. V. Balasubramanyam and O. P. Malik, "Static VAr Compensator Performance with Adaptive Stabilizer", 2002, (Internal report).
- [80] T. Abdelazim and O. P. Malik, "Intelligent SVC Control for Transient Stability Enhancement", IEEE, Power Engineering Society General Meeting, Vol. 2, 12-16 June 2005, pp 1701 - 1707
- [81] Tamer Abdelazim, "Adaptive fuzzy logic based PSSs", Ph. D. Thesis, Department of Electrical Engineering, University of Calgary, Canada, 2005.
- [82] E.V. Larsen and D.A Swann, "Applying Power System Stabilizers, Part I-III", IEEE Trans. on Power Apparatus and Systems, vol. PAS-100, June 1981, pp. 3017-3046.
- [83] E. Z. Zhou, "Application of Static VAr Compensator to Increase Power System Damping", IEEE Trans. On Power Systems, vol. 8, No. 2, May 1993.
- [84] M. A. El-Sayed, E. M. Abu El-Zahab, M. B. Eteiba and A. A. Emam, "Damping Inter-Area Oscillations in Multi-Machine Power Systems Using Fuzzy Logic SVC", The Tenth International Middle East Power Systems Conference, Ref. No. PW37, pp 699-704 Dec. 13-15, 2005, Port Said, Egypt.
- [85] IEEE Excitation System Model Working Group, "Excitation System Models for Power System Stability Studies", IEEE Standard p421.5-1992, Aug. 1992.
- [86] B. Adkins and R.G. Harley, The General theory of Alternating Current machines: Application to Practical Problems", Chapman and hall, London, England, 1975.

- [87] M. Eitzmann, "Excitation System tuning and Testing for Increased Power System Stability", GE Energy BROOC10605, 2004.
- [88] Hong Wang, "Neural Network Based SVC Controller", MSC. Dissertation, The University of Calgary, Calgary, Canada, October, 2004.
- [89] R. M. Mathur and R. K. Varma, "Thyristor-Based FACT Controller for Electrical Transmission System", Piscataway, NJ, IEEE, New York, Wiley, 2002.
- [90] R. E. Kalman, "New Approach to Linear Filtering and Prediction Problems", Transaction of the ASME-Journal of Basic Engineering, 82 (Series D), 35-45, 1960.
- [91] K. S. Dasgupta, "Transmission Line Impedance Protection Using an Optimal Kalman Filter", PH.D. Dissertation, The University of Calgary, Calgary, Canada, May, 1984.
- [92] Y.C. Ho "On the Stochastic Approximation Method and Optimal Filtering Theory", Journal of Mathematical Analysis and Application, 6, 152-154, 1962.
- [93] K.J. Astrom and B. Wittenmark, "Problems of Identification and Control", Journal of Mathematical Analysis and Application, 34, 101-113, 1971.
- [94] E. W. Kimbark, "How to Improve System Stability without Risking Subsynchronous Resonance", IEEE Trans. on Power Apparatus and Systems, vol. PAS-96, no. 5, September/October 1977, pp. 1608-1619.

APPENDIX A

SINGLE MACHINE POWER SYSTEM

The structural diagram of the single machine infinite bus power system model is shown in Fig. 4.2. The generating unit is modeled by seven first order differential equations.

A.1. Generator Model

The generator is modeled by seven first order differential equations [86].

$$\dot{\delta} = \omega_o \omega \quad (\text{A.1})$$

$$\dot{\omega} = \frac{1}{2H} (T_m + g + K_d \dot{\delta}_o - T_e) \quad (\text{A.2})$$

$$\dot{\lambda}_d = e_d + r_a i_d + \omega_o (\omega + 1) \lambda_q \quad (\text{A.3})$$

$$\dot{\lambda}_q = e_q + r_a i_q - \omega_o (\omega + 1) \lambda_d \quad (\text{A.4})$$

$$\dot{\lambda}_f = e_f - r_f i_f \quad (\text{A.5})$$

$$\dot{\lambda}_{kd} = -r_{kd} i_{kd} \quad (\text{A.6})$$

$$\dot{\lambda}_{kq} = -r_{kq} i_{kq} \quad (\text{A.7})$$

where:

ω_o : Nominal rotational speed,

H : Inertia constant,

K_d : damping coefficient,

r_a : Armature resistance,

r_f : Field resistance,

r_{kd} : Direct-axis resistance,

r_{kq} : Quadrature-axis resistance.

The generator parameters are given in Table A.1.

Table A.1. Generator parameters used in simulation studies

$r_a = 0.007$	$H = 3.46$	$r_f = 0.00089$	$r_{kd} = 0.023$
$r_{kq} = 0.023$	$X_d = 1.24$	$X_f = 1.33$	$X_{kd} = 1.15$
$X_{md} = 1.126$	$X_q = 0.743$	$X_{kq} = 0.652$	$X_{mq} = 0.626$
$K_d = -0.0027$			

All resistances and reactances are in pu and time constants in seconds.

A.2. Governor Model

The governor used in the system has the following transfer function.

$$g = \left[a + \frac{b}{1 + sT_g} \right] \dot{\delta} \quad (\text{A.8})$$

The Governor parameters used in the simulation studies are given in Table A.2.

Table A.2. Governor parameters used in simulation studies

$$a = -0.001328 \quad b = -0.17 \quad T_g = 0.25$$

A.3. AVR and Exciter Models

The AVR and exciter combination used in the system are from the IEEE Standard P421.5-1992, Type ST1A shown in

Fig. A.1 [85]. The parameter values are given in Table A.3.

Table A.3. AVR and exciter parameters used in simulation studies

$R_C = 0.0$	$X_C = 0.0$	$T_R = 0.04$	$K_A = 190$
$K_C = 0.08$	$K_F = 0.0$	$K_{LF} = 0.0$	$I_{LR} = 0$
$T_B = 10.0$	$T_C = 1.00$	$T_A = 0.01$	$T_F = 0.0$
$T_{BI} = 0.0$	$T_{CI} = 0.0$	$V_{OEL} = 999$	$V_{UEL} = -999$
$V_{IMAX} = 999$	$V_{IMIN} = -999$	$V_{AMAX} = 999$	$V_{AMIN} = -999$
$V_{RMAX} = 7.8$	$V_{RMIN} = -6.7$		

The AVR control action is determined by the lead lag compensator with time constants T_B , T_C , T_{BI} and T_{CI} and by the voltage regulator of proportional integral action of time constant T_A and gain K_A . The local control loop is closed by the proportional derivative action block time constant T_F and gain K_F .

Excitation systems with high gain and fast response times greatly aid transient stability but at the same time tend to reduce small signal stability [87]. Consequently, to increase the system stability an additional controller is needed which is called the power system stabilizer.

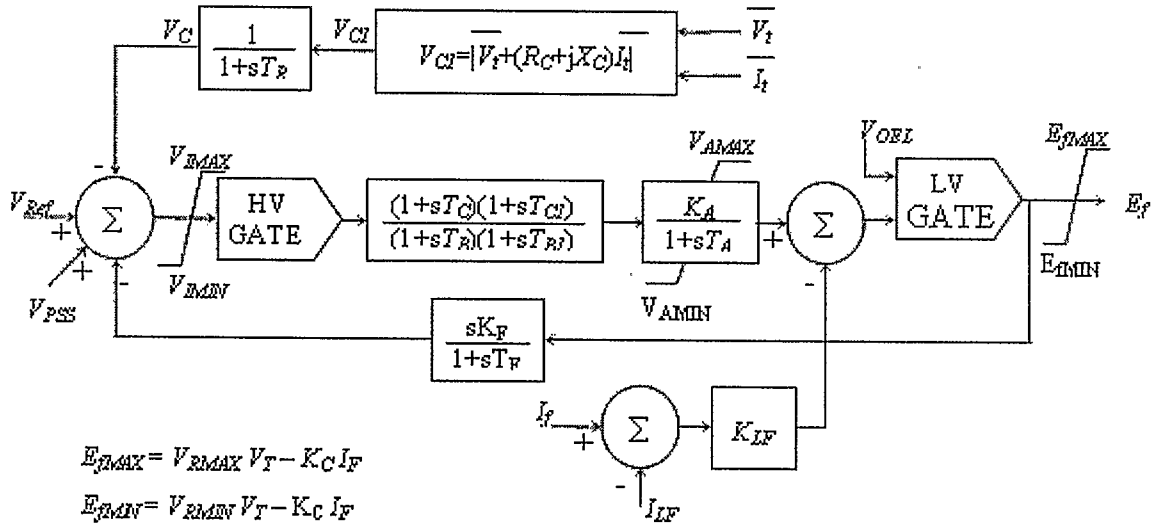


Fig. A.1. AVR and excitation model type ST1A, IEEE standard P421.5-1992

A.4. SVC

According to [88], the SVC can be represented as a voltage source behind a step up transformer. The voltages along the d and q axes are a function of the magnitude and angle of the DC voltage. The value of "m" can be controlled to adjust the output of the SVC.

$$e_d = (1 + m)V_{dc} \cos(\psi) \quad (A.9)$$

$$e_q = (1 + m)V_{dc} \sin(\psi) \quad (A.10)$$

From the SVC voltage resource to the middle bus, the SVC unit can be expressed as:

$$v_{md} = e_d + r_T i_{sd} - x_T i_{sq} \quad (A.11)$$

$$v_{mq} = e_q + r_T i_{sq} - x_T i_{sd} \quad (A.12)$$

The SVC parameters used in the simulation studies are given in Table A.4.

Table A.4. SVC parameters used in simulation studies

$K_{svc} = 2.5$	$T_{svc} = 0.15 \text{ s}$	
$B_{ini} = 0.04$	$B_{max} = 0.15$	$B_{min} = -0.15$

A.5. CPSS for Generator AND SVC

The CPSS Parameters used in the simulation studies are shown in Table A.5.

Table A.5. CPSS parameter used in simulation studies

$T_1 = 0.2$	$T_2 = 0.05$	$T_3 = 0.2$	$T_4 = 0.05$
$T_w = 2.5$	$K_{pss} = 0.01$	$V_{STMAX} = 0.1$	$V_{STMIN} = -0.1$

A.6. Transmission System

From the generator bus to the middle bus, the system can be written as:

$$v_{gd} = v_{md} + r_e i_d - x_e i_q \quad (\text{A.13})$$

$$v_{gq} = v_{mq} + r_e i_q - x_e i_d \quad (\text{A.14})$$

From the middle bus to the infinite bus, the system can be written as:

$$v_{md} = v_b \sin \delta + r_e (i_d + i_{sd}) - x_e (i_q + i_{sq}) \quad (\text{A.15})$$

$$v_{mq} = v_b \cos \delta + r_e (i_q + i_{sq}) - x_e (i_d + i_{sd}) \quad (\text{A.16})$$

Table A.6. Transmission line parameters used in simulation studies

$r_e = 0.0$	$X_e = 0.6$
-------------	-------------

All resistances and reactances are in pu and time constants in seconds.

APPENDIX B

MULTI-MACHINE POWER SYSTEM

B.1. Generator Model

The generating units shown in Fig. 5.1 are modeled by five first order differential equations (Equations (B.1) through (B.5)) [10].

$$\dot{\delta} = \omega_o \omega \quad (\text{B.1})$$

$$\dot{\omega} = \frac{1}{2H} (T_m + g + k_d \omega - T_e) \quad (\text{B.2})$$

$$T'_{do} \dot{e}_q = ef - (x_d - x'_d) i_d - e'_q \quad (\text{B.3})$$

$$T''_{do} \ddot{e}_q = e'_q - (x'_d - x''_d) i_d - e'_q + T'_{do} \dot{e}_q \quad (\text{B.4})$$

$$T''_{qo} \ddot{e}_d = (x_q - x''_q) i_q - e''_d \quad (\text{B.5})$$

B.2. Parameters of the Power System

The parameters for the five machines power system given in Fig. 5.1 are defined in Table B.1. The AVR and simplified ST1A exciter parameters are defined in Table B.2. The governor parameters are given in Table B.3. Finally, the power grid transmission line parameters are given in Table B.4.

Table B.1. Generators parameters used in simulation studies

	G_1	G_2	G_3	G_4	G_5
X_d	0.1026	0.1026	1.0260	0.1026	1.0260
X_q	0.0658	0.0658	0.6580	0.0658	0.6580
X_d'	0.0339	0.0339	0.3390	0.0339	0.3390
X_d''	0.0269	0.0269	0.2690	0.0269	0.2690
X_q''	0.0335	0.0335	0.3350	0.0335	0.3350
T_{do}'	5.6700	5.6700	5.6700	5.6700	5.6700
T_{do}''	0.6140	0.6140	0.6140	0.6140	0.6140
T_{qo}''	0.7230	0.7230	0.7230	0.7230	0.7230
H	80.000	80.000	10.000	80.000	10.000

All resistances and reactances are in pu and the time constants are in seconds.

Table B.2. AVR and ST1A exciter parameters used in simulation studies

	G_1	G_2	G_3	G_4	G_5
T_R	0.04	0.04	0.04	0.04	0.04
K_A	190	190	190	190	190
K_C	0.08	0.08	0.08	0.08	0.08
T_B	10.0	10.0	10.0	10.0	10.0
T_C	1.00	1.00	1.00	1.00	1.00

All time constants are in seconds.

Table B.3. Governor parameters used in simulation studies

	G_1	G_2	G_3	G_4	G_5
T_g	0.25000	0.25000	0.25000	0.25000	0.25000
A	-0.00015	-0.00015	-0.00133	-0.00015	-0.00133
B	-0.01500	-0.01500	-0.17000	-0.01500	-0.17000

All time constants are in seconds.

Table B.4. Transmission line parameters used in simulation studies

Bus #	R	X	Bus #	R	X
1 – 7	0.00435	0.01067	4 – 8	0.00524	0.01184
2 – 6	0.00213	0.00468	5 – 6	0.00711	0.02331
3 – 6	0.01002	0.03122	6 – 7	0.04032	0.12785
3 – 6	0.01002	0.03122	7 – 8	0.01724	0.04153

All resistance and reactance values are in pu.

B.3. Loads and Operating Condition

The power system described in Fig. 5.1 contains three loads, their parameters are given in Table B. and tested under the power flow parameters given in Table B.6.

Table B.5. Load parameters used in simulation studies

L_{o1}	L_{o2}	L_{o3}
$7.5 - j5.0$	$8.5 - j5.0$	$7.0 - j4.5$

Table B.6. Power flow parameters used in simulation studies

	G_1	G_2	G_3	G_4	G_5
P	5.1076	8.5835	0.8055	8.5670	0.8501
Q	6.8019	4.3836	0.4353	4.6686	0.2264
V	1.0750	1.0500	1.0250	1.0750	1.0250
δ	0.0000	0.3167	0.2975	0.1174	0.3051

All electrical powers and voltages are expressed in pu and the power angles are in rad.